Hydrogeological study of Strømbo waterworks, Øvre Eiker municipality, Norway

Master´s thesis in Geoscience

Madelen Teigland

Department of Geosciences

Faculty of Mathematics and Natural Sciences

UNIVERSITY OF OSLO

August 2022

2022

Hydrogeological modelling of Strømbo Waterworks, Øvre Eiker municipality, Norway.

Print. Reprosentralen, University of Oslo.

Abstract

Strømbo waterworks supplies approx. 60% of the inhabitants of Hokksund and Skotselv with drinking water and consists of six supply wells in unconsolidated sediments located close to Drammen river. The hydrogeological conditions of Strømbo waterworks were investigated to find a solution to increase the capacity in their supply wells by the end of summer 2022 due to an increasing population growth. The waterworks have also at times struggled with to high concentrations of iron and manganese in the groundwater. For this purpose, 9 observation wells were drilled in February 2022 to monitor the groundwater in the aquifer around the supply wells and sediment samples were collected to assess the hydraulic properties of the sediments around the wells. A previous study conducted by Rambøll in 2019 of the iron and manganese concentration in each of the six supply wells were investigated and a previous study conducted by Rambøll in 2020 of the iron and manganese concentrations from the raw water in the entire waterworks were compared with precipitation events looking for correlations. A numerical groundwater model was designed to explore the river-aquifer interaction following a change in pumping rate and surface recharge with MODFLOW. In addition, MODPATH with particle tracing was used to investigate which directions the wells draw water from, and in particular whether they draw water from Drammen river. The wells capture zones were also examined to check if the wells maintain a residence time of 60 days which ensures that bacteria from the river die before reaching the wells. The result shows that the sediments around the wells consists of a mixture of sand and gravel. The sensitivity analysis showed that the model is not very sensitive to changes in hydraulic conductivity or recharge, but the wells capture zones are sensitive to changes in porosity. In addition, there is a linear relationship between river leakage and pumping rate where an increase in pumping rate leads to an increase in river leakage. There is also a linear relationship between river leakage and surface recharge where an increase in surface recharge leads to a decrease in river leakage. In addition, all wells draw water from the river and maintain a residence time of 60 days except from the supply well located closest to the river which maintain a 50-days limit. This supply well have also higher concentrations of manganese and is the only well that just draw on river water. Furthermore, the north-eastern part of the study area was found to be the most suitable location for a new supply well. This area is less affected by the pumping from the other wells. If a new supply well is to be established here, it will not only draw on river water and it will maintain a residence time of at least 60 days. Thus, this well will probably not have problems with manganese concentrations above maximum limit value.

Acknowledgements

I would like to thank my supervisor Carlos Duque Calvache for his guidance and advice over the past year. I have benefited greatly from your experience and your vast store of knowledge. I must honestly admit that I at first was worried about having a supervisor that was not physically available. But I quickly realized that my worries were completely unnecessary as I got all the help I needed through digital meetings. The teaching you gave me through these meetings benefited my understanding of how a hydrogeologist thinks. It was also very nice that you came to visit the university before my thesis was submitted. I have noticed that you have spent a lot of time correcting my thesis and giving me feedbacks which I have greatly appreciated. I know for sure that this thesis would not have turned out so well without your help.

I would also like to thank my other supervisor, Jonas Thu Olsen. You have been my security over the last year, and I am extremely grateful for all the help and advice. Without your guidance and great understanding of hydrogeology and groundwater modeling, this master´s thesis would have been much more difficult for me to complete. I want to thank you for always being available digitally, by email and phone, and for allowing me to come to your office as much as I wanted. I would also like to extend a big thank you to your colleagues at Rambøll for welcoming me with open arms and being very inclusive. I also had a very nice day with you out in the field where I was enriched with a lot of experience.

I would also like to thank Anna Vårheim for joining me for the first 2 days of the fieldwork. You helped me get started with sediment sampling and I got a nice lesson in how a hydrogeologist thinks in the field. I want to thank you for welcoming me in Rambøll with open arms and for all the nice conversations we have had.

Finally, I must thank my family and friends for supporting me over the past year. You have been very understanding and arranged for me to be able to sit and work in peace during this time. You have also motivated me in difficult periods when I have been tired and given me positive energy.

Table of contents

List of figures

Chapter 1
Introduction

Groundwater is an important water resource in many countries around the world. In Norway, groundwater only accounts for 15% of all water consumption (Geological Survey of Norway, 2017). Norway has a large supply of surface water due to the dominating presence of bedrock and quaternary geology (Morland, 1996). The knowledge of groundwater resources is important in areas where groundwater constitutes the only available source of drinking water. The proportion of Norway´s population that is supplied with groundwater and who lives in densely populated areas is only 4,2%. About 30% of the population who live in sparsely populated areas have groundwater as the main source of water supply (Morland, 1996). Groundwater is often more economical and because it can be difficult to connect to pipes if the distance is too large. However, as the knowledge about the utilization of groundwater increases, several factors have emerged that make it a better alternative in the water supply than surface water. For example, good quality, stable temperature, better protection against pollution, and low investment and operating costs (Morland, 1996). While groundwater is better protected against pollution than surface water, groundwater can also be exposed to chemical and biological sources of pollution. The quality and quantity of the groundwater depend on the geological and climatical conditions like precipitation and evapotranspiration. The contamination of groundwater can occur both naturally or from human activities depending on the wide range of environmental and physical variables, including depth to groundwater and aquifer size (Evans and Myers, 1990). Therefore, mapping the aquifer´s vulnerability, i.e., the natural protection and potential sources of pollution, is essential to ensure water quality for human supply (Gaut, 2009).

In Norway, most of the groundwater facilities are in small aquifers where the amount stored is based on infiltration from streams or lakes (Colleuille *et al*., 2004). Induced recharge is common in many Norwegian waterworks where wells are established in the sedimentary deposits near a watercourse. Induced recharge involves increasing the infiltration of water from a river to the aquifer by pumping water in wells located near the riverbank where the groundwater level is lowered below the level of the river (Casanova *et al*., 2016). If the aquifer gets less recharge from precipitation, an induced recharge will increase the groundwater supply capacity. There are several groundwater works in Norway that depend on

induced infiltration such as Ringerike and Sunndal waterworks. Both waterworks have also experienced major problems with high concentrations of manganese or iron, which has led to the establishment of new wells and expensive water treatment plants (Stenvik and Hilmo, 2020). Thus, changes in flow pattern entails a change in the aquifer's geochemical processes which affect the mobility of iron and manganese (Farnswort and Hering, 2011).

Groundwater flow models are tools frequently used to monitor the availability and quality of the groundwater as well as the extraction potential for the supply wells. They are also widely used to simulate the aquifer conditions, to estimate aquifer parameters and to predict groundwater conditions (Hashemi *et al*., 2013). In planned operations such as pumping that leads to a change in water level or quality, the model can simulate the behavior of the aquifer (Bear and Verruijt, 2012). The model can also be used to explore the river-aquifer interactions and how changes in hydrological conditions affect the groundwater. Numerical groundwater models can consider more realistic hydrological conditions in the river-aquifer system compared to analytical methods (NVE, 2005). Groundwater models are only simplified mathematical representations of complex natural systems, so they need to be assessed and compared with field observations and data.

1.1 Justification of study

Øvre Eiker municipality located in south-east Norway is situated approximately 3 km north of Hokksund along Drammen river and have two main waterworks were Strømbo waterworks supplies around 63% of the inhabitants in Hokksund and Skotselv city with drinking water. In recent years, the waterworks has faced two main challenges. First, due to increasing population growth, increased capacity is needed to provide more drinking water by the end of summer 2022. Currently, the water demand is covered when water is pumped from 4 of the 6 supply wells. Data from Statistics Norway (SSB) show that the population will increase from approximately 20.000 inhabitants in 2022 to over 23.000 inhabitants in 2035. For this reason, Rambøll have suggested to establish a new supply well in the waterworks. The municipality wants the new supply well to be located close to the current pipeline network which sets limits on where the well can be established. Second, the waterworks have problems with too high concentrations of iron and manganese in their supply wells, and previous research has not revealed the main reason for these high concentrations. The population complains about

the taste, smell and the color of the water. The two northernmost supply wells near Drammen river as including one of the wells in the south have been taken out of operation due to these high concentrations. It is especially the manganese concentrations that are high and above the maximal limit value. Thus, the municipality have considered a new water treatment plant to reduce the concentrations. Before investing, the municipality wants to consider other alternative solutions.

1.2 Objectives of study

The main goal of this study is to examine the hydrogeological conditions of Strømbo waterworks to find a solution to increase the capacity in the waterworks. For this purpose, a numerical groundwater flow model of the study area is constructed to explore the aquifer-river interaction by changing the pumping and recharge rate. Particle tracking was used to explore the well capture zones to investigate which direction the wells draw water from and especially if they draw water from the river. To find the most suitable location for a new supply well without it being affected by already existing supply wells in the area, the wells pumping depression cones were also investigated. Since the waterworks at times have high concentrations of iron and manganese, a previous study conducted by Rambøll in 2019 of the iron and manganese concentration in each of the six supply wells was investigated and the iron and manganese concentrations from the raw water in the entire waterworks in 2020 was compared with rain precipitation events looking for correlations.

Chapter 2

Study area

2.1 Geographical location

The waterworks in Øvre Eiker municipality are located in the south-eastern part of Norway, approximately 3 km north of Hokksund on the eastern side of Drammen river (Figure 2.1). The municipality has a population of 19,842 inhabitants and covers an area of 457 km^2 (Statistics Norway, 2021). Strømbo waterworks is one of two main municipal waterworks and has currently six groundwater supply wells with different capacities.

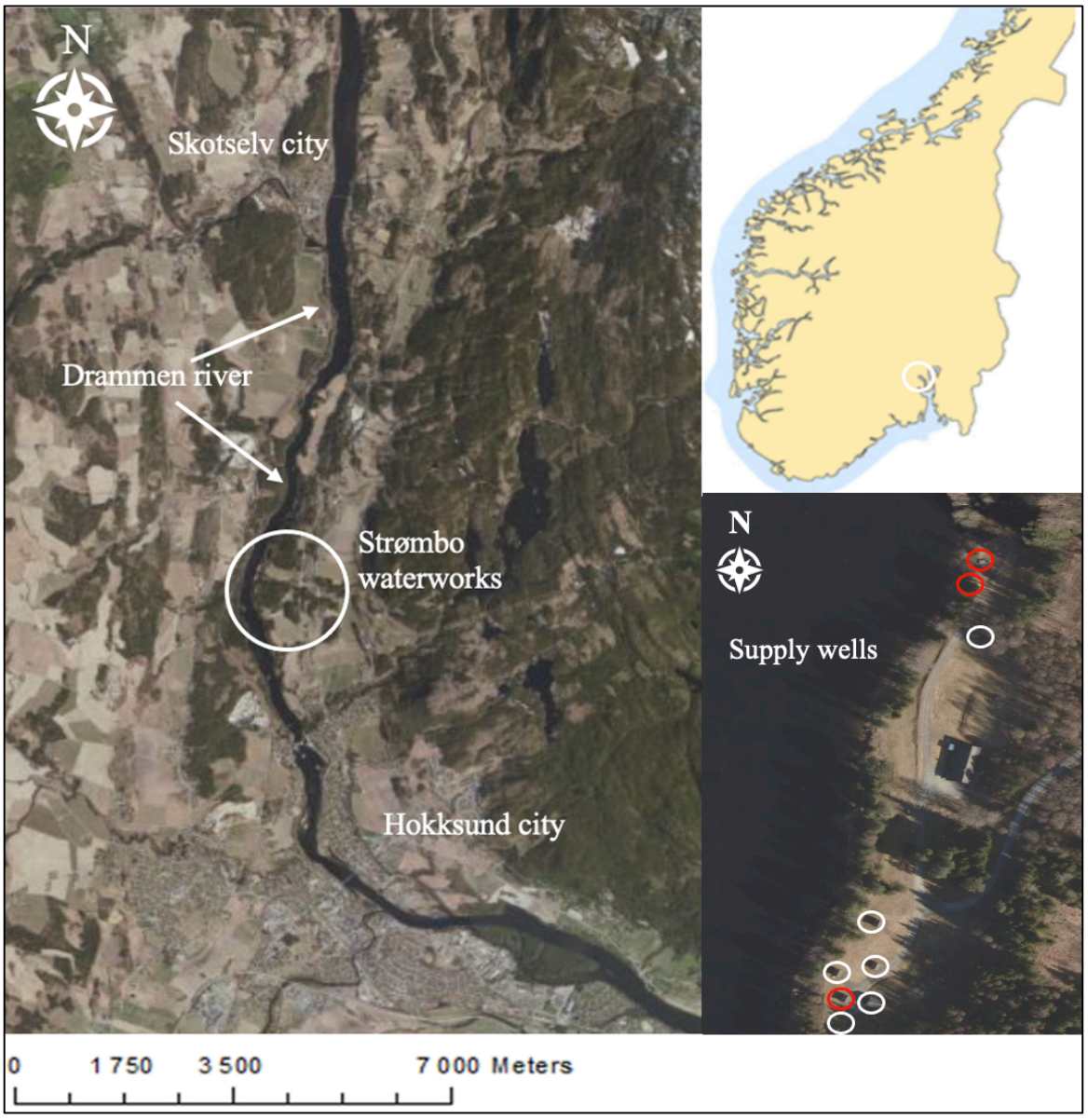

Figure 2.1. Geographical location of the study area. The red circle is showing supply wells out of operation.

2.2 Background information

2.2.1 Water Treatment plant

At Strømbo, a water treatment plant has been installed that purifies the groundwater as there are traces of dissolved iron and manganese in the groundwater. Iron and manganese are redox-sensitive elements that are oxidized and precipitated as hydroxides in oxygen-rich environments and are reduced and dissolved in oxygen-poor water conditions (Stenvik and Hilmo, 2020). All six supply wells at Strømbo are deep enough where there is little or no oxygen present. Thus, before the water is sent through the distribution systems, it is necessary that iron and manganese are decreased. Iron and manganese behave differently in the aquifer, but they are both dissolved in the water under reducing concentrations as divalent Fe^{2+} and Mn^{2+}. Under oxidizing conditions, the substances will lose electrons, typically to oxygen, and act with high oxidation numbers, low solubility and form hydroxide minerals which precipitate from the water phase. In reducing condition without access to oxygen, iron and manganese will be more soluble, and act as dissolved ions in the water phase (Stenvik and Hilmo, 2020).

If reduced groundwater is used in drinking water production, iron and manganese must be removed to avoid operational problems, as they precipitate on the wiring network when they come in contact with oxygen. However, iron and manganese can give other unwanted effects in drinking water, such as poorer taste and color (Mettler *et al*., 2001). Today, the raw water from the wells is treated with chlorine for disinfection and water glass for corrosion control as well as aeration at the inlet to the clean water basin. The water is then pumped up to the clean water magazine which is located up the terrain east of the waterworks where it is stored before it goes out into the supply network.

2.2.2 New supply well and groundwater infiltration

In the short-term scenario, the municipality wants to establish a new supply well to increase the capacity by the end of summer 2022. For this purpose, new observation wells have been drilled to determine the location of the new supply well, including the depths and sizes of the filter. On the other hand, in the long-term scenario to increase the capacity, the municipality wants to infiltrate water from Drammen river to the aquifer as river water contains low iron and manganese concentrations and high oxygen concentration. However, river water will have greater humus content and is more prone to contamination and bacteria, but a residence time of minimum 60 days from the river to the supply well ensures that bacteria from the river die before reaching the well. Nevertheless, pumping groundwater from the northern wells to the aquifer may be healthier and less contaminated or contain bacteria (Figure 2.1). However, the northern wells are not in production today as they had manganese concentrations above the maximal limit value of 0.05 mg/l.

2.2.3 Groundwater flow and contamination transport

The high concentrations of iron and manganese in the groundwater at Strømbo waterworks appear to originate from natural sources within the aquifer. The natural sources include organic and inorganic compounds or elements found in rocks and soils such as degraded organic material, iron, manganese, arsenic, chlorides, fluorides, sulfates or radio sources (Belk, 1994). The solution of iron and manganese in groundwater depends on the availability of oxygen and the acidity (pH). Periods with high recharge may lead to an influx of oxygen-rich water, which together with low pH level leads to the dissolution of iron and manganese. Oxidation with chlorine is effective in reducing the concentration of iron and manganese, and it also provides protection against microbial contamination. Oxidation together with adsorption and biological degradation are the three natural processes that take place in soil layers in the unsaturated zone, and which all help to reduce the concentration of pollutants and stop pollution from reaching the groundwater (Belk, 1994). Thus, the understanding of the groundwater flow pattern is crucial in the monitoring of the groundwater and the groundwater flow is also often strongly affected by recharge and interaction with the surface water.

2.3 Geological setting

The study area consists mainly of glacial- and glacifluvial deposits over a bedrock basement (Figure 2.2). The glaciofluvial deposits in the north were deposited by flowing meltwater from the glacier or from areas within or below the glacier and represents coarse and relative well-sorted material with large blocks embedded (Hansen *et al*., 2005). Previous drilling shows that the upper layers closer to the surface consist of fine-grained and well-sorted sediments while the lower layers closer to the bedrock are gravelly (Norconsult, 2011). In addition, since they are deposited at the end of the ice age, the content of organic material is small or absent (Colleuille *et al*., 2004). While the glacial deposits south of the well area were deposited by the glacier itself and represents fine-grained and well-sorted material.

Metagabbro and quartzite are the dominant bedrock and was formed during mountain chain folds in Precambrian times. The bedrock is visible in the surface several places in the study area, both in the north and south as well as an area in the middle (Figure 2.3). Upstream the well area in the north there is a ravine that descends towards the wells which is caused by streambank erosion. South of the well area are two terrace edges which is stepped edges in the terrain. Further upstream the well area is a thin moraine mass which are glacial deposits that have been deposited or transported by a glacier that has torn or crushed the material from rocks or loose sediments. There are also several eskers which extends from northeast to southwest and consist of glaciofluvial material deposited in rivers on or sub-glaciers and contain coarse and well-sorted material (sand, gravel, and round stone). Finally, there is a dead ice pit southwest from the well area. The formation of dead ice pits corresponds to icebergs that have either been completely or partially buried when the sediments have melted. This has led to the ice depositing rock materials in mounds and ridges, so that deeper ponds and water have formed (Colleuille *et al*., 2004).

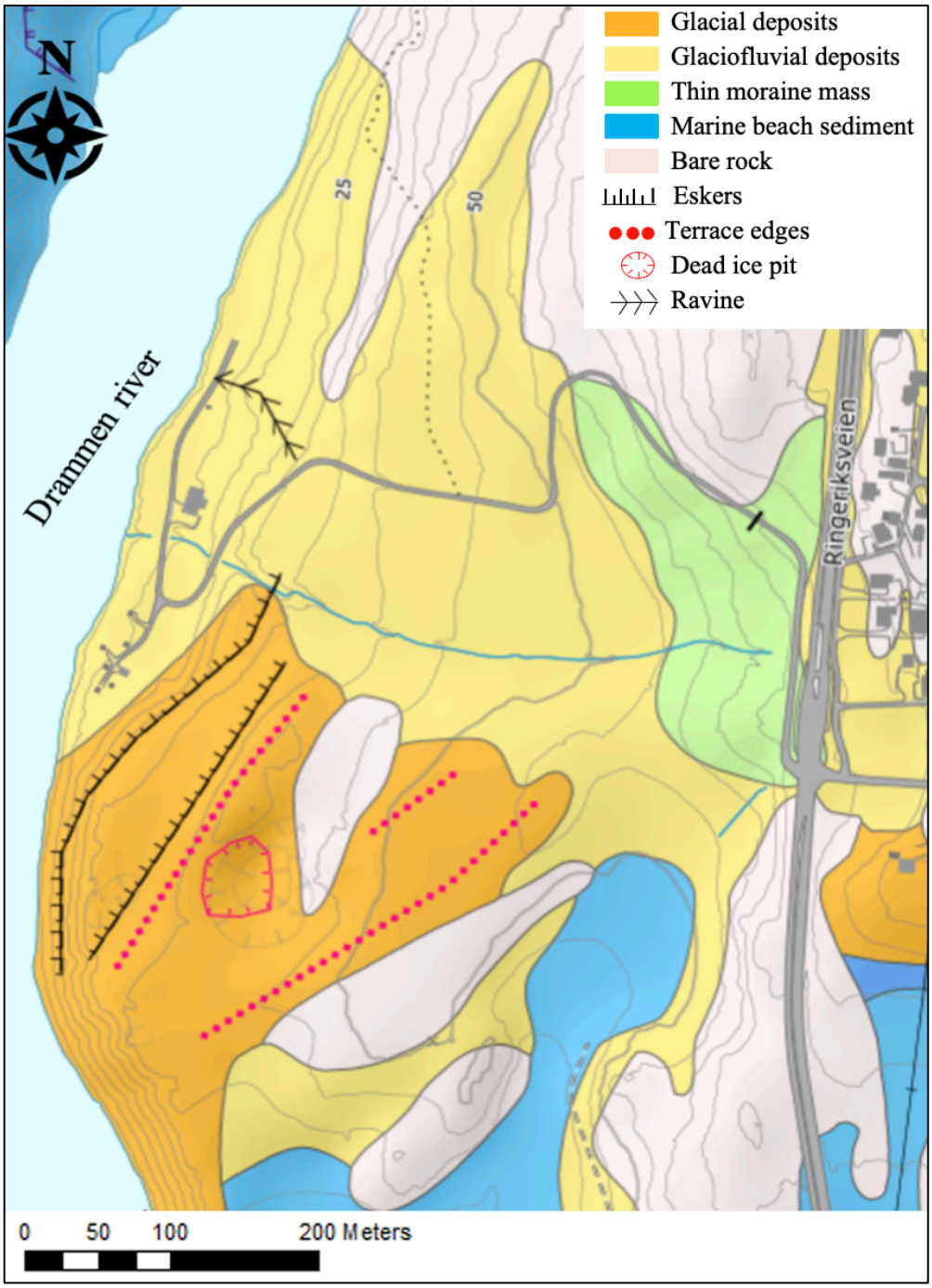

Figure 2.2. Sediment and geomorphological map of the study area (NGU, 2022).

2.3.1 Topographical condition

At Strømbo, the maximum elevation in east is of around 75 meters above sea level (m.a.s.l.) to the lowest elevation is in the west of about 7 m.a.s.l. where it meets Drammen river (Figure 2.3). In the western area near the river, where all six supply wells are located, there is an open landscape while the rest of the study area is covered by forest or agriculture. The recharge comes mostly from the snowmelt in the spring (445mm) for a yearly precipitation of 871 mm (SeNorge, 2022).

Figure 2.3. Topographical map of the study area retrieved from NGU.no

2.4 Supply wells

The waterworks at Strømbo currently consists of six supply wells drilled in 1996 and 2007 (Figure 2.4). Since the wells have been drilled in different periods, different types of filters have been installed in different depths with different slot openings. The last letter in the well name stands for the wells locations in the north, south or in the middle of the waterworks.

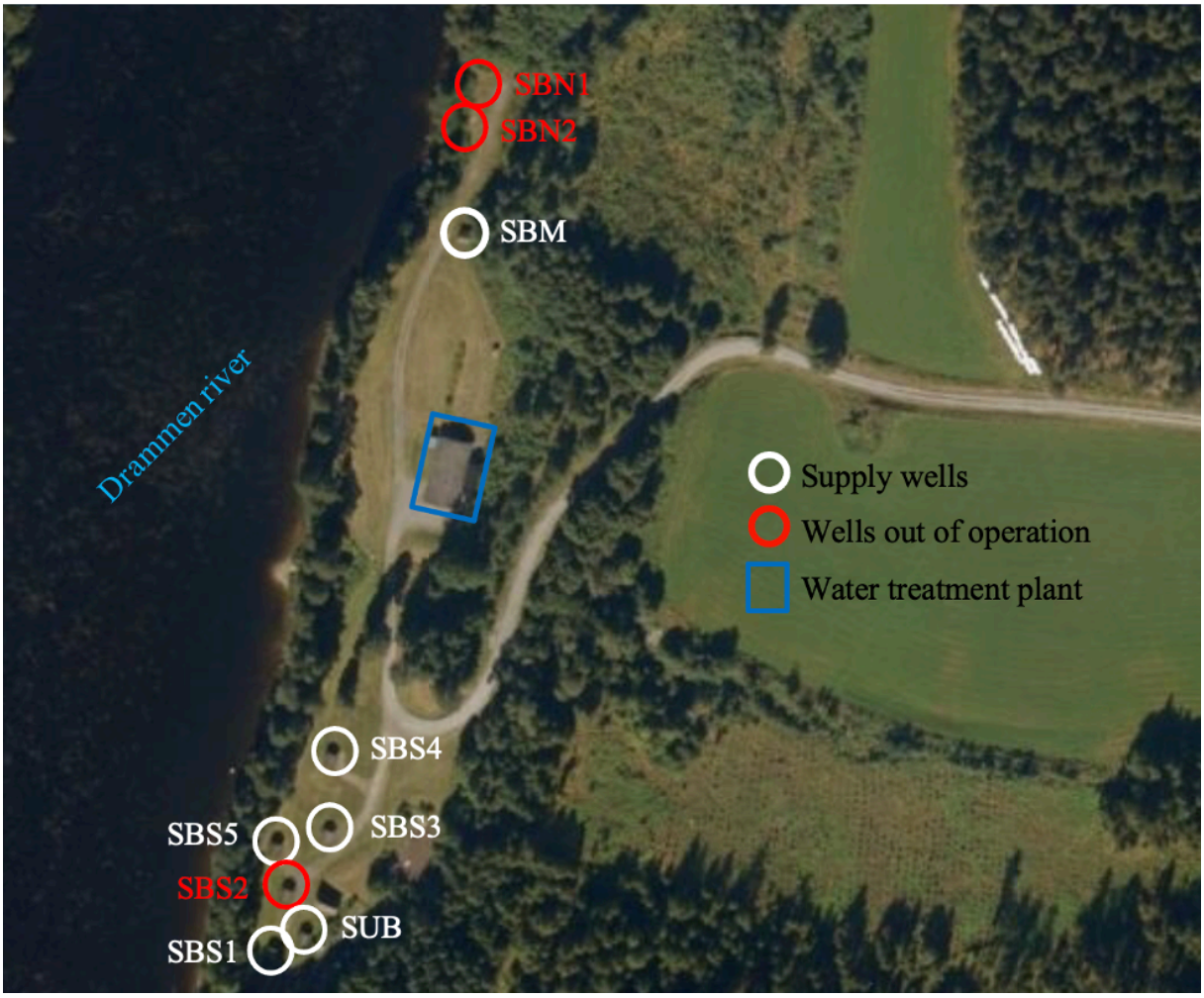

Figure 2.4. The location of all current supply wells and the water treatment plant in the study area.

The wells have different extraction capacity ranging from 1296 to 1987 m^3/d and are all set in relatively heterogeneous sediments consisting of a mixture of sand and gravel. All supply wells consist of well pipes and well filters where the water intake takes place (Table 2.1). All wells except those established in 2007 were set with sump pipes that collect fines entering the well.

Table 2.1. Well information.

Name	SBM	SBS1	SBS3	SBS4	SBS5	SUB
Establishment date	1996	1996	1996	2007	2007	1996
Responsible for establishment	NGU	NGU	NGU	NGU	NGU	NGU
ØV-coordinates	549930	549875	549891	549892	549876	549884
NS-coordinates	6630044	6629837	6629871	6629894	6629867	6629841
Surface level (masl)	12.34	15.55	14.76	15.07	14.33	16.21
Well depth (m)	30	21	21	19	19.5	24
Diameter (mm)	213	355	355	188	280	355
Type of filter	Conslot stainless	Conslot stainless	Conslot stainless	Plastic	Plastic	Conslot stainless
Filter location (m)	17-27	12-19	12-19	14-19	13-19.5	14-22
Sump (m)	3	2	2	0	0	2
Slot opening (mm)	0.7 – 1.5	1 – 2.5	0.8 - 1	1.25	1.5	0.6 - 1
Pump capacity (l/s)	23	19.5	20	15	16	20
Pump capacity (m^3/d)	1987	1685	1728	1296	1382	1728
Groundwater depth (m)	unknown	11.1	unknown	8.5	9.0	9.0

2.5 Previous work

In the last 30 years, 15 geophysical and hydrogeological surveys have been conducted at Strømbo. Most are not relevant today as they deal with experiments performed on supply wells that are out of operation, but the area has been geologically mapped and several water quality analyses have been carried out. A short overview of previous studies is:

a) Compilation of pumping results from the groundwater wells and grain size distribution analysis:

Asplan Viak (1995) carried out hydrogeological surveys to find the hydraulic conductivity in the sediments around the waterworks as well as long-term sample pumping of groundwater wells both in the northern, southern and mid part of the study area. The northern wells are not in production today (Figure 2.4). The results showed that the highest hydraulic conductivity values were found in the northern area of the waterworks and decreases towards the southern area (Table 2.2). In addition, the maximal pump capacity for SBM located in the mid area is

23 l/s. Two different methods were performed to calculate the hydraulic conductivity, data from pumping tests as well as Hazen´s formula with grain size distribution data, which explains the variations (Table 2.2).

Table 2.2. Calculated hydraulic conductivity values in the study area (Asplan Viak, 1995).

Well area	**North**	**Mid**	**South**
Average hydraulic conductivity (m/s)	$1.8 - 57\ x\ 10^{-4}$	$7.5 - 12\ x\ 10^{-4}$	$2.0\ x\ 10^{-4}$
Average hydraulic conductivity (m/d)	15.5 – 492	64.8 – 103.7	17.3

b) Evaluation of exiting data basis for automatic monitoring at the plant and from pumping tests in 1999 and 2000, and design of well filter against grain distribution analysis:

Norconsult (2005) evaluated previous pumping tests at Strømbo and investigated the high turbidity values in some of the supply wells. They found that all supply wells were set without gravel pack in relatively heterogeneous sediments. In addition, the filter tubes for each well had different slot openings where the dimensioning of filter tubes in natural phenomenon (without gravel casting) is made in relation to the loose material composition and the relative heterogeneity (sorting degree) in the sediments where the filter is placed. The grain size distribution curves from the wells showed that the filter openings were dimensioned too large (lager than d_{60} for the entire filter length) (Table 2.3). This is contrary to common practice regarding filter dimensioning and is a possible origin of some of the turbidity in the wells.

Table 2.3. Assessment of slot opening in relation to grain size distribution curves (Norconsult, 2005).

SBS1	No grain size distribution curve
SBS2	Slot openings from d_{70} to d_{90} for interval 11-19m
SBS3	No grain size distribution curve
SBM	Slot openings > d_{60} for interval 17-24m; no grain size distribution curve for interval 24-27m
SUB	Slot openings from d_{75} to d_{85} for interval 14-22m

c) Ground investigation – establishment of two supply wells and test-pumping:

Norconsult (2008) carried out ground investigations with the subsequent establishment of wells SBS4 and SBS5 (Figure 2.4). After establishment, the supply wells were test pumped over a 4-month period to assess capacity and water quality. Both wells had satisfactory water quality with slightly higher turbidity than desired between 1 and 4 Formazin Nephelometric Units (FNU). The concentrations of iron and manganese were below the maximum limit. In addition, the maximal pump capacity was calculated to be 31 l/s for both wells.

d) Suggestion to reduce iron and manganese concentrations – infiltrating water from Drammen river:

Norconsult (2011) proposed to reduce the iron and manganese concentrations by infiltrating water from Drammen river which have low iron and manganese concentrations as well as higher oxygen saturation. The wells were originally designed to raise alkalinity (buffering capacity) in the groundwater but have not been in use since the early 2000s. The aim was to achieve reduction zones of iron and manganese concentrations by diluting and raising oxygen in the groundwater.

e) Analyses of iron and manganese concentrations in supply wells:

Rambøll carried out analyzes of the groundwater in each of the 6 supply wells at Strømbo in 2019. The results showed that all wells contained both iron and manganese, where the well located closest to the river had the highest manganese concentrations while the second most southerly well had the highest iron concentrations (Rambøll, 2021).

f) Analyses of iron and manganese in the raw water at Strømbo waterworks:

Rambøll investigated the raw water in the entire waterworks in 2020 for iron and manganese concentrations throughout the year. The result showed that the manganese concentrations was for long period above the maximal limit value of 0.05mg/l, while iron remained stable below the maximal limit value of 0.2mg/l (Rambøll, 2021).

Chapter 3

Methods

3.1 Field work

Geophysical surveys were performed by Rambøll October 29th, 2021, to investigate the conditions in the ground and depth to the groundwater. On February 16th 2022, a field study was carried out in the area to acquire information about landforms, topography and drainage associated with the aquifer. In week 7 and week 10 2022, all observation wells were drilled (Figure 3.1).

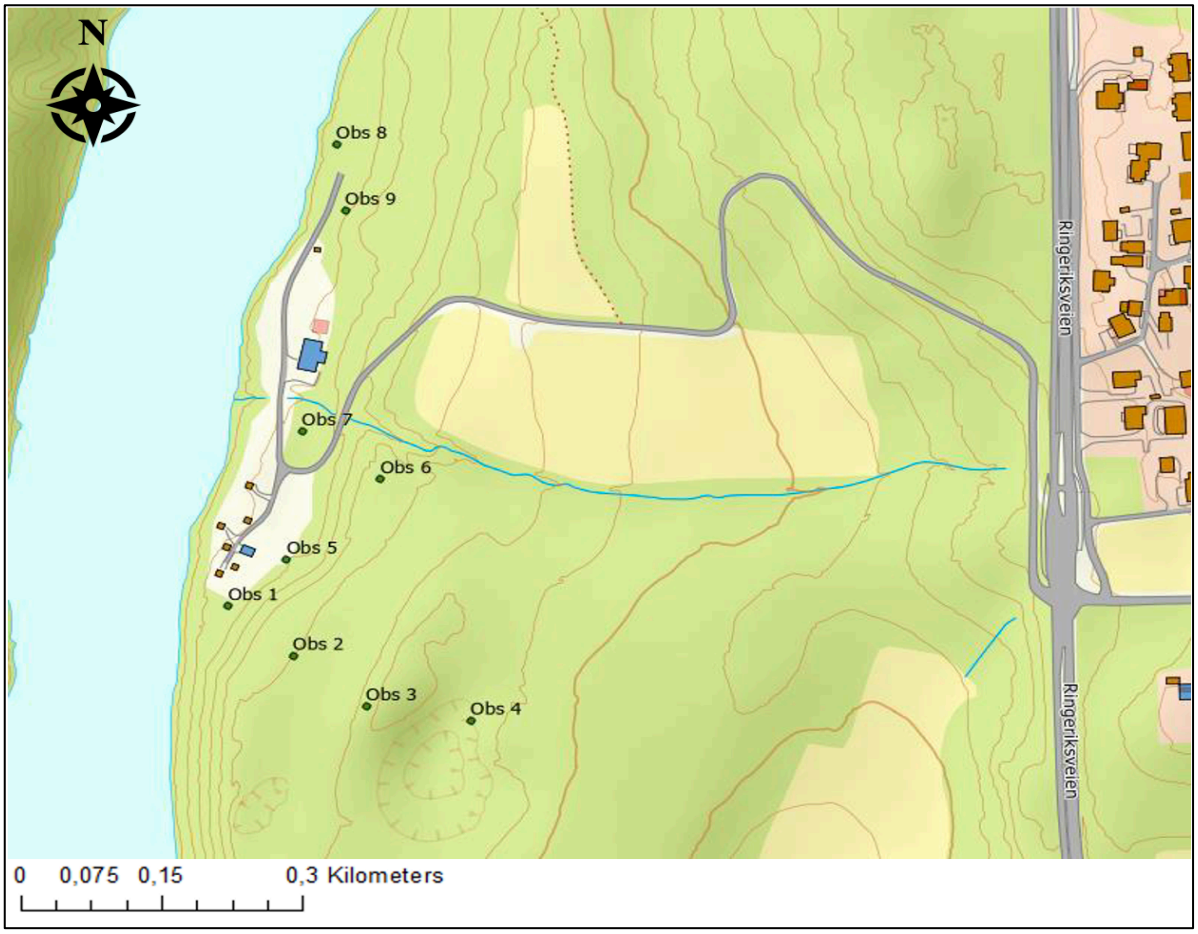

Figure 3.1 The location of the observation wells marked as Obs 1 – Obs 9.

3.1.1 Geophysical ground survey – Drilling of observation wells

A total of 9 observation wells were drilled to identify the approximate depth and thickness of the aquifer as well as to study the chemical and physical properties of the sediments. The

locations of the observation wells were based on results from the geophysical survey conducted in October 2021 as well as information from previous ground surveys (Norconsult, 2011) (Figure 3.1).

Total sounding is a method that is often used in an initial phase to investigate the loose sediments and map the bedrock elevation. The method consist of a combination of rotary pressure sounding and rock control drilling (NGF, 1994). where the stratification of loose sediments, the depth to solid ground and the position of the groundwater table can be determined. The execution involves using a drilling rig to rotate an observation pipe into the ground (Figure 3.2). When the pipe is almost completely down, it is welded on a new pipe. This process continues until the bedrock is reached. However, several challenges may arise during rotation. If the pipe meets solid or hard layers, the penetration will not be maintained. Thus, the rotation speed can be increased or flushing or hammering mode can be activated (NGF, 1994).

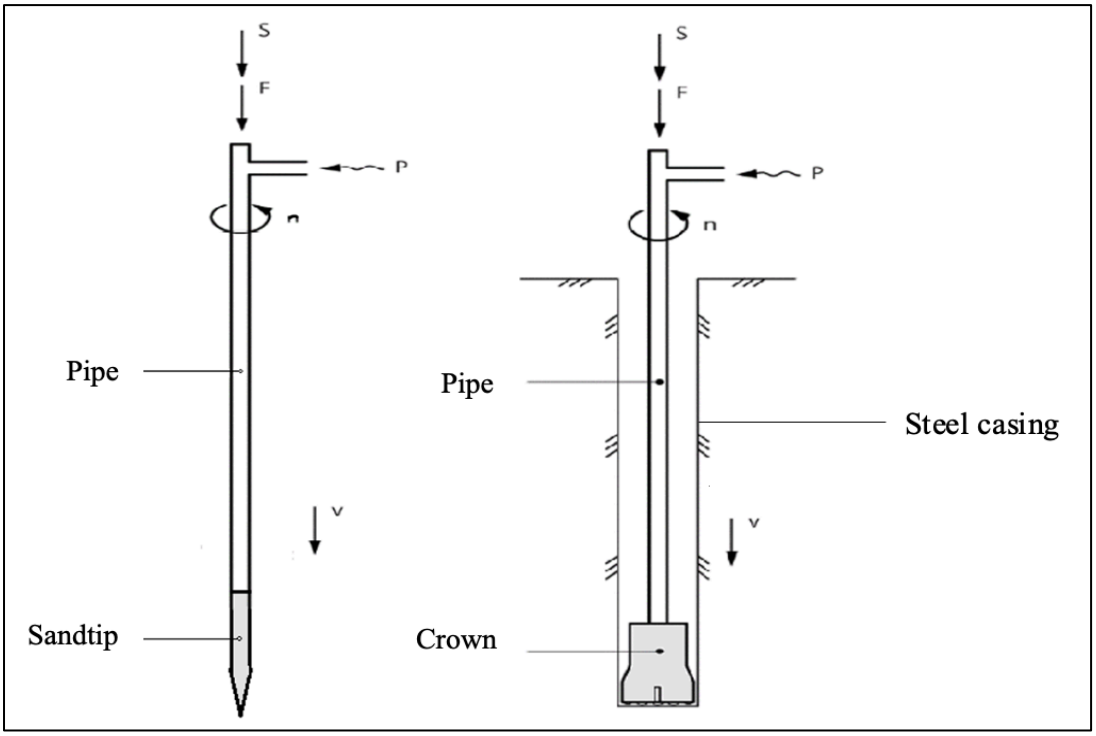

Figure 3.2. Principle for performing total sounding with sandtip and crown. S is stoke, F is depression force, P is water flush, n is rotation and v is depression rate (Kolstad, 1987).

For obs1, obs8, and obs9, pipes of 2m length and 51mm width were used (Figure 3.3). When the drilling rig failed to push the pipes further down due to hard sediments, all pipes were

lifted of the ground before a sand tip was mounted on the bottom of the first pipe (Figure 3.2). Then, the pipe was pushed even further into the ground until the bedrock was reached

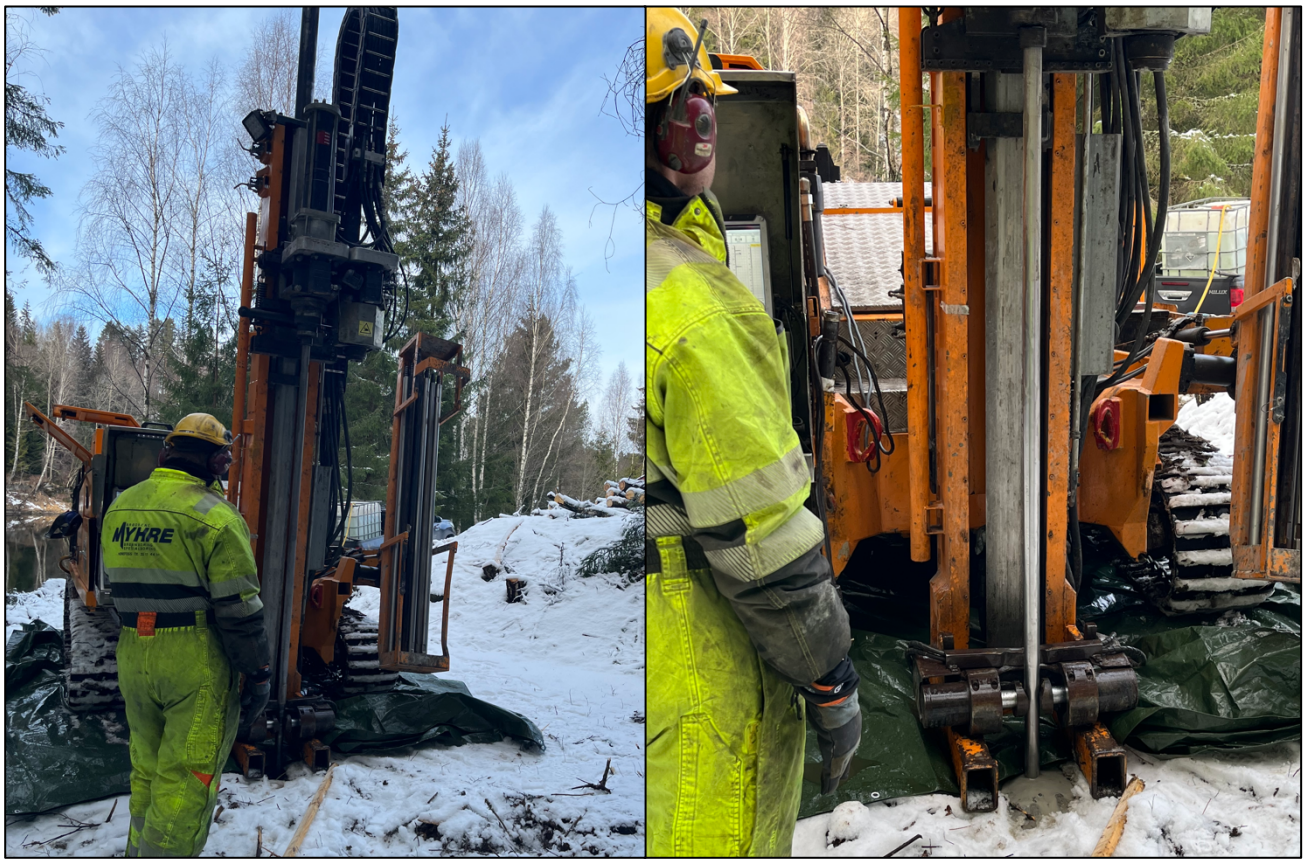

Figure 3.3 Drilling rig used in the establishment of one of the observation wells.

For the remaining wells, an Odex crone (Overburden drilling excentric) was used as the subsurface was harder (Figure 3.4). The pipes had a length of 2 m and 102mm width. The advantage of to establishing wells with this width is that the well is full-fledged well with less uncertainty around filter depth and well design. With this drilling technique, a special drill is lowered into a steel pipe or an outer casing (Figure 3.2). When drilling starts, the Odex drill bit quickly cuts in front of the steel casing, allowing a number of "wings" on the drill bit to open. This bit can drill a hole with a diameter that is slightly larger than the steel casing. The pipes are pressed and rotated into the ground once at a time and follows the same procedure as mentioned above. When the desired depth is reached, the drill can be turned once in reverse. The wings are then folded back so that the drill can be pulled up inside the casing while the casing stays in place (Bruce, 1989). In addition, it is easy to take sediment samples as sediments are continuously flushed up by the pipe during drilling. For each meter, sediment samples were collected to make observations of color and grain size.

Figure 3.4. The drilling rig with odex crown showing the establishment of one of the observation wells.

3.1.2 Hydraulic conductivity by grain size distribution

Hydraulic conductivity is a measure of the ability of the deposit to pass through water (Colleuille and Kitterød, 1998) and is related to the grain-size distribution (sorting), the effective porosity, grain shape, and packing in sediments (Rogas *et al*., 2014). Groundwater can flow through many different materials with the properties of the medium to be affecting the nature and the speed of the flow. Thus, the hydraulic conductivity is an important parameter to investigate in connection with the establishment of groundwater wells.
Since the hydraulic conductivity is related to the particle size and is inversely related to standard deviations of the particle size, coarser and well sorted grains have higher hydraulic conductivity than finer and unsorted grains. In unconsolidated materials, the size of the grains is a key characteristic of the material, and the distribution of grain sizes determines how much pore space is available to hold water and how easily water is transmitted through the material (Fitts, 2013). To define the hydrogeological conditions of the sediments, grain size distribution analysis was performed for the 4 observation wells that were located in areas that

was most suitable for establishing a new supply well (Obs1, Obs2, Obs5 and Obs9). To evaluate the hydraulic properties, samples were taken with an interval of 1-2m depth during drilling. The hydraulic conductivity can be derived from a grain-size distribution of sediment samples using empirical relations between grain size and permeability (Rosas *et al*., 2013).

3.1.2.1 Hazen´s method

Using an empirical formula, the hydraulic conductivity can be estimated. The Hazen method involves using the cumulative grain size curve to extract the effective grain size diameter to derive an estimate of the hydraulic conductivity and can be used for sand with an effective grain size (d_{10}) between 0.1 and 3.0 mm (Colleuille and Kitterød, 1998):

$$K = C(d_{10})^2 \qquad \text{Eq.1}$$

where K is the hydraulic conductivity (cm/s), d_{10} is the effective grain size (cm) corresponding to the weight percentage of 10% and C is an empirical coefficient which is between 40-80 for poorly sorted fine sand, 80-120 for poorly sorted coarse sand and well sorted medium sand, and 120-150 for well sorted coarse sand. The requirement to use Hazen method is that $d_{60}/d_{10} \leq 5$ where d_{60} is the effective grain size (cm) corresponding to the weight percentage of 60%.

The hydraulic conductivity values depend on the geological material. Fetter (1994) estimated the hydraulic conductivity in unconsolidated sediments (Table 3.1).

Table 3.1. Representative values for unconsolidated sediments (Fetter, 1994).

	K in m/s
Clay	10^{-11} - 10^{-8}
Silt, sandy silt	10^{-8} - 10^{-6}
Silty sand, fine sand	10^{-7} - 10^{-5}
Well sorted sand	10^{-5} - 10^{-3}
Well sorted gravel	10^{-4} - 10^{-2}

3.1.2.2 Procedure

Each sample was placed in plastic bags from Eurofins marked with well name, depth, and date before being transported to the University of Oslo. Then, approximately 50g of each interval sample was poured into a marked plastic box and placed in a drier for minimum 24 hours at 80°C until the samples were completely dry. When the samples were dry, they were weighted and poured in a grain size distribution analyzer with 9 different sieve sizes (Table 3.2). To separate the material, each sample were shaken in the analyzer for 5 minutes before the sediment retained in each sieve was measured using a precision weight (Figure 3.5).

Table 3.2. Sieves and sizes.

Sieve	Size (mm)
1	8
2	4
3	2
4	1
5	0.5
6	0.25
7	0.125
8	0.063
9	<0.063

Figure 3.5. Left: All 9 sieved used to sort the sediments, right: some of the sieves used.

The retained sediment can then be plotted in a semilogarithmic plot with cumulative weight on the y-axis and the grain size on the x-axis. From here, the d_{60} and d_{10} can be read (Figure 3.6).

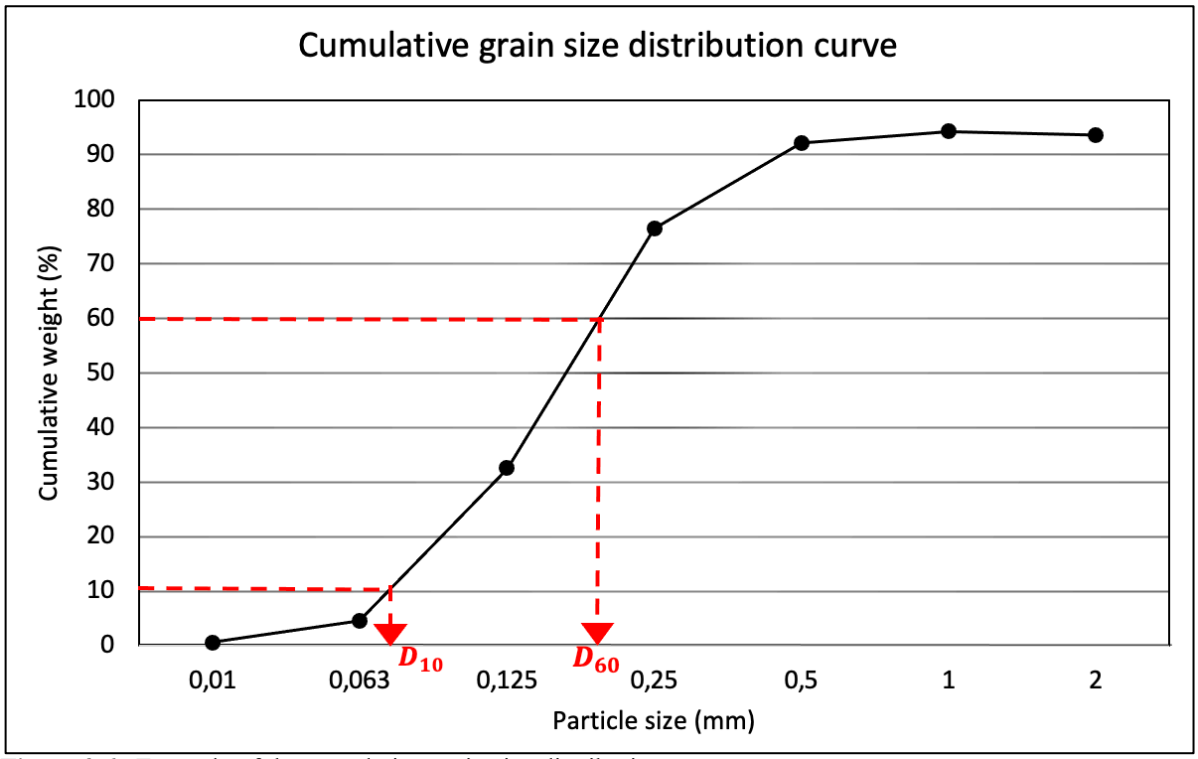

Figure 3.6. Example of the cumulative grain size distribution.

3.1.3 Near-surface geophysical methods

To find stratigraphic information about the bedrock depth and the groundwater level in the study area, GPR and ERT surveys were conducted by Geovista on behalf of Rambøll October 29th, 2021. A total 1,2km profiles (3 pcs of 400m long profiles) were measured (Figure 3.7). The GPR profiles were measured with a Topocon GRS-1 RTK-GPS. Profile 1 crosses metal fences along the first 30 to 80 meters which results in a strong object in the model and the model cannot be interpreted near these disturbances. Profile 2 runs from north to south, mainly along a ridge. The profile extends over a flat terrain where the first 80m are on cultivated land. Profile 3 runs from the river in the northwest, over the ridge where profile 2 is located, down into a depression and ends in in the southeastern direction.

The data from this survey was processed and visualized with the program ReflexW where the radar diagrams are filtered from noise and the signal is amplified to depth. The direct wave was moved to time "0". The radar diagram was visualized with a depth scale based on the

radar speed of 0.1 m/ns. Topographic correction is performed based on measurements and a digital elevation model. The ERT profiles were performed with a multi-electrode system and the instrument Terrameter LS2 (Guildline Geo).

The measurements were performed with a gradient configuration, which allows high sensitivity for both lateral and vertical structures. Cables with a minimum electrode distance of 5m have been used, which has resulted in a relatively high resolution of the upper 20 meters and a maximum examination depth of approx. 70 m in the middle of the profile. Data processing and modeling are done with the program Res2Dinv (Geotomo software). All modeling is done regarding the topography (measured coordinates).

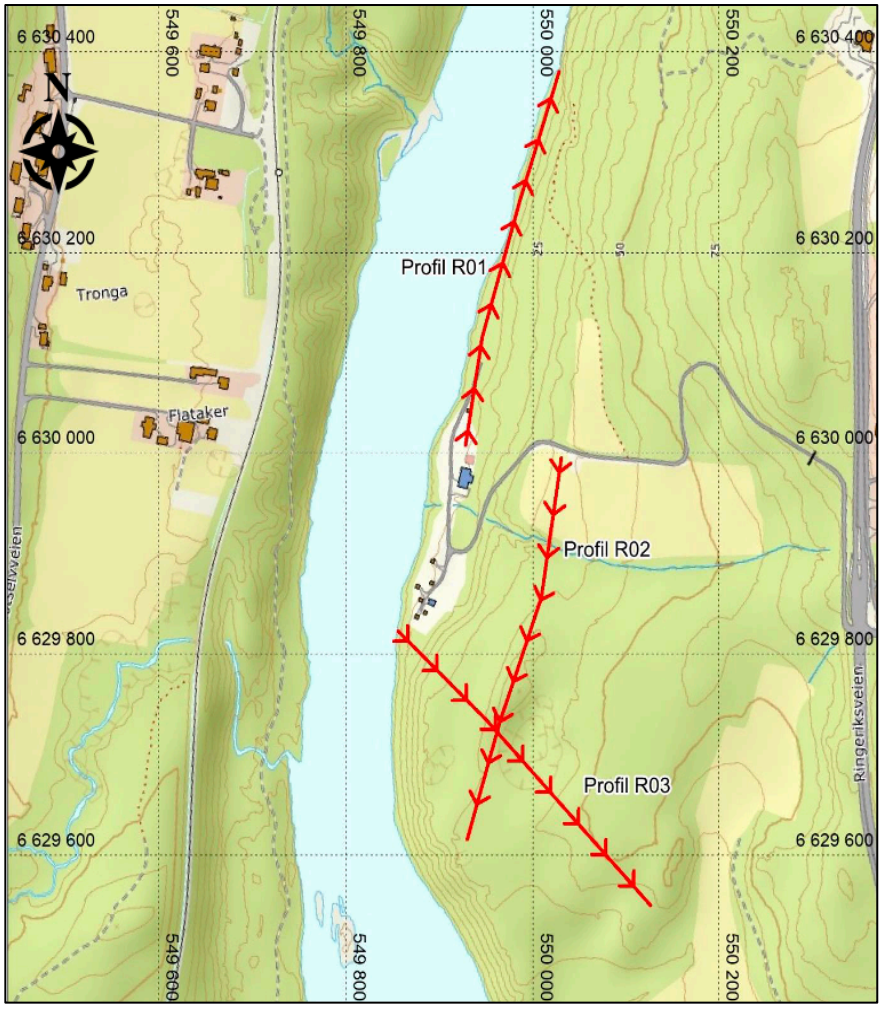

Figure 3.7. Location for geophysical methods (GPR and ERT).

GPR uses electromagnetic pulses in the frequency range 10 to 2000 MHz to visualize the ground down to a depth of a few decimeters to tens of meters depending on the nature of the ground and the selected antenna frequency. Different objects will reflect the electromagnetic waves back to a radargram with different velocities. The study area consists mostly of glacial

and glaciofluvial deposits (sand and gravel) that are transparent to radiowave signals.

The resistivity of a material is described as the ability of the material to conduct electrical current and is controlled by the porosity and water content of the soil, dissolved salts, and clay mineral. There is usually high resistivity in crystalline rocks, but low resistivity can occur because of crushing, zones with fracture, mineralization, or mineral transformation. A resistivity measurement is performed by sending current between two electrodes to measure the potential difference simultaneously between them. If the electrode distance is known, the apparent resistivity of the ground can be calculated. Using a data program, one can in a subsequent data processing generate one or more resistivity models by modeling the "true" resistivity. With knowledge of the electrical properties of different materials, a model can be created where it is possible to identify different soil layers, groundwater levels, rock levels and fracture zones and possible mineralization's. The resistivity survey was used to investigate the bedrock depth and distinguish interfaces in the subsurface.

3.2 Water balance

The basic concept of mass conservation is called the hydrological balance and is given by:

$$\text{Flux}_{\text{in}} - \text{Flux}_{\text{out}} = \text{rate of change in water stored within} \qquad \text{Eq.2}$$

The water balance of aquifers depends on the aquifer matrix, proximity to recharge area and groundwater recharge and discharge (Alsharhan and Rizk, 2020).
The water balance states that all water entering an area as precipitation will evaporate, form runoff or be stored (Fitts, 2002). Thus, the water balance defines the input and output of the groundwater system. The water balance is expressed as:

$$P = E + R \qquad \text{Eq.3}$$

Where P is precipitation, E is evapotranspiration and R is runoff.

3.3.1 Precipitation

The main part of the hydraulic cycle is precipitation which falls as rain, snow, sleet, hail, and fog on the surface (Dingman, 2015). Precipitation is measured by several gauges by each county in Norway, both by local and national meteorological agencies. For this thesis, precipitation data in 2020 was retrieved from senorge.no which is an open portal on the internet that shows daily updated maps of water conditions and climate for Norway.

3.3.2 Evapotranspiration

Evapotranspiration refers to the combined processes of direct evaporation at the ground surface, direct evaporation on plant surfaces, and transpiration (Fitts, 2013). Evapotranspiration is a collective term for all the processes by which water in the liquid or solid phase at or near the earth´s land surface become atmospheric water vapor (Dingman, 2015). There are daily and seasonal variations in evapotranspiration and the evapotranspiration is generally lower in winter than in summer in regions with strong seasonal climate variations because less water can evaporate into cool air than into warm air (Fitts, 2013). Temperature, air, wind, and vegetation cover are all factors that control evapotranspiration. In this thesis, evapotranspiration was retrieved using Tamm`s formula expressed as:

$$E = 221{,}5 + 29T \qquad \text{Eq.4}$$

Where E is evapotranspiration and T is temperature (°C). Tamm´s formula assumes that radiation is the governing factor for evapotranspiration (Tamm, 1959).

3.3.3 Recharge

Groundwater recharge is a hydrological process in which water moves to the groundwater from the surface. The water flows down into an aquifer and often occurs in the vadose zone below the plant roots. Materials with high permeability have pore spaces connected to one another allowing water to flow from one to another, unlike materials with lower permeability where the pore spaces are isolated (Reference). Groundwater recharge is often expressed as a flux to the water surface. Recharge takes place both naturally through the water cycle and through man-made processes, where rainwater and/or recycled water is led to the subsoil (Campling *et al*., 2008).

The primary source of recharge is infiltration of surface water derived from precipitation and the majority of groundwater recharge in Norway occurs during snow melting in spring. In this thesis, recharge is calculated from the water balance where the total amount of evapotranspiration is subtracted from the total amount of precipitation in the area:

$$R = P - E \qquad \text{Eq.5}$$

In this case, recharging takes place north and east of the well area where there is steeper topography. In addition, as the study area is dominated by sand and gravel with high porosity and permeability, most of the precipitation will infiltrate directly into the ground.

3.3 Porosity

The porosity indicates how large the pore volume is in a rock or soil type and is expressed as the percentage of pore volume in the total volume (Fitts, 2013). The total volume is given as the sum of pore volume and solids:

$$n = 100\ x\ \frac{V_v}{V_{tot}} \qquad \text{Eq.6}$$

where V_v is the volume of voids in a total volume of material V_{tot}. The porosity is a dimensionless parameter in the range of $0 < n < 1$ and depends on grain packing, grain distribution and grain shape (Bear, 2013). Porosity is often expressed as a percentage by multiplying Eq.7 by 100, and typical values for different materials are given in Table 3.3. In this thesis, the porosity was used to interpret the capture zone for each of the six supply wells. The porosity was set to 30% as a material with a mixture of sand and gravel usually has a porosity between 20-35% (Fetter, 1994).

Table 3.3. Total porosity of different materials (Fetter, 1994)

	Porosity
Well-sorted sand and gravel	25 – 50 %
Mixture of gravel and sand	20 – 35 %
Silt	35 – 50 %
Moraine	10 – 20 %

3.4 Groundwater table

To calibrate the numerical model against field observation, the groundwater was measured in all 9 observations wells during field work on 12.05.2022. For the measurement, a water level probe was used. Thereafter, the length of the casing was subtracted from the total length of the well to get the depth to the groundwater from the surface. The measurements were used for the calibration of the numerical groundwater model.

3.5 Numerical modeling of groundwater flow

3.5.1 Mathematical background

The standard equations that govern groundwater flow are derived using the principle of continuity and Darcy´s law. Darcy´s law is expressed in terms of hydraulic head and is derived:

$$Q = -KA\frac{dh}{dl} \qquad \text{Eq.7}$$

where Q is discharge velocity in units of volume pr unit time, K is the hydraulic conductivity, A is the flow cross-sectional area of the aquifer and dh/dl is the hydraulic gradient of the groundwater (Fetter, 2001).

By combing Darcy´s law with the water mass balance equation, the governing equation for flow can be derived:
For groundwater flow in 3-D, MODFLOW solves the governing equation:

$$\frac{\partial}{\partial x}\left(K_x \cdot \frac{\partial h}{\partial x}\right) + \frac{\partial}{\partial y}\left(K_y \cdot \frac{\partial h}{\partial y}\right) + \frac{\partial}{\partial z}\left(K_z \cdot \frac{\partial h}{\partial z}\right) - W = S_s \cdot \frac{\partial h}{\partial t} \qquad \text{Eq.8}$$

Where K_x, K_y and K_z is the values of hydraulic conductivity along the x, y and z coordinates, h is the potentiometric head (L), t is time and S_s is the specific storage of the porous material (L^{-1}). Thus, the groundwater flow is described in three dimensions, W is added or extracted flow to/from the groundwater system and the term on the right-hand describes time-dependent changes in storage (Fitts, 2013).

3.5.2 MODFLOW

MODFLOW (McDonald and Harbaugh, 1988) was developed by the U.S. Geological Survey for three-dimensional flow modelling (Fitts, 2013). MODFLOW can simulate aquifer systems where saturated flow conditions exist, Darcy's law applies, the density of groundwater is constant and where the principal directions of horizontal hydraulic conductivity or transmissivity do not vary within the system (USGS, 1997).

MODFLOW is originally developed by McDonald and Harbaugh in 1984 (Harbaugh *et al*., 2000) using the finite difference method. By dividing the modeled area into rectangular cells where the head is loose in the middle of each cuboid cell, one can, with the help of Darcy´s equations and equations of mass, this head can be related to surrounding cells which in turn have homogeneous properties (K_x, K_y, K_z, S). For groundwater flow in 3-D, MODFLOW solves Eq 11.

3.5.3 MODPATH

MODPATH (Pollock, 1989) was developed by the U.S. Geological Survey for three-dimensional flow modelling used to compute three-dimensional flow paths using output from steady-state or transient groundwater flow simulation by MODFLOW (Pollock, 2012). MODPATH uses groundwater velocity in every model cell from cell-by-cell output files generated from MODFLOW to compute paths of particles of water moving through the groundwater flow system (Palmer, 2013). In addition, MODPATH requires information about the MODFLOW head output and porosity of each layer that has a water table that can be run (Pollock, 1994). When using MODPATH in a steady-state model, one can add particle tracking to each well to find travel paths in forward or reverse directions (Reyne *et al*., 2013). Using particle tracking, one can find the groundwater residence time around each well and thus investigate vulnerability to pollution. In forward tracking, particles are placed in the model domain and are traced as they move downgradient toward a well while reverse tracking involves placing particles at a well and tracking them in the reverse (upgradient) flow direction to their sources (Reyne *et al*., 2013).

3.5.4 Modeling approach

The first step in the modeling process was to create an image of the study area based on information from previous studies and consists of boundary conditions, aquifer geometry and hydrological parameters. Boundary conditions are critical as they, among other things, determine flow directions and are determined from the hydrological conditions along the boundaries identified in the conceptual model (Anderson *et al*., 2015). The aquifer was assumed to be in steady state.

An initial regional model was built based on the collected information and from it, a local model was extracted. The local model was established as the regional model did not converge as the eastern part of the model got a very thin sediment layer due to steeply sloping terrain. Therefore, the local model was centered around the well area in the waterworks. The boundary along the cut-off were modeled as a no-flow boundary based on the regional model result. A sensitivity analysis was performed on the local uncalibrated model to investigate the sensitivity of hydrological parameters which was further used as limits in the calibration process. After the local model was calibrated by the trial-and-error method, different scenarios were tested (Figure 3.8).

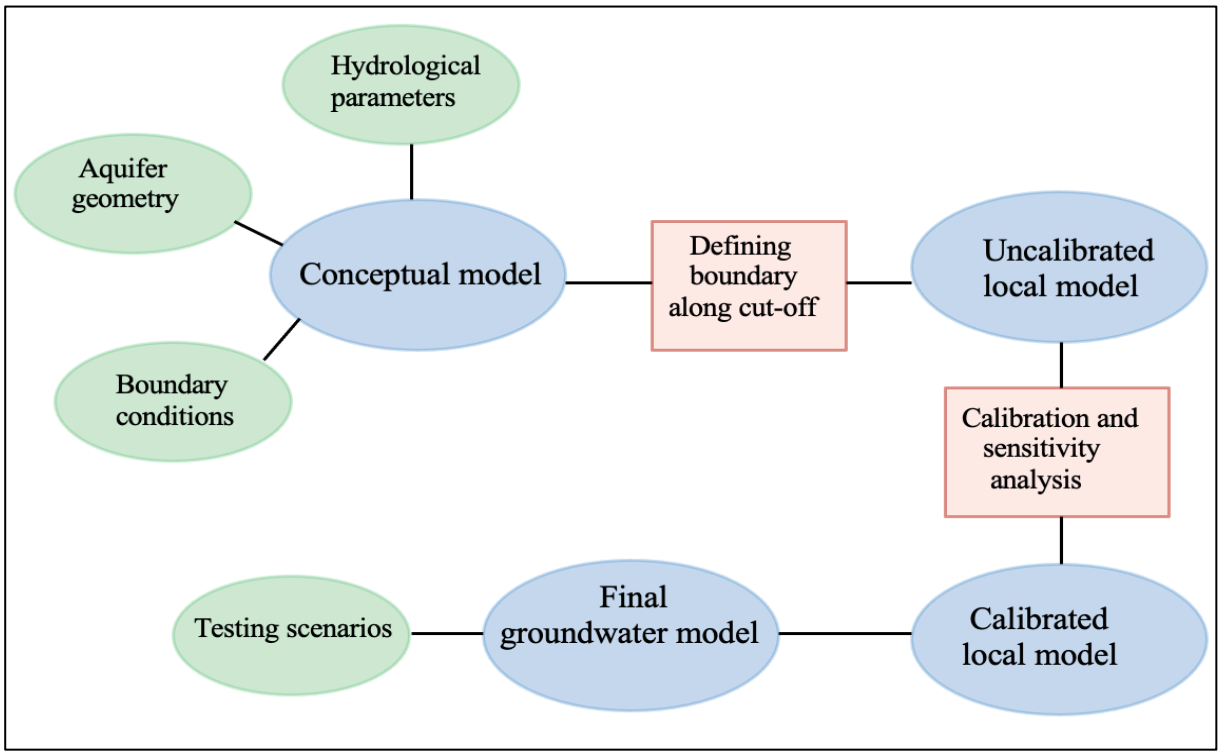

Figure 3.8. Flow chart of the modeling procedure.

3.5.5 Conceptual model

The accuracy of a numerical model depends on how closely the conceptual model is to the real aquifer system (Anderson *et al*., 2015). Building the conceptual model is time consuming and consists of several interpretations/assumptions about the natural system behavior like the model domain, boundary conditions and model stratigraphy. Simplifications are needed as it is not possible to construct the true reality.

A conceptual model was created based on geology, hydrology and meteorology (Figure 3.10). A sediment map was used to define the boundaries in the aquifer (Figure 2.2).

A topographical map was used to define the drainage network, surface water bodies and water related activities (Figure 2.3) (Alley *et al*., 1999). Meteorological and hydrological data of precipitation and evaporation were used to calculate how much water that enters the aquifer and to calculate the groundwater recharge. The small stream that crosses the study area horizontally in the middle is omitted, as it was observed as relatively dry during field and will thus have no effect on the result (Figure 3.9).

Figure 3.9. The dry stream in the middle of the study area.

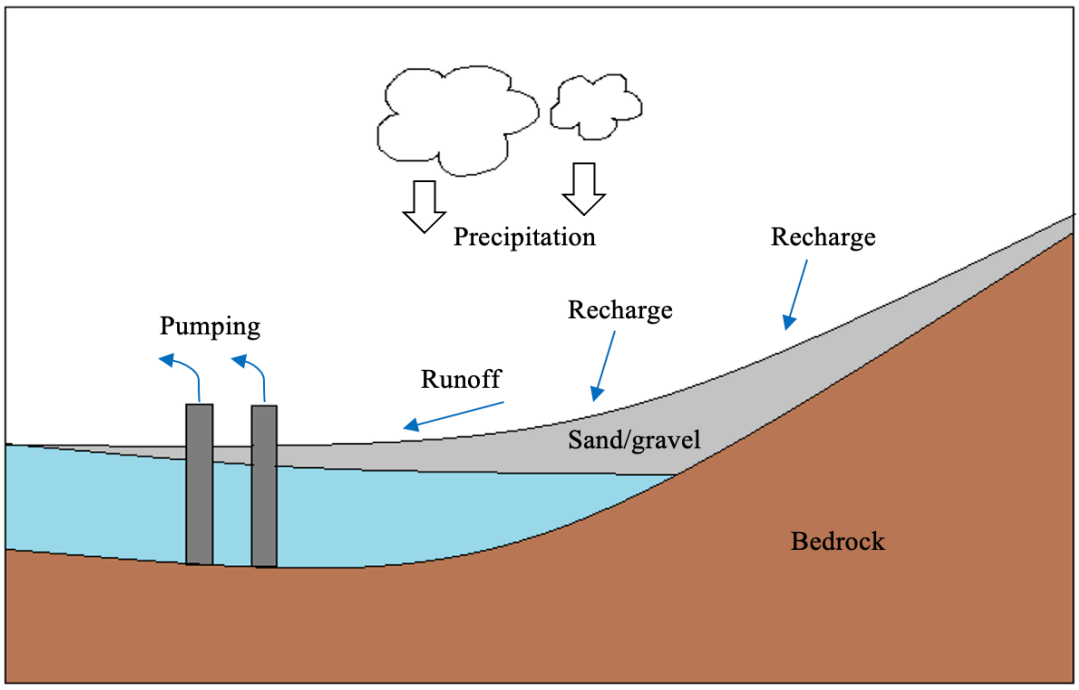

Figure 3.10. Schematical representation of the hydrological system at Strømbo.

3.5.6 Regional model

A 1-layer model consisting of a mixture of sand and gravel was first created. A geological map was used to construct the boundaries around the aquifer and to get an overview of the areas with visible bedrock. While a DTM image was used to simulate the surface elevation of the layer. The drilling logs of all observation wells were used to define the bottom of the layer. But there were problems converging the model as the layer got very thin in the eastern part of the model where the bedrock rises steeply. Therefore, an additional layer consisting of bedrock was added to the model. This layer was assigned a very low hydraulic conductivity value to keep it saturated and to ensure that the layer never dries. The regional model was given a cell size of 6x6 meters as the simulation converted faster and provided an improved grid compared to lager cell sizes.

3.5.6.1 Boundary conditions

Mathematically, boundary conditions are classified mathematically into three types: Specified head boundary (Dirichlet conditions), Specified flow boundary (Neumann conditions) and Head-dependent boundary (Cauchy conditions) (Anderson *et al*., 2015). Boundary conditions are not only mathematical constraint in groundwater flow problems but do also represents the sources and sinks within the system (Reilly and Harbaugh, 2004). The boundary conditions in the model are determined from the hydrological conditions along the boundaries identified in the conceptual model (Anderson *et al*., 2015). A total of 5 boundary conditions were assigned the model (Figure 3.11):

1. The Drammen river boundary was defined as a general head boundary. The hydraulic heads along the river were generated from a DTM image imported from høydedata.no to retrieve a gradient in the river. The head stage in the northern limit was assigned 7.5 masl and the head stage in the southern limit was assigned 7.3 masl. The GHB package is used to simulate the exchange of water between the aquifer and river. The reason for modelling the river with the GHB package is that GHB is useful when simulating distant boundaries outside the model domain. A conductance of 1 m^2/d was assigned to the boundary and relates the head difference to the flow rate, Since the river is at a higher elevation than the groundwater, this boundary condition will cause water to flow from the river and into the aquifer where the flow rate is proportional to the head difference.

2. The northern and southern borders of the model was assigned as no-flow boundaries to represent the margin between the aquifer and the regions consisting of bedrock. According to Anderson and Woessner (1992) will a contrast in hydraulic conductivity of a factor of 100 between two materials may serve as a no-flow boundary. Thus, it is assumed that there is no flow coming from these areas as glaciofluvial and glacial deposits meet bedrock.

3. The eastern side of the study area was assigned as a specified flow setting the flow at the boundary as a function of position and time (Andersson *et al*., 2015). The flow was calculated by multiplying the catchment area of the small stream with yearly precipitation and subtract the evapotranspiration. The calculated flow assigned to the model was 30 m^3/d.

4. Groundwater extraction from each well was assigned with the Well-packages and given different flowrates using field data.

5. Recharge in the form of precipitation was assigned as a specific flow boundary. The calculated recharge was assigned constant in the entire model as 0.0016 m/d.

While the additional layer consisting of bedrock was assigned a specified flow to the entire polygon to make it saturated with water.

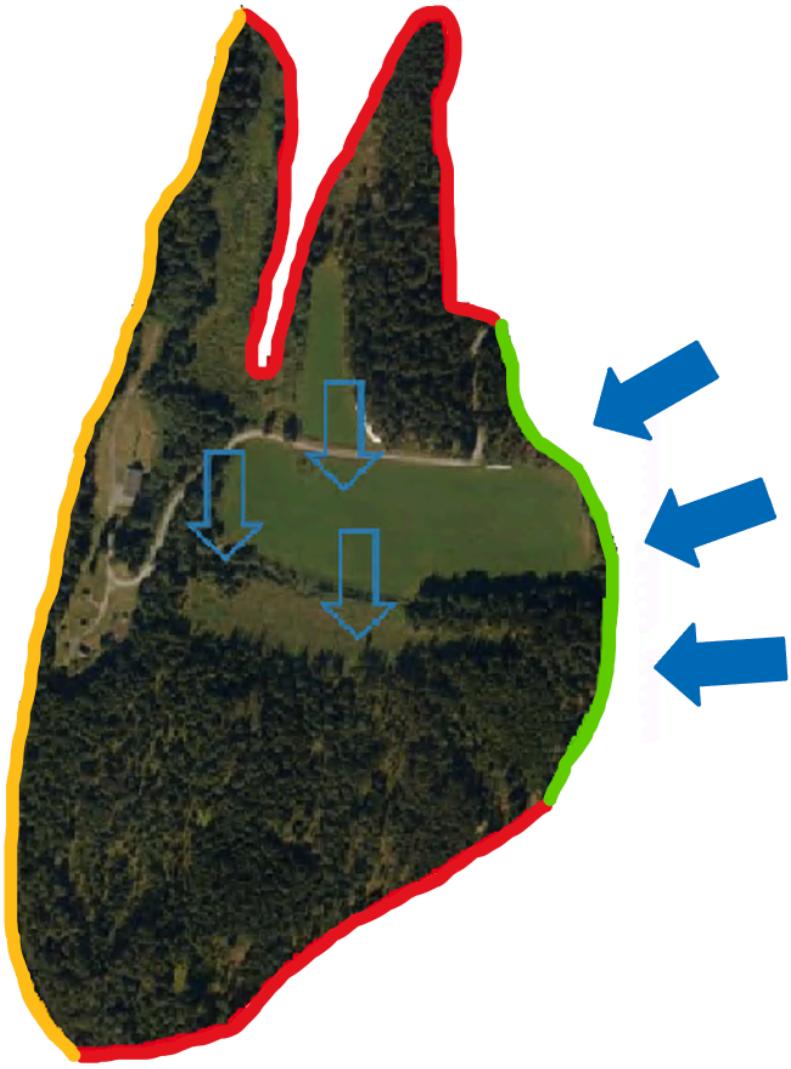

Figure 3.11. Conceptual model of the study area showing the different boundary conditions applied to the model; yellow color represents general head (Drammen river), red color represents no-flow boundaries, green color represents specified flow (eastern boundary), light blue arrows represent recharge, and the dark blue arrows represent flow from eastern border.

3.6.6.2 Recharge

By subtracting the yearly evapotranspiration from the yearly precipitation in the area, the recharge was assigned constant to the whole model surface. The reason why only one recharge value was chosen for the whole site it because it is very small. It is also important to remember that recharge does not mean the amount of precipitation that falls on the study area, but how much of the precipitation that goes down into the groundwater.

3.6.6.3 Model geometry

A simple cross-section of the model area was made to illustrate the geology in the study area (Figure 3.12). The top elevation of layer 1 consisting of sand and gravel corresponds to the topography in the study area and was determined from a digital terrain map (DTM) retrieved from høydedata.no. Data of the bottom of layer 1 were collected during drilling of the 9 observation wells and interpolated to the model. However, since all these wells were drilled in a limited area close to each other in the western part of the model close to Drammen river as well as some up the terrain in the middle part of the model, the rest of the model area lacked information about the bedrock elevation. Therefore, it was necessary to gather more information from other sources. The GPR and ERT surveys were carried out for this purpose, but as the results showed that the bedrock fluctuated between larger elevation differences, it was difficult to use them in the model. Thus, the sediment map (Figure 2.2) shows several areas where there is visible bedrock in the surface both in the northern and southeastern area of the model as well as an area in the middle of the model. This map was used in conjunction with høydedata.no to extract coordinates and associated elevations for several inferred points around the model where it was visible bedrock to prevent interpolation artifacts in these areas. Kriging was the chosen interpolation method as it gave the most realistic bottom geometry after comparing with the other interpolation methods available. Thus, kriging is an appropriate interpolation method for geological topics (Davis and Sampson, 1986).

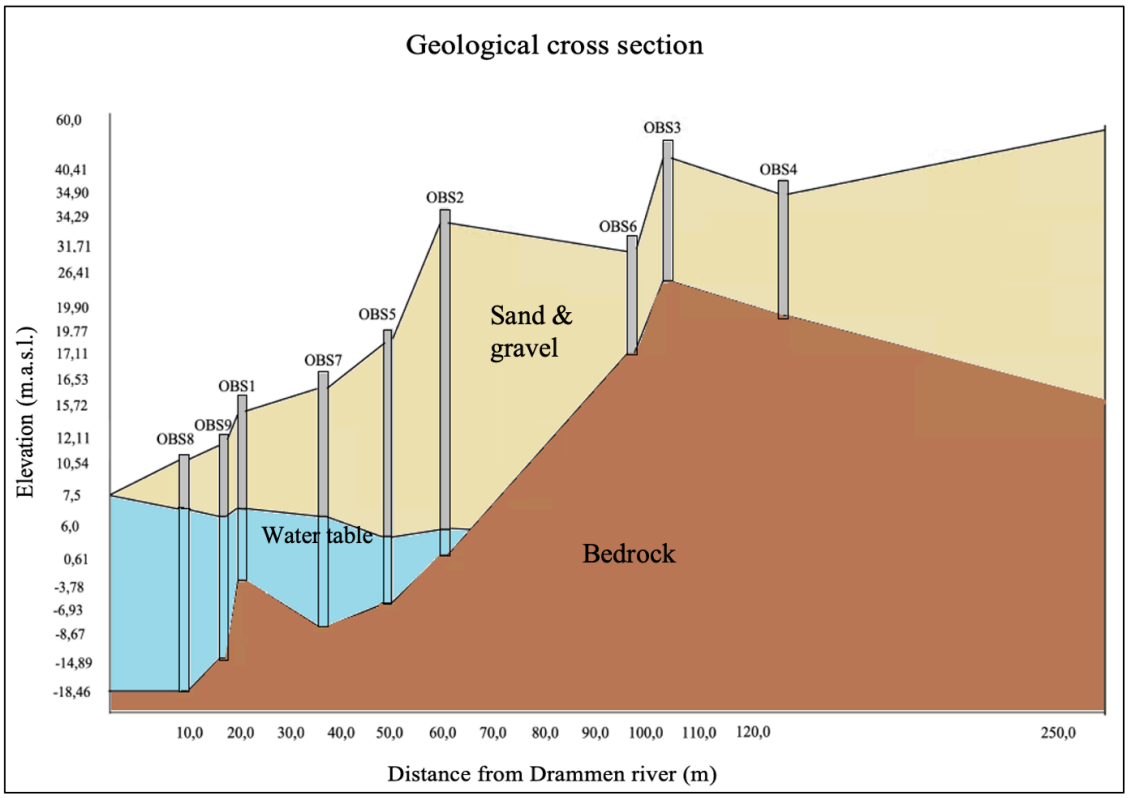

Figure 3.12. Cross-section of the bedrock elevation at Strømbo.

3.4.6.4 Hydraulic conductivity

The model was assigned two hydraulic conductivity zones in layer 1 based on the results of the grain size distribution analysis for 4 of the observation wells (Figure 3.13). The small river that crosses the model in the middle was used as a division between the zones where the northern zone were assigned an average hydraulic conductivity value based on the results from the drilling of Obs9, and the southern zone was assigned an average hydraulic conductivity value based on the results from the drilling of Obs1, Obs2 and Obs5. The northern zone was assigned a hydraulic conductivity of 320 m/d and the southern zone was assigned a hydraulic conductivity of 160 m/d. While layer 2 which consist of metamorphic bedrock were assigned a very low hydraulic conductivity of $1x10^{-9}$ m/d. The idea was to avoid dry cells in the eastern part of the model were layer 1 is very thin by keeping layer 2 saturated with water.

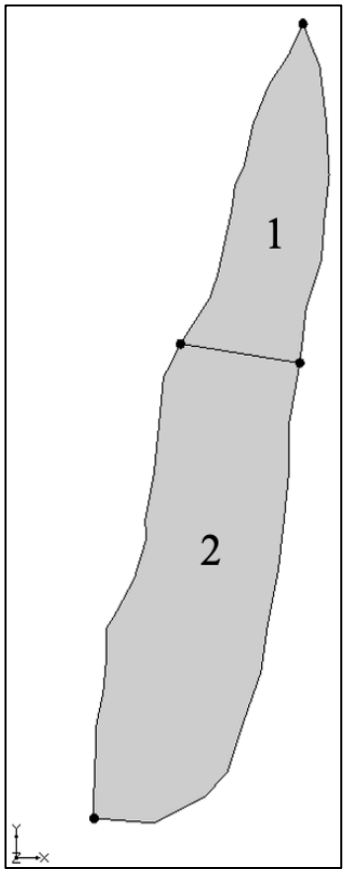

Figure 3.13. The hydraulic conductivity zones for layer 1for the local model.

3.5.7 Local model

A local model was extracted from the regional model as there were problems converging the model due to the steep slope that caused layer 1 to be very thin in the eastern part of the study area. The regional model was also assigned an additional layer to help the model converge, but the results were not satisfying as the model result was incorrect. The local groundwater model is located in the western part of the regional model along Drammen river (Figure 3.14). The extent of the model was based on the regional model output. The cell size of the local model was set as 5x5 meters. Since the 3 observation wells in the eastern area up the terrain was dry, it was decided to cut the model there.

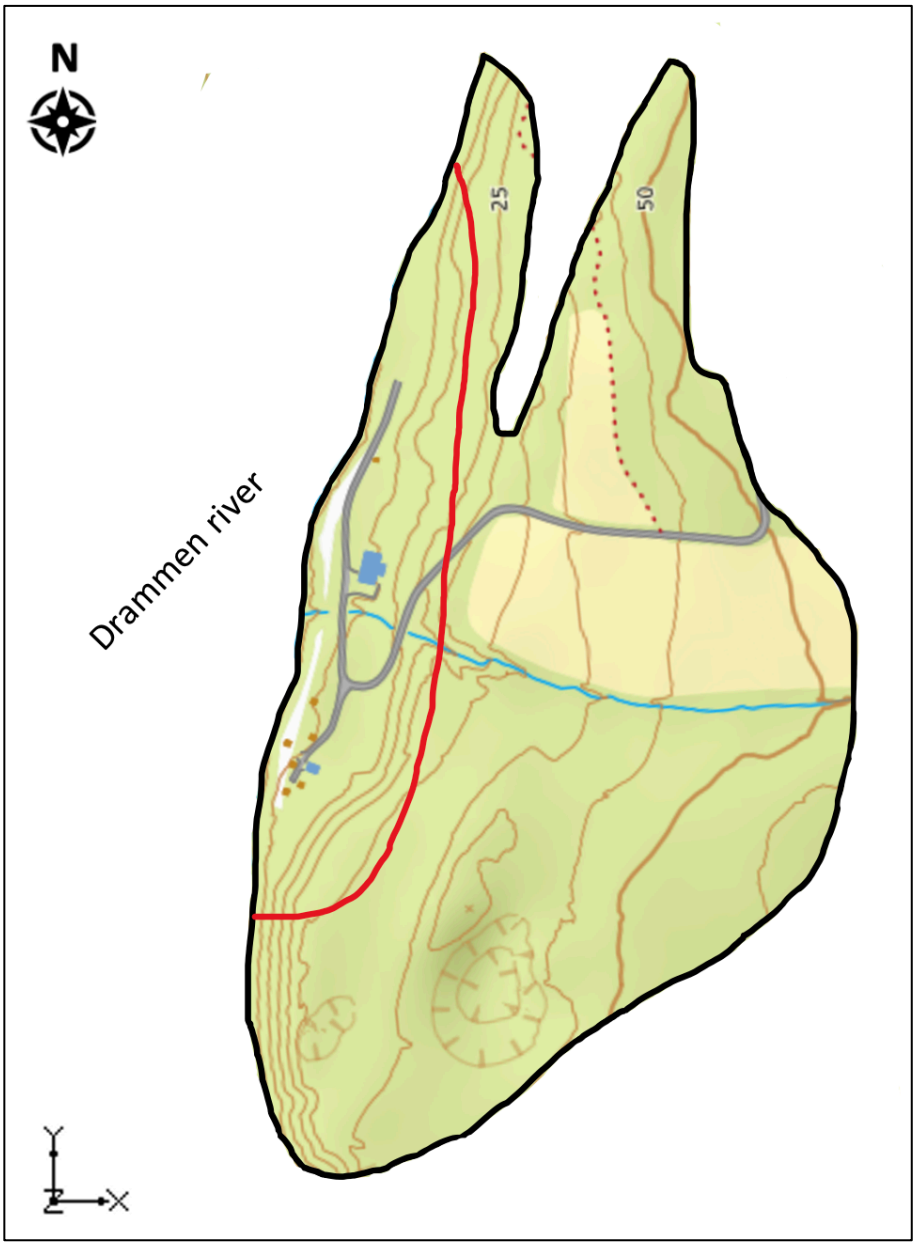

Figure 3.14. Regional model delineated with black line and the red line shows the local model cut.

3.6.7.1 Boundary conditions

The boundary conditions for the local model were chosen based on the regional model results.

1. The Drammen river boundary was still defined as a general head boundary. The hydraulic heads along the river were generated from the same DTM image imported from høydedata.no. The head stage in the northern limit was assigned 7.4 masl and the head stage in the southern limit was assigned 7.3 masl.
2. The rest of the boundary was defined as no flow boundary based on the results of the regional model assuming that no water flows from this boundary to the model area. This boundary condition was chosen because there is possibly a hilltop to the east of this boundary that extends from the area with visible bedrock in the north to the area with visible bedrock in the south, which creates a physical barrier where water cannot penetrate.

3.6.7.2 Recharge

The local model was assigned a recharge value of 0.0016 m/d by using precipitation data from year 2020 so it corresponds to pumping data from the same year.

3.6.7.3 Hydraulic conductivity

The hydraulic conductivity was assigned in 2 different zones in the local model. As for the regional model, the river that crosses the model was used as a division between the zones (Figure 3.13). Zone 1 includes the northern supply well and the grain size distribution analysis of Obs9 which was assigned an average hydraulic conductivity value of 320 m/d. Zone 2 includes all other supply wells and grain size distribution analysis of Obs1, Obs2 and Obs5 which was assigned an average hydraulic conductivity value of 160 m/d.

3.6.7.4 Supply wells

Production data from the six supply wells were extracted from the Gurusoft operational reporting system for the years 2010-2020 (Appendix 1). The average pumping rate in 2020 was assigned to each well in the local model.

3.6.7.5 Model geometry

The model geometry after the cut was performed gave a top elevation of approximately 34.5 m.a.s.l. in the south-eastern part of the model boundary. The top elevation corresponds to the topography in the area and the bottom elevation was based on the same geological map

information as the regional model, as well as results from boreholes and geophysical surveys. The local model was designed with only one layer consisting of sand and gravel as there were no problems converging the model as the steep slope were cut. Thus, it was no longer necessary to have an additional layer saturated with water to help the model converging. The local model area consists of a flat surface and based on the results from the boreholes, the bedrock does not have large elevation differences.

3.5.8 Sensitivity analysis

A sensitivity test was performed on the local uncalibrated model to analyze the parameters in the groundwater model that are most sensitive during the calibration, as well as how changes would affect the model´s average RMSE error and groundwater level. The sensitivity analysis involves changing a single parameter while holding the other parameters constant. If a parameter is sensitive in the model, additional data about the parameter will help to improve the calibration (Tesfaye, 2009). The sensitivity was first tested for hydraulic conductivity and recharge. The model is sensitive to the variable tested if there is a larger change in groundwater level, while the model is insensitive to the variable tested if there is small change in groundwater level. Then, a sensitivity test were performed to analyze how the well capture zones changes when porosity increases and decreases.

3.5.9 Calibration

The manual (trial and error) calibration process started by first adjusting the recharge value as the initial simulated results showed to high groundwater heads. Then, the hydraulic conductivity was adjusted in each of the two zones to get a good agreement between observed and computed head values. The recharge value assigned to the model after calibration was 0.02 m/d, while the hydraulic conductivity values assigned was 80m/d in the southern part and 300 m/d in the northern part of the model. This agrees with the grain distribution analyses which show that Obs 8 established in the northern part of the model has higher conductivity than Obs 1, Obs2 and Obs 5 established in the southern part of the model. The calibration targets were 6 of the drilled observation wells, where 3 were neglected as they were dry during measurement. In addition, 3 old observation wells found during field work was also used in the calibration process. The measurements of hydraulic head in all observation wells were carried out during fieldwork 12.05.2022 (Table 3.4). The summary statistics RMSE

(Eq.9) was used to interpret the result where an acceptable error of 0.165m or less was allowed as suggested by Anderson *et al*. (2015).

$$RMSE = \left[\frac{1}{n}\sum_{i=1}^{n}(h_o - h_c)_i^n\right]^{0.5} \quad \text{Eq.9}$$

Where n is the number of targets, h_o is observed head (m) and h_c is computed head (m).

Table 3.4. Observed hydraulic head of observation wells.

Observation wells	Observed hydraulic head (m.a.s.l)
Obs1	6.27
Obs2	5.95
Obs5	5.84
Obs7	6.12
Obs8	6.64
Obs9	6.06
G2	6.79
G3	3.61
G4	6.0

3.6.10 Modeling different scenarios

After the calibration and sensitivity analysis, the model was used to test different scenarios based on increasing the capacity in the waterworks. The model was used to explore the aquifer-river interaction by changing the pumping rates and recharge rate. MODPATH with particle tracking was used to find the wells capture zones and to investigate which wells draw water from the river. In addition, the wells pumping funnels were investigated to explore which areas in the waterworks are most suitable for the establishment of a new supply well.

3.6.10.1 River leakage by change in pumping rates

Increasing the pumping rate in each well from their average pumping rate in 2020 with 10%, 20% and 30% were investigated to explore how much the river leaks into the groundwater when the pumping rate is adjusted (Table 3.5). Since the municipality needs to increase the capacity in the waterworks, it is expected that the supply wells need to pump more water in the years to come.

Table 3.5. Average pumping rate (m^3/d) for each well in 2020 and the pumping rate when increasing with 10, 20 and 30%.

Wells	Average in 2020 (m^3/d)	Increase 10%	Increase 20%	Increase 30%
SBM	379.9	417.80	455.88	493.87
SBS1	23.9	26.29	28.68	31.07
SBS3	397.7	437.47	477.24	517.01
SBS4	147.9	162.69	177.48	192.27
SBS5	25.7	28.27	30.84	33.41
SUB	273.4	300.74	328.08	355.42

3.6.10.2 River leakage by change in surface recharge

The original surface recharge was increased and decreased with 50% while the supply wells were set to pump their average pumping rate in 2020. Surface recharge varies throughout the year and it was investigated how the aquifer reacts in different seasons with more and less recharge.

3.6.10.3 Well capture zones

To investigate the most suitable location of a new supply well without it being affected by the already existing supply wells in the area, the well capture zones and the groundwater flow paths were investigated using MODPATH. The importance of defining capture zones is based on expected residence times and flow in the supply well to ensure good groundwater quality. The groundwater flow paths were investigated using backward particle tracking. A residence time of 60 days is the minimum limit the groundwater needs to use from the river to the supply wells to ensure that bacteria from the river die before reaching the wells. The average amount of water pumped out of each supply well in 2020 was used to calculate the capture zones.

3.6 Chemical properties of water

The results from a previous study of the iron and manganese concentration in each of the six supply wells carried out by Rambøll on July 10th, 2019, were examined and compared with literature studies. It was investigated whether there is any connection between the location of the well in relation to the river and the concentration of iron and manganese. In addition, a previous study conducted by Rambøll of the iron and manganese concentrations in the entire waterworks in 2020 was compared with annual monthly precipitation data looking for correlation. It was investigated whether periods with more precipitation would increase the groundwater's oxygen content and lead the aquifer to a partially oxidized state where iron and manganese are present in the groundwater as oxides and whether periods with less precipitation makes it more difficult for iron and manganese to dissolve since the groundwater will contain less oxygen.

Chapter 4

Results

4.1 Water balance

4.1.1 Precipitation

The study area has a humid continental climate where the annual average precipitation in 2020 was 1046mm with monthly variations (Figure 4.1). This year, the study area had less precipitation from January until the summer where it increased. In August the precipitation was at its lowest before it increased considerably in the autumn and early winter, except for November. December was the month with most precipitation (Appendix 2).

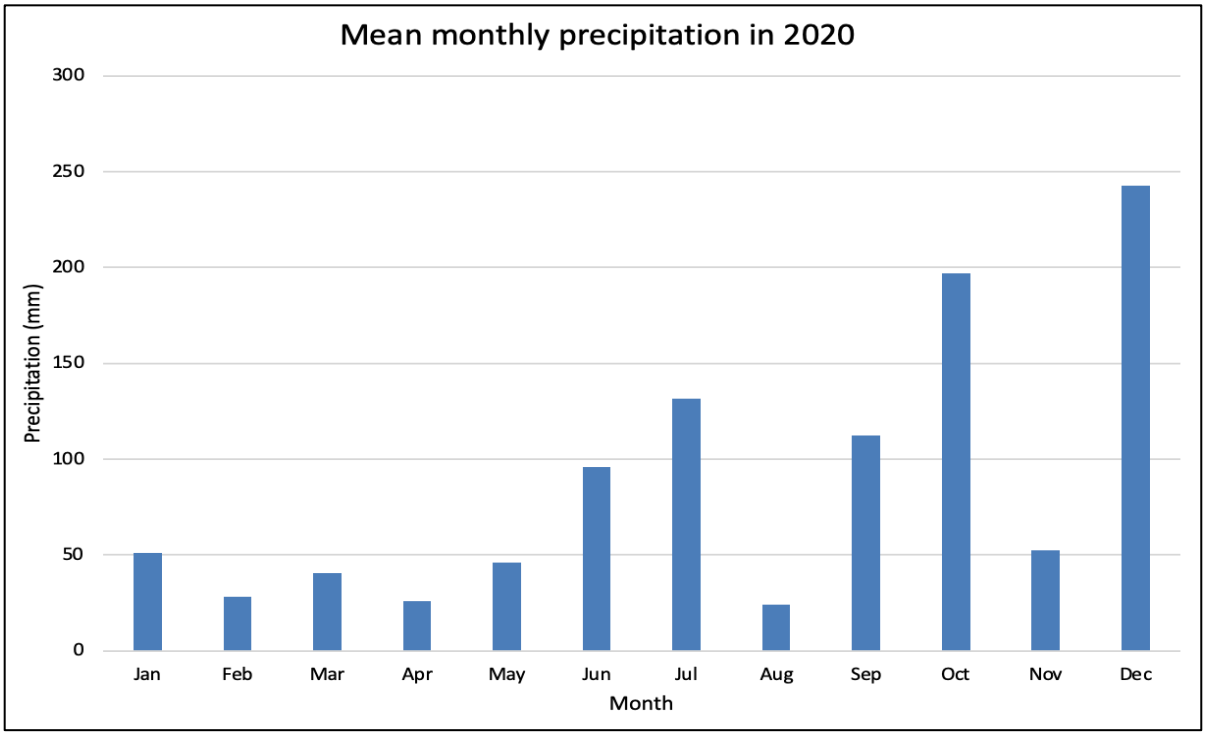

Figure 4.1. The mean monthly precipitation (mm) in the study area in 2020.

4.1.2 Temperature

The study area has a humid continental climate where summer temperatures rarely exceed 22°C. The humid continental climate leads to changing weather conditions with long and mild summers as well as cold temperatures in the winter months. The annual average temperature

in 2020 was 8.6 ºC (Figure 4.2). The low temperatures in the winter months are caused by a dominant westerly wind that brings high pressure from the Norwegian sea.

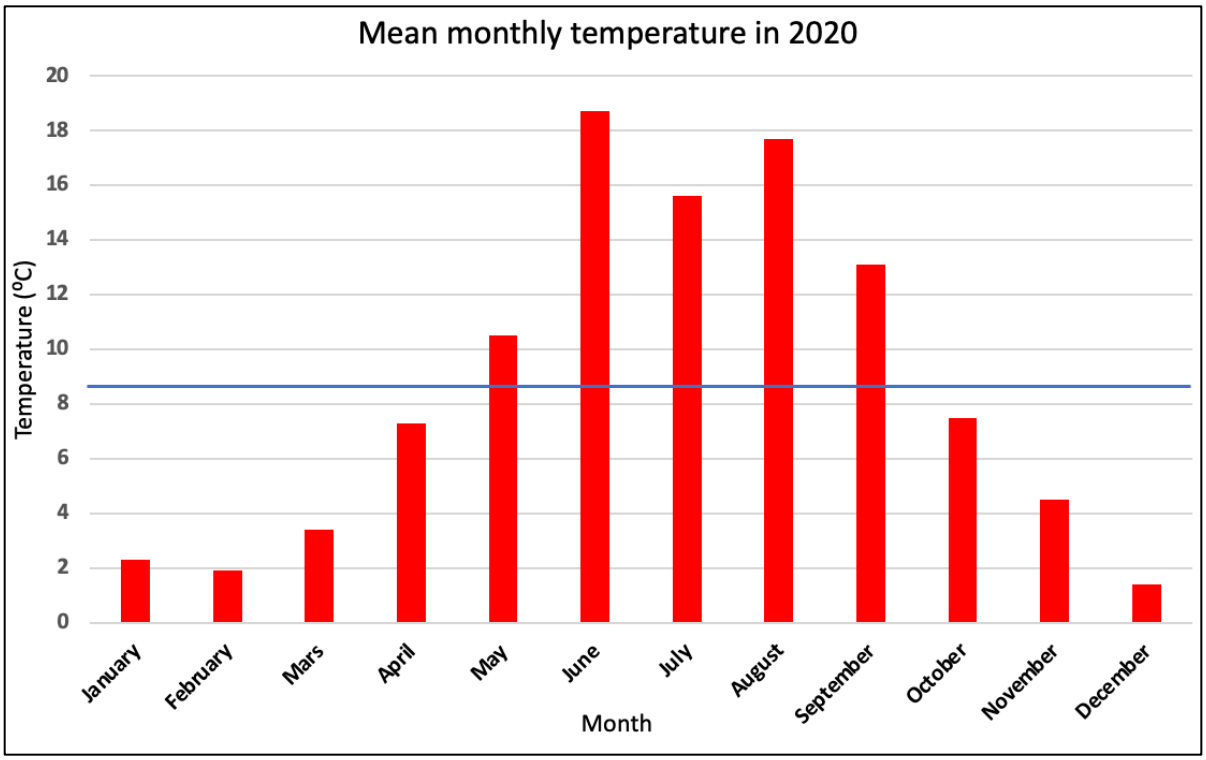

Figure 4.2. Mean monthly temperature (ºC) in the study area in 2020. The blue line represents the average temperature true the year.

4.1.3 Evapotranspiration

The evapotranspiration was calculated to be 453 mm/year taking into consideration that this is a yearly estimation and that there will be daily and seasonal variations. Thus, about 43% of the precipitation will evaporate before reaching the groundwater.

4.1.4 Recharge

The recharge value for the study area was calculated to be 593mm/year. In the study area, most of the surface recharge occurs in October and December as these are the months with most precipitation (Figure 4.3).

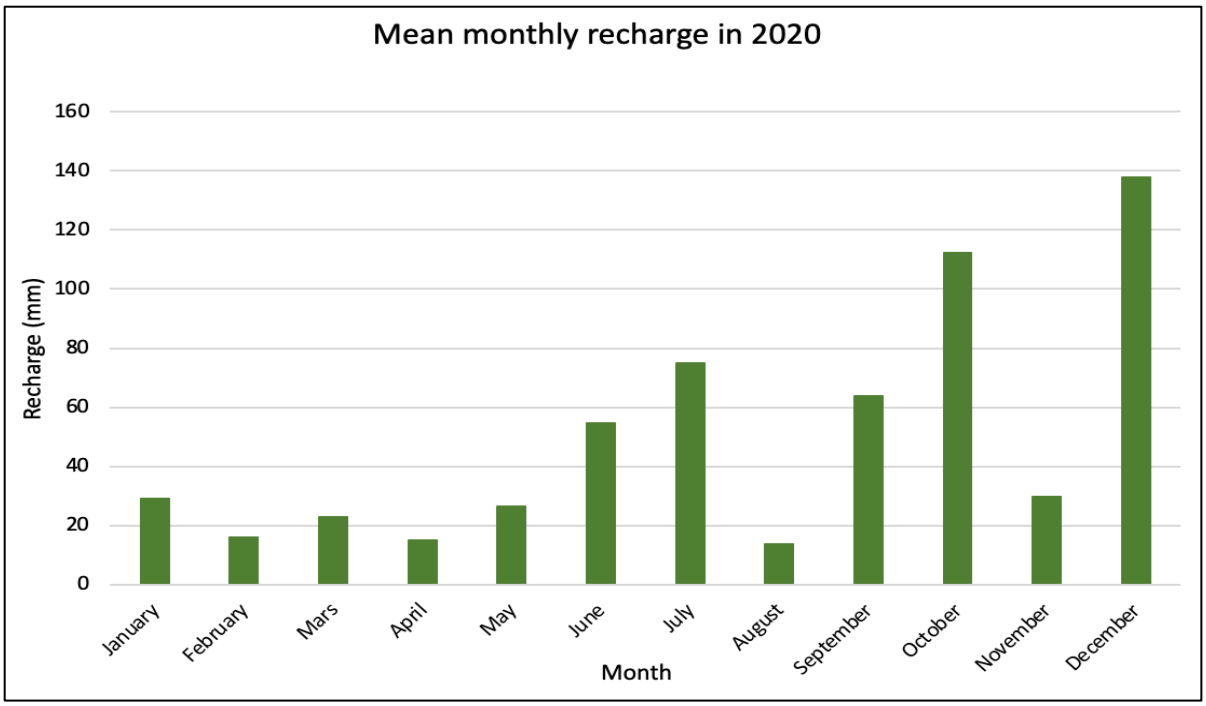

Figure 4.3. Mean monthly recharge in the study area in 2020.

4.2 Groundwater table

The hydraulic head was obtained from the measurement in the observation wells in spring 2022 (Figure 4.4). The groundwater moves from the norther wells to south as well as from the river to the eastern direction in the lower part of the study area. Observation wells G2, G3 and G4 are old wells that may have affected the groundwater as the wells have no lid or can be clogged. Observation well G3 is located right next to one of the supply wells which was pumping during measurement which led to a lower hydraulic head during the measurement.

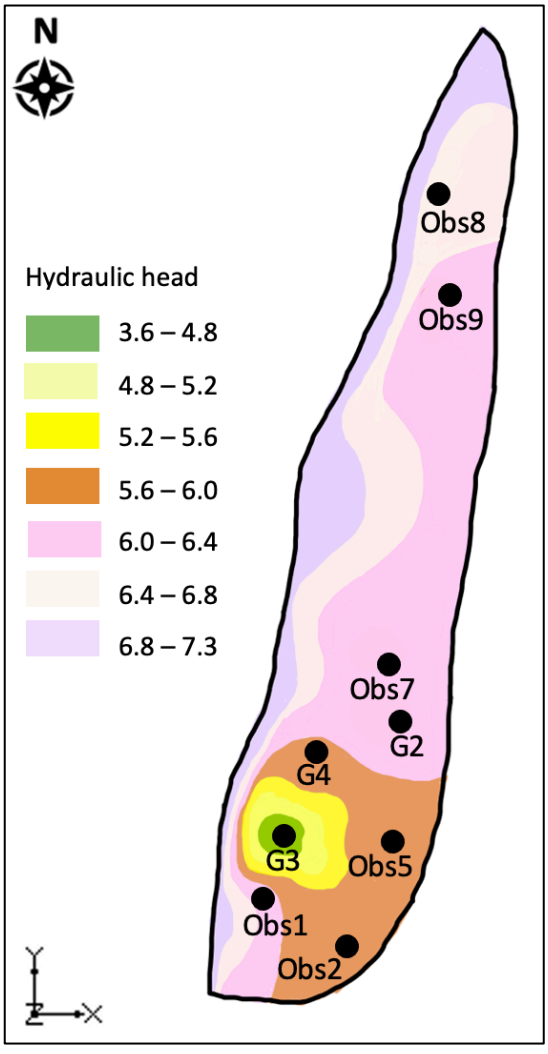

Figure 4.4. Hydraulic head measurements.

4.3 Aquifer geometry

The results from the geophysical investigations combined with data from the drilling logs of the 9 observation wells led to the description of the aquifer geometry which was further implemented to the groundwater model.

4.3.1 Ground Penetrating Radar and Electrical Resistivity Tomography

The results from the GPR data show good depth penetration and low noise level. The depth to the bedrock is interpreted to be between -8 to 8 m.a.s.l and is located in the area between the dashed black lines (Figure 4.5). According to the legend there is low resistivity in the first 50 to 100m of the section and shows the groundwater depth which is interpreted to be between 8 and -15 m.a.s.l. There are higher resistivity in the upper 5-10m of the section and below 10m depth the legend gives indications of a more irregular reflectivity.

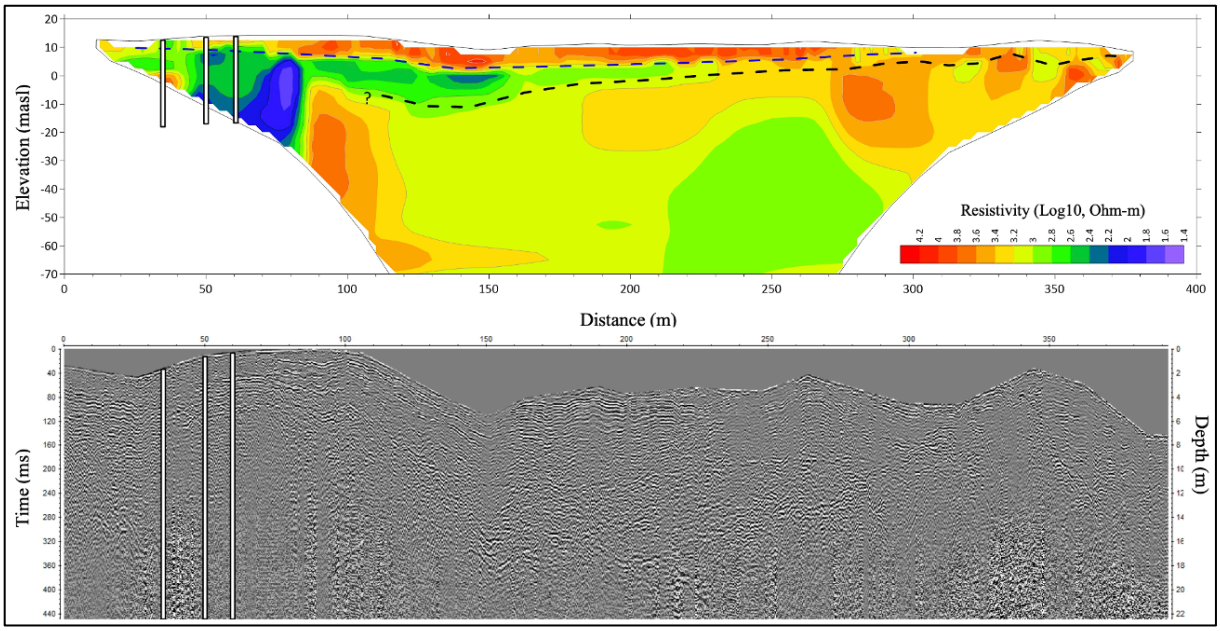

Figure 4.5. Profile 1. The upper section shows ERT model, and the lower section shows GPR data. Note that the radar profile indicates depth (m) while the resistivity section indicates height (m.a.s.l.). Low resistivity is interpreted as groundwater (blue color).

For Profile 2, the resistivity model indicates low resistivities closest to the ground surface in the north, which indicates that there is clay. The resistivity model also indicates an upper drained layer that is about 5m thick. The depth to the bedrock is around 15 to 30 meters below surface located in the area between the dashed black lines (Figure 4.6). Like profile 1, this profile does not give any clear information about the water table elevation.

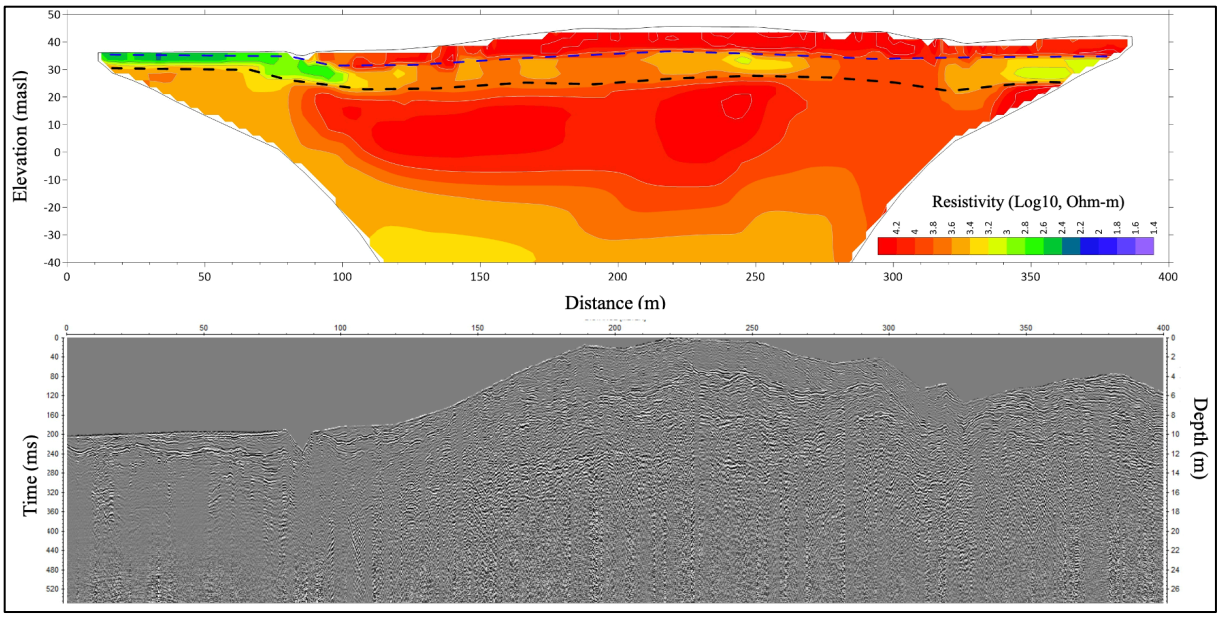

Figure 4.6. Profile 2. The upper section shows ERT model, and the lower section shows GPR data. Note that the radar profile indicates depth (m) while the resistivity section indicates height (m.a.s.l.).

At the first 30-80 m in profile 3, a probable artifact occurs in the resistivity model (Figure 4.7). Along the sections 100-250 m and 300-400 m, the model shows an upper, drained "dry crust" that is 5-10 m thick. The bedrock surface is interpreted to be at level 15-30 m.a.s.l and shows high resistivities, in the range 6.000 – 15.000 Ohm-m, which corresponds to fractured crystalline bedrock. The groundwater surface follows the topography. Along the first 150m of the profile, the GPR data indicate a large number of flat layers that probably consist of different sedimentary layers to a depth of 10-15 m below the ground surface. Along large parts of the stretch from 100-350 m there are a large number of hyperbolas which are caused by point-shaped objects. Thus, in this geological environment it is reasonable to assume that the hyperbolas can be linked to larger rocks. Along the last 50 m of the profile, the signal goes out under a superficial, flat reflector. Disturbances from fencing occur in the resistivity models along shorter parts of profile 3. Near these disturbances, the models cannot be interpreted. For profile 3, the signal quality is significantly worse. It is probable that poorer dip penetration of profile 3 can be linked to geological conditions, e.g. a rich occurrence of boulders, indicated by a large number of hyperbolas as along profile 3, which leads to the spread of the signal.

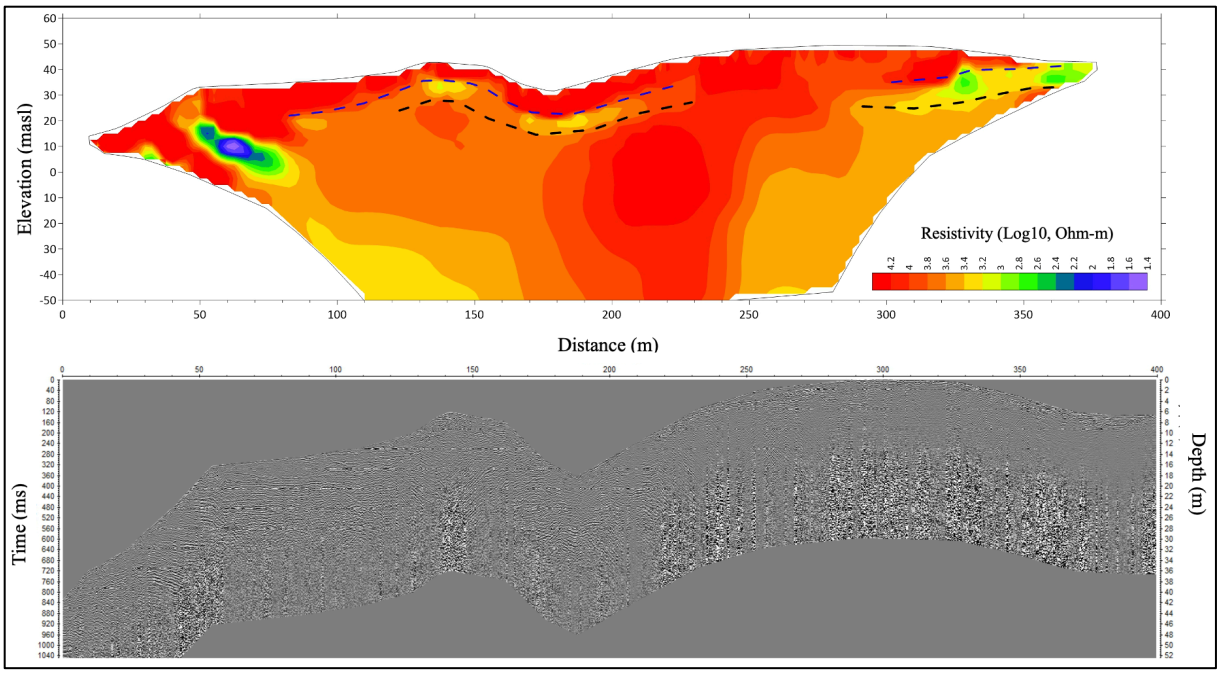

Figure 4.7. Profile 3. The upper section shows ERT model, and the lower section shows GPR data. Note that the radar profile indicates depth (m) while the resistivity section indicates height (m.a.s.l.). Low resistivity is interpreted as groundwater (blue color).

The results from the GPR and ERT surveys show that the unconsolidated sediments have a thickness of 10-20m and the rock surface north of the waterworks is within the level range -8 to 8 m.a.s.l. While south and east of the waterworks, the rock surface is located at 15-30 m.a.s.l., the water table is interpreted according to the topography and lies at 0-2m depth below the topographic surface near Drammen river and at 1-10m depth below the surface east and south of the waterworks. Furthermore, the GPR data indicate clear sedimentary layer divisions that are 5-10m thick in the area around the waterworks.

4.4 Aquifer properties of Hydrogeological parameters

4.4.1 Grain size distribution analysis

The results from the grain size distribution analyses show that the drilled observation wells mostly consist of a mixture of sand and gravel (Figure 4.8; Figure 4.9; Figure 4.10; Figure 4.11). The grain size distribution analysis for the southernmost well Obs1 located close to Drammen river shows alternating sediments of sand and gravel (Figure 4.8). The samples were collected with 2m intervals down to 20m below surface where it reached bedrock. The upper 2m closest to the surface contains poorly sorted sand before a 4m thick layer consisting

of poorly sorted gravel. From 8 to 16m below surface there is again poorly sorted sand while the 4m closest to the bedrock basement consists of poorly sorted gravel.

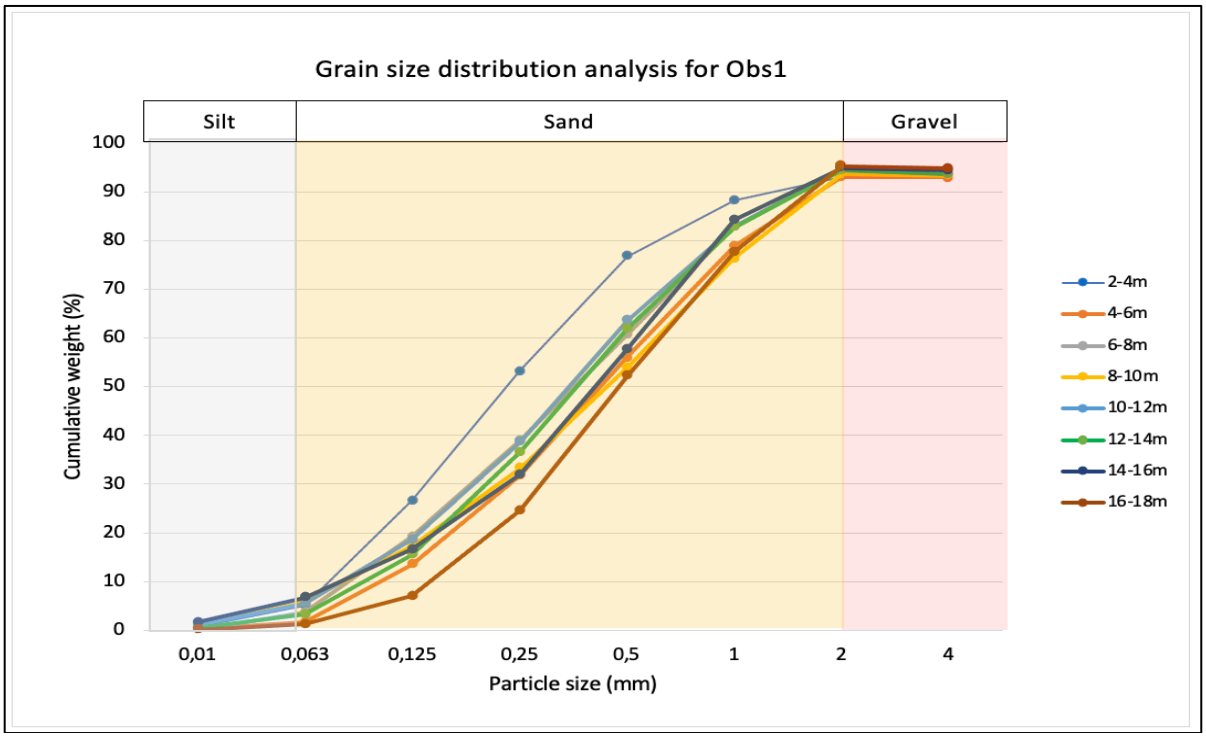

Figure 4.8. Grain size distribution analysis for Obs 1.

The grain size distribution for Obs2 located southeast of Obs1 shows poorly sorted sand the first 20m below the surface before a mixture of poorly sorted sand and gravel from 20 to 27m below surface (Figure 4.9). The observation well reached bedrock at 27m depth. The samples were collected with 1m intervals.

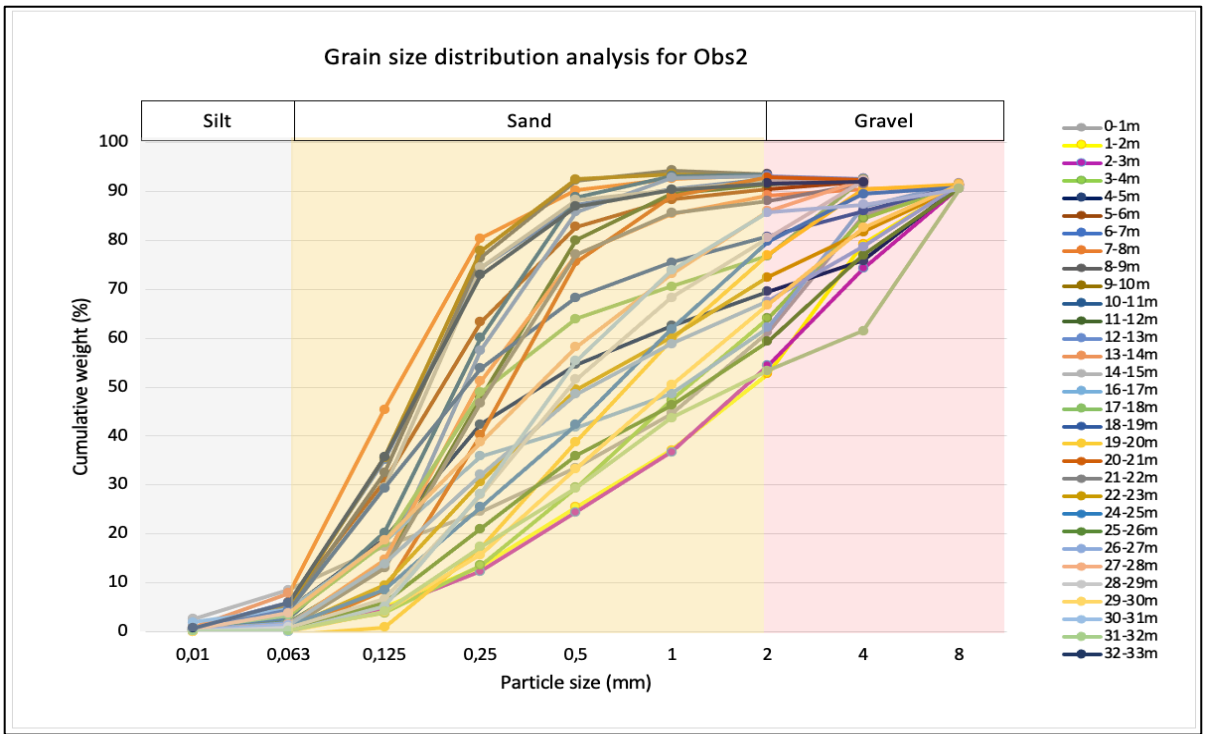

Figure 4.9. Grain size distribution analysis for Obs 2.

The grain size distribution for Obs5 located in the middle part of the study area some distance away from Drammen river shows only poorly sorted sand (Figure 4.10). The samples were collected at 1m intervals starting at 10m below surface and down to 27m where it reached bedrock.

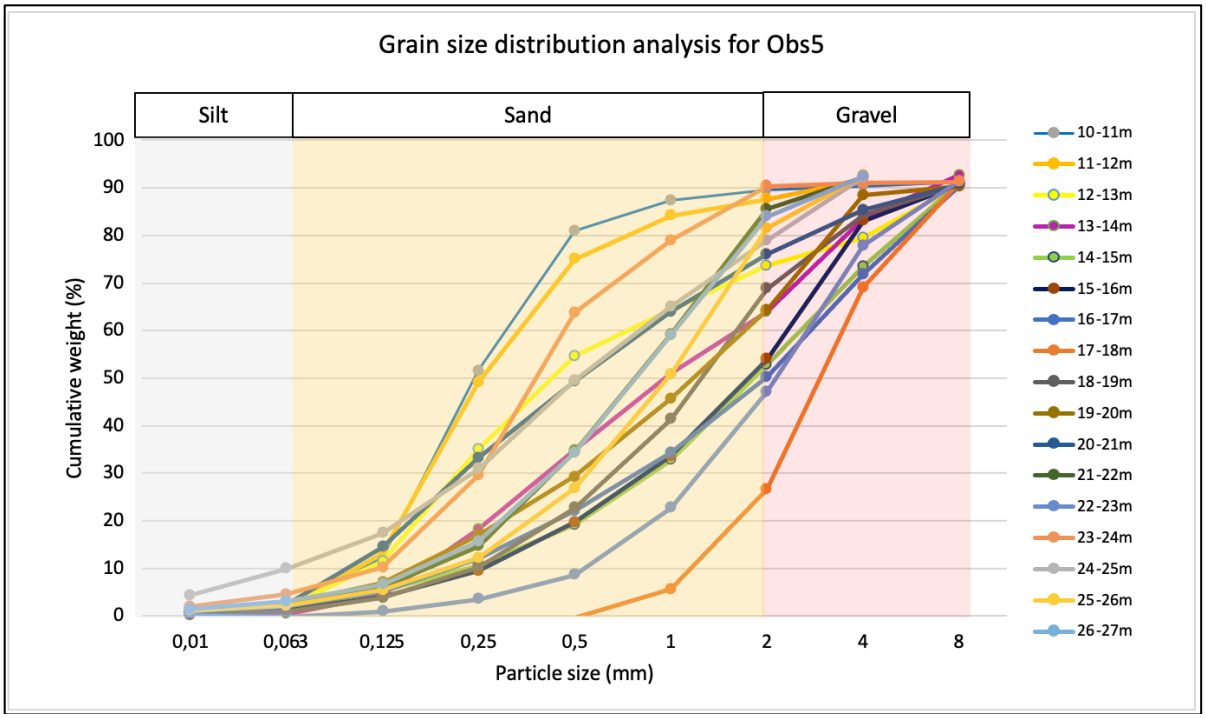

Figure 4.10. Grain size distribution analysis for Obs 5.

The grain size distribution for Obs9 located in the northern part of the study area close to Drammen river shows poorly sorted sand 0 to 20m below surface before a mixture of poorly sorted sand and gravel from 20 to 27m below surface where it reached the bedrock basement (Figure 4.11). The samples were collected at 1m intervals.

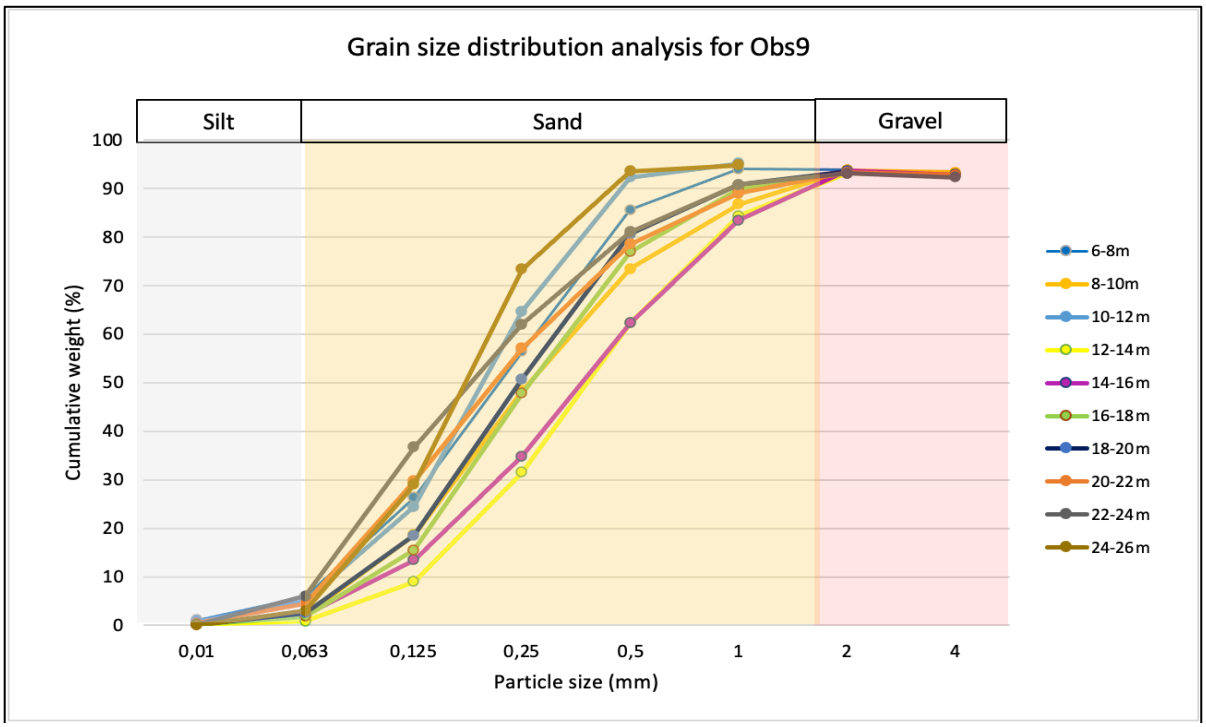

Figure 4.11. Grain size distribution analysis for Obs 9.

4.4.2 Hydraulic conductivity by grain size distribution

For the grain size distribution analysis, the Hazen method was chosen as it is the most common applied method and as it gives good estimations for site-specific hydraulic conductivity. The results were used to explore any variation in the soil layers for the 4 observation wells. The results shows that Obs1, Obs2 and Obs9 have a top soil layer consisting of poorly sorted sand before a mixture of poorly sorted sand and gravel the remaining meters towards the bedrock basement. While Obs5 consisted only of poorly sorted sand (Appendix 3-6). The results show variances in hydraulic conductivity of 3 orders of magnitude varying from $10x^{-2}$ to $10x^{-5}$. Compared to the results of Fetter (1994), the grain size distribution analyses show that the sediments stay within the geological range for sand and gravel.

4.5 Numerical modelling

4.5.1 Regional model

The study area has a type of environment with thin aquifer and large variances in topography that MODFLOW struggles to simulate. The results in layer 1 showed a larger area in the north, south and eastern part of the model (Figure 4.12) with head value of 7.64. Thus, the model does not show a good approximation to reality as the 3 observation wells located in this area were dry during measurement. Layer 2 corresponding bedrock was assigned a very low hydraulic conductivity value of 1 x 10^9m/d to keep it saturated and to ensure that the layer never dries. Assigning the model an additional layer helped the model to converge, but the result was not satisfactory. In addition, the groundwater flows from the north-western side of the area towards the south-eastern side when the wells are pumping.

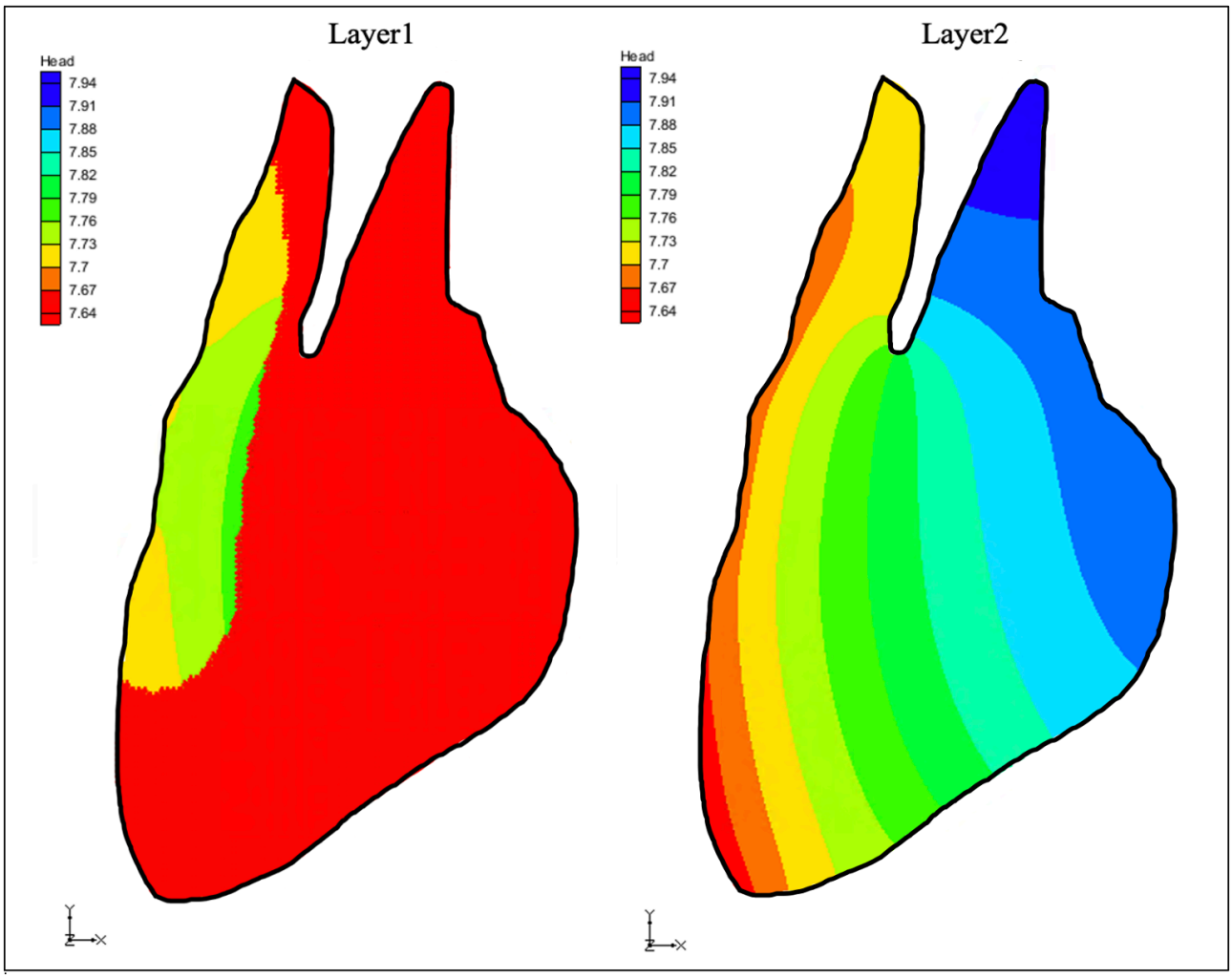

Figure 4.12. The groundwater model before the cut was performed.

4.5.1.1 Model geometry

The drilling logs of all observation wells were used to define the bottom of the first layer (Appendix 7). The results show that the bedrock rises steeply in the eastern part of the study area. From the observation wells that are located closest to Drammen river, the drilling log for Obs8 and Obs9 in the northern part of the study area show a bedrock elevation of -18.46 m.a.s.l. and -14.89 m.a.s.l. East of these wells, the bedrock is visible in the surface (Figure 4.13). The drilling log for Obs1 in the southern part of the study area shows a bedrock elevation of -3.78 m.a.s.l. Further east of Obs1, the drilling log of Obs2 shows a bedrock elevation of 0.61 m.a.s.l. Even further east, the drilling log of Obs3 shows a bedrock elevation of 26.41 m.a.s.l. North-east of this well, the bedrock is also visible in the surface. Furthermore, the drilling log of Obs 6, which was drilled near the middle of the study area show that the bedrock elevation is at 17.71 m.a.s.l. Thus, the drilling logs from all the observation wells indicate that the bedrock rises steeply in the eastern part of the model. A simple illustration was made to show a possible hilltop that extends between the visible bedrock in the north and the visible bedrock in the middle part of the study area (Figure 4.13). Between these points, the sediment layer is very thin. North-east of the southernmost point in the illustration, the bedrock elevation decreases again. Furthermore, the bottom of the second layer consisting of bedrock was assigned a constant value of -30 masl as the bottom elevation of the bedrock is unknown. This is approximately 10m below the deepest drilled observation well.

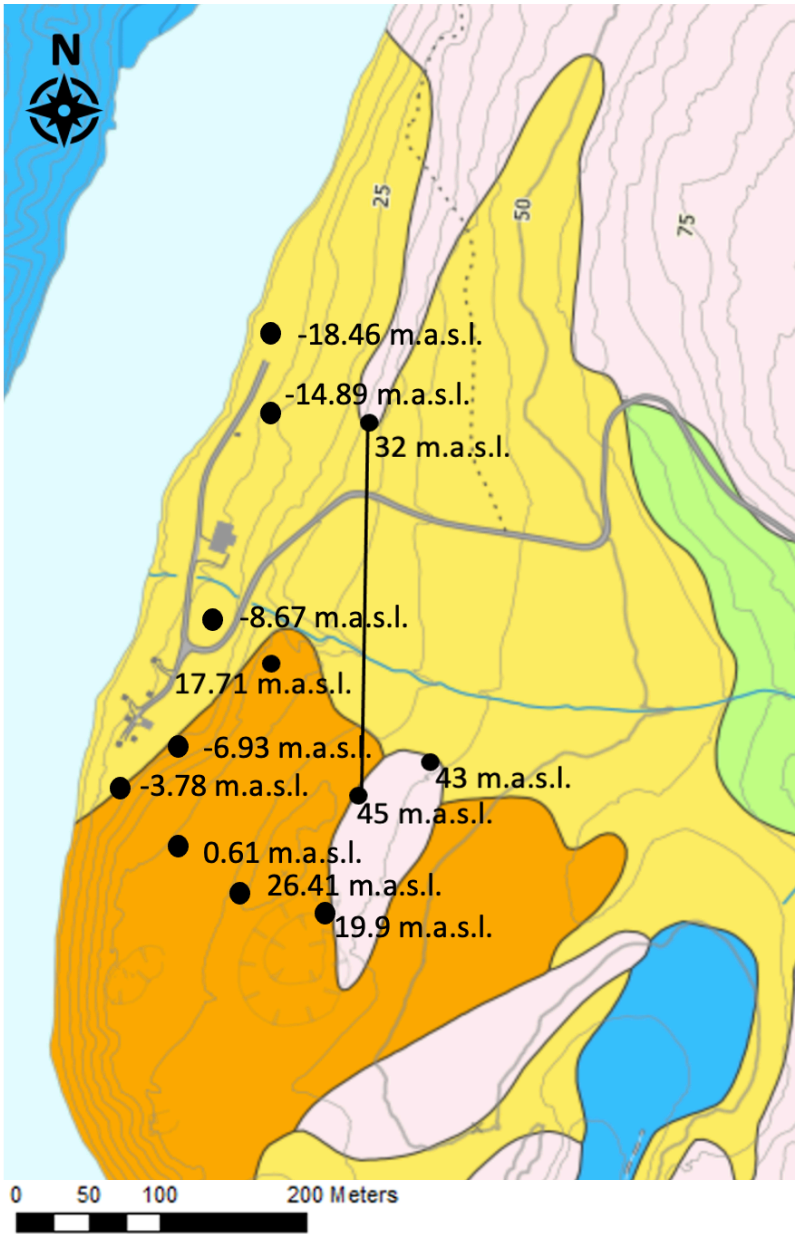

Figure 4.13. Map showing the areas with visible bedrock where the black dots is showing the bedrock elevation (m.a.s.l.) and the black line is illustrating the hilltop.

3.5.2 Local model

The local model was extracted from the regional model (Figure 3.14). The steep slope in the eastern part of the study area has been excluded from the model, which means that the model's surface is relatively flat compared to the regional model. The aquifer thickness for the local model is 54m and the surface elevation is lowest along the Drammen River and extends from 6 m.a.s.l. near the river to 36 m.a.s.l. in the south-eastern part of the model (Figure 4.14).

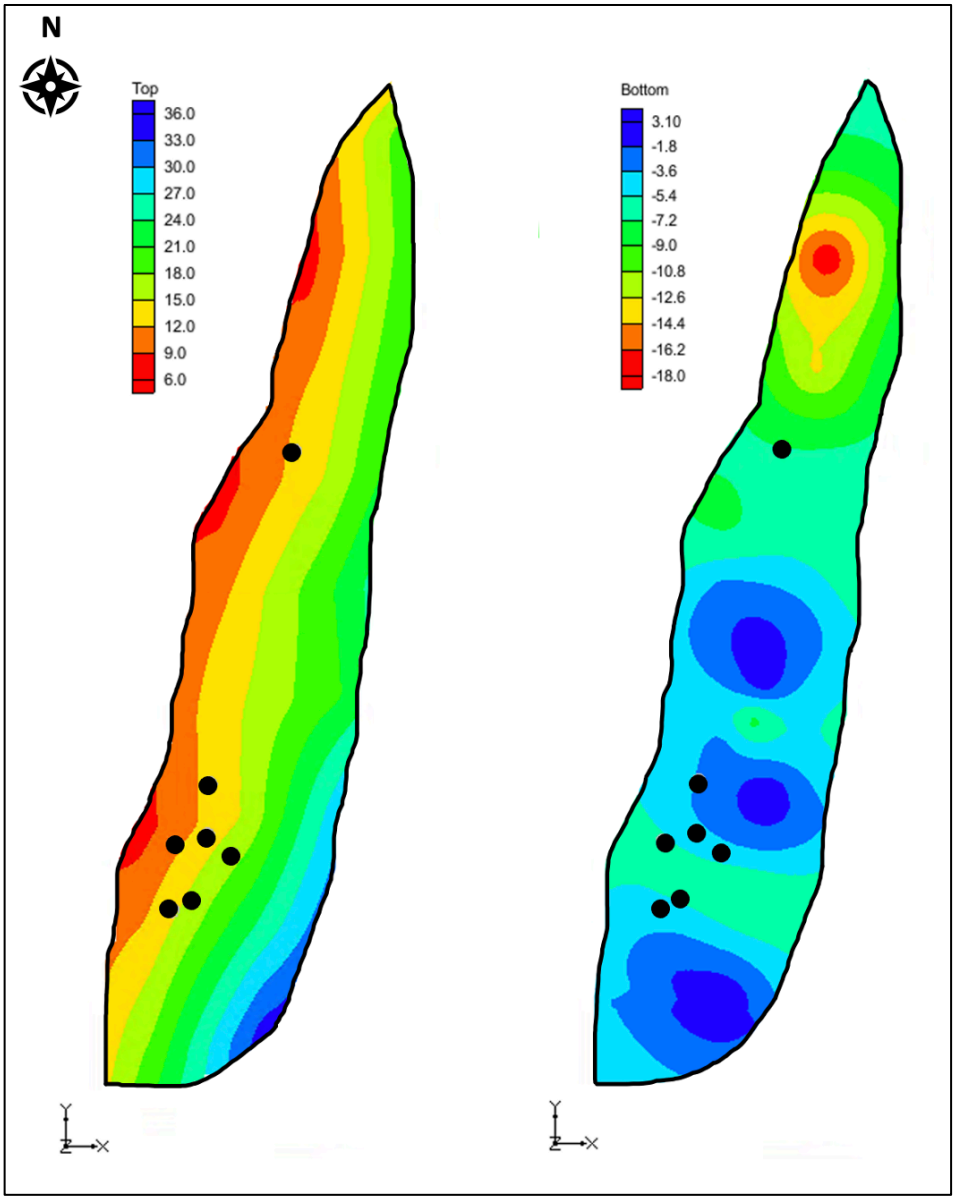

Figure 4.14. Top and bottom elevation of the local model where the black dots is showing the supply wells.

4.5.2.1 Sensitivity analysis

The sensitivity analyses were done to increase the understanding of the aquifer behavior when recharge, hydraulic conductivity and porosity varies. The sensitivity to a change in hydraulic conductivity was tested by increasing the initial hydraulic conductivity by 30% and decreasing it by 30%. The RMSE results show that the model is affected by a change in hydraulic conductivity, but the calculated RMSE value is within what is acceptable as suggested by Anderson *et al*. (2015) (Table 4.1). There is a small change in hydraulic head where an increase in hydraulic conductivity of 30% leads to a decrease in hydraulic head of 0.05m, while a decrease in hydraulic conductivity of 30% leads to an increase in hydraulic head of 0.1m (Figure 4.15). The capture zones with a residence time of 60 days remains unchanged when hydraulic conductivity varies.

Table 4.1. Sensitivity to hydraulic conductivity.

Run	Hydraulic conductivity (m/d) North	South	RMSE
1	320 (initial)	160 (initial)	0.96
2	Increased 30%	Increased 30%	0.97
3	Decreased 30%	Decreased 30%	0.95

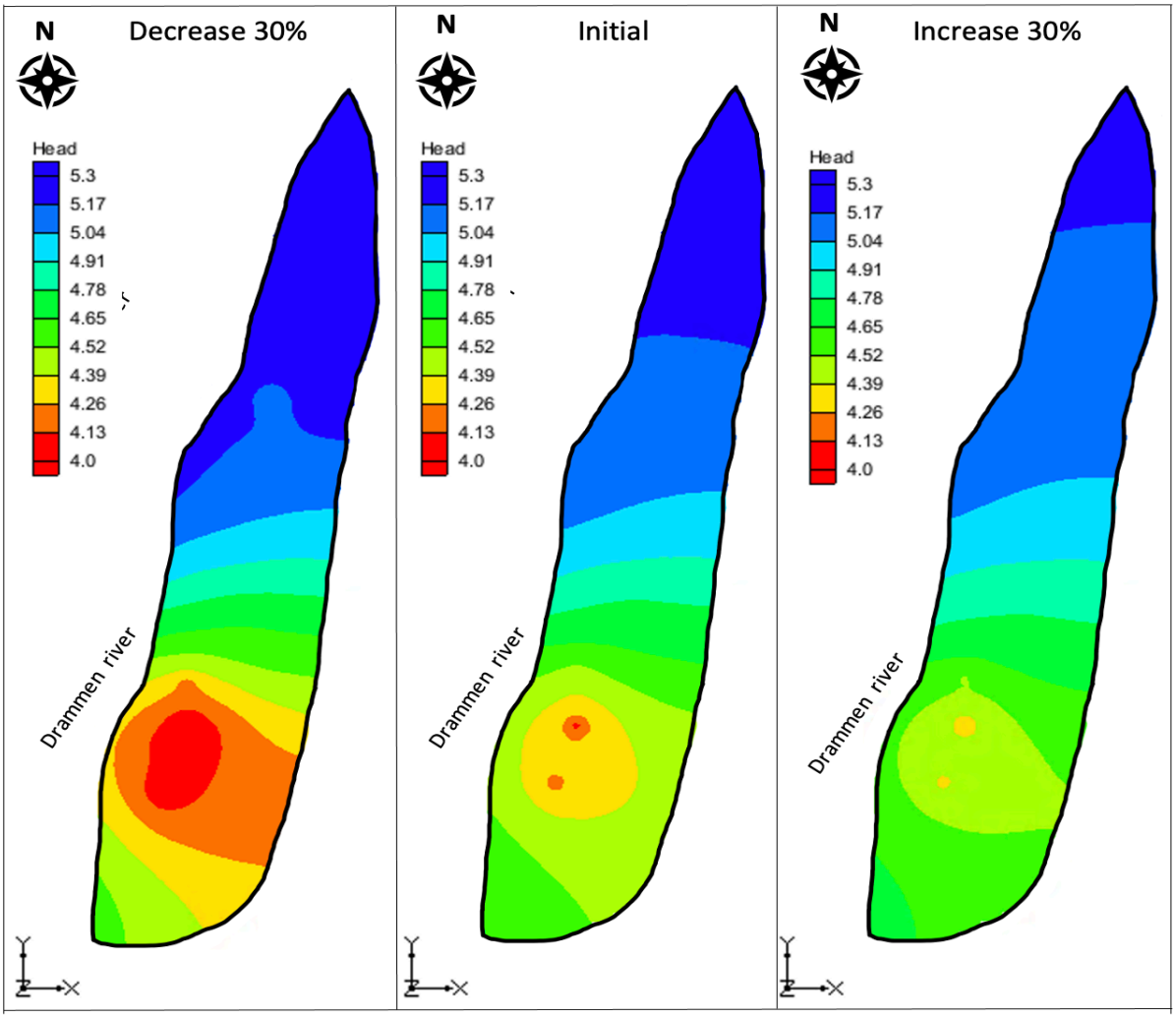

Figure 4.15. Sensitivity analysis showing a decrease and an increase in hydraulic conductivity of 30%.

The sensitivity analysis indicated that the model is more sensitive to changes in recharge than hydraulic conductivity, but the calculated RMSE value is within what is acceptable as suggested by Anderson *et al*. (2015) (Table 4.2). The hydraulic head decreases with increased recharge values which is normal in unconfined aquifers where the hydraulic head is affected by recharge provided by precipitation. When the recharge is decreased with 30% is the hydraulic head increasing with 0.1m and when the recharge is increased with 30% is the hydraulic head decreasing with 0.1m (Figure 4.16). The capture zones with a residence time of 60 days remains unchanged when recharge varies.

Table 4.2. Sensitivity to recharge.

Run	Recharge (m/d)	RMSE
1	0.0016 (initial)	1.66
2	Increased 30%	1.63
3	Decreased 30%	1.65

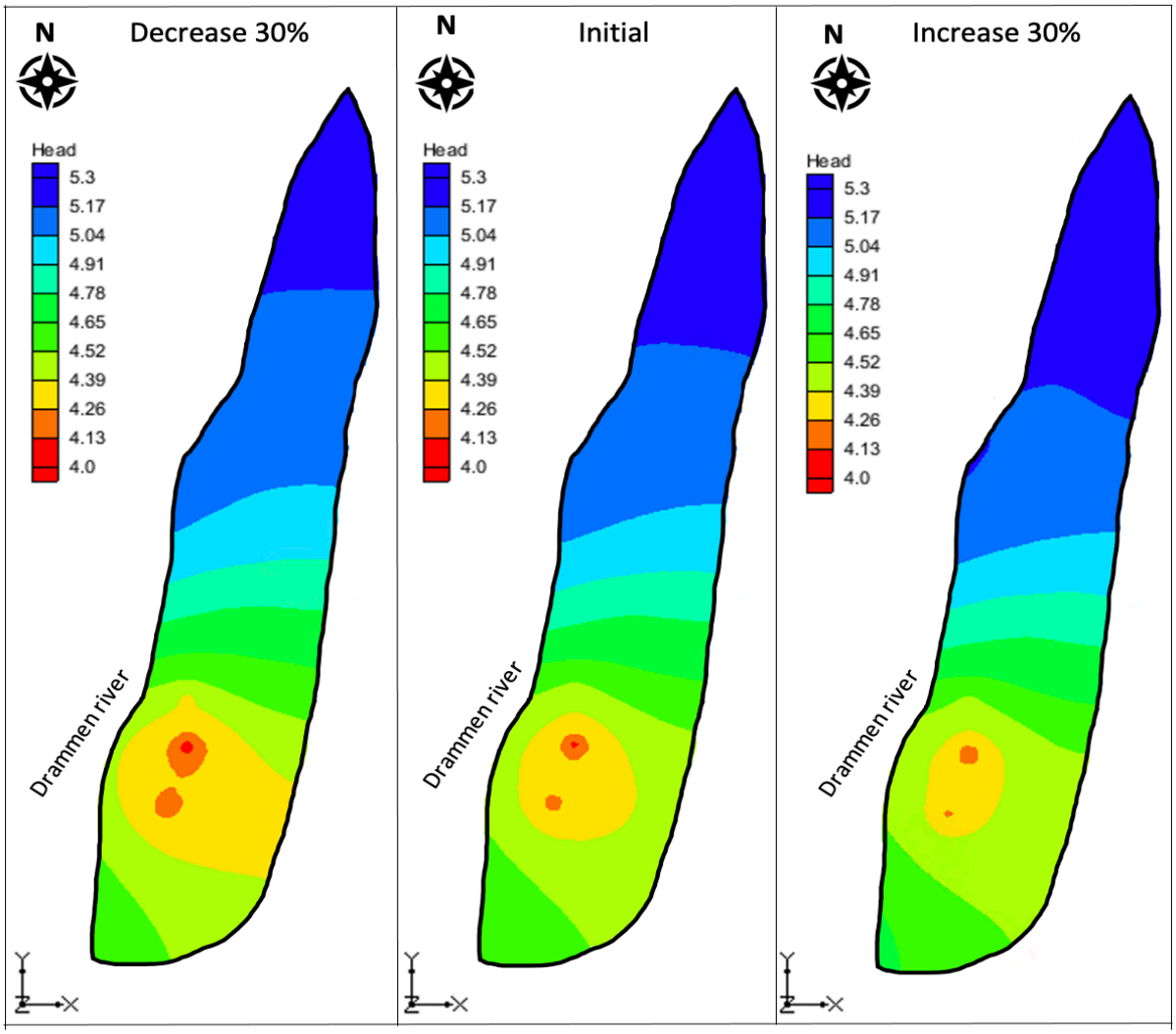

Figure 4.16. Sensitivity analysis showing a decrease and an increase in recharge of 30%.

The sensitivity analysis indicates that the capture zones with a residence time of 60 days are sensitive to changes in porosity where a higher porosity value increases the capture zones (Figure 4.17).

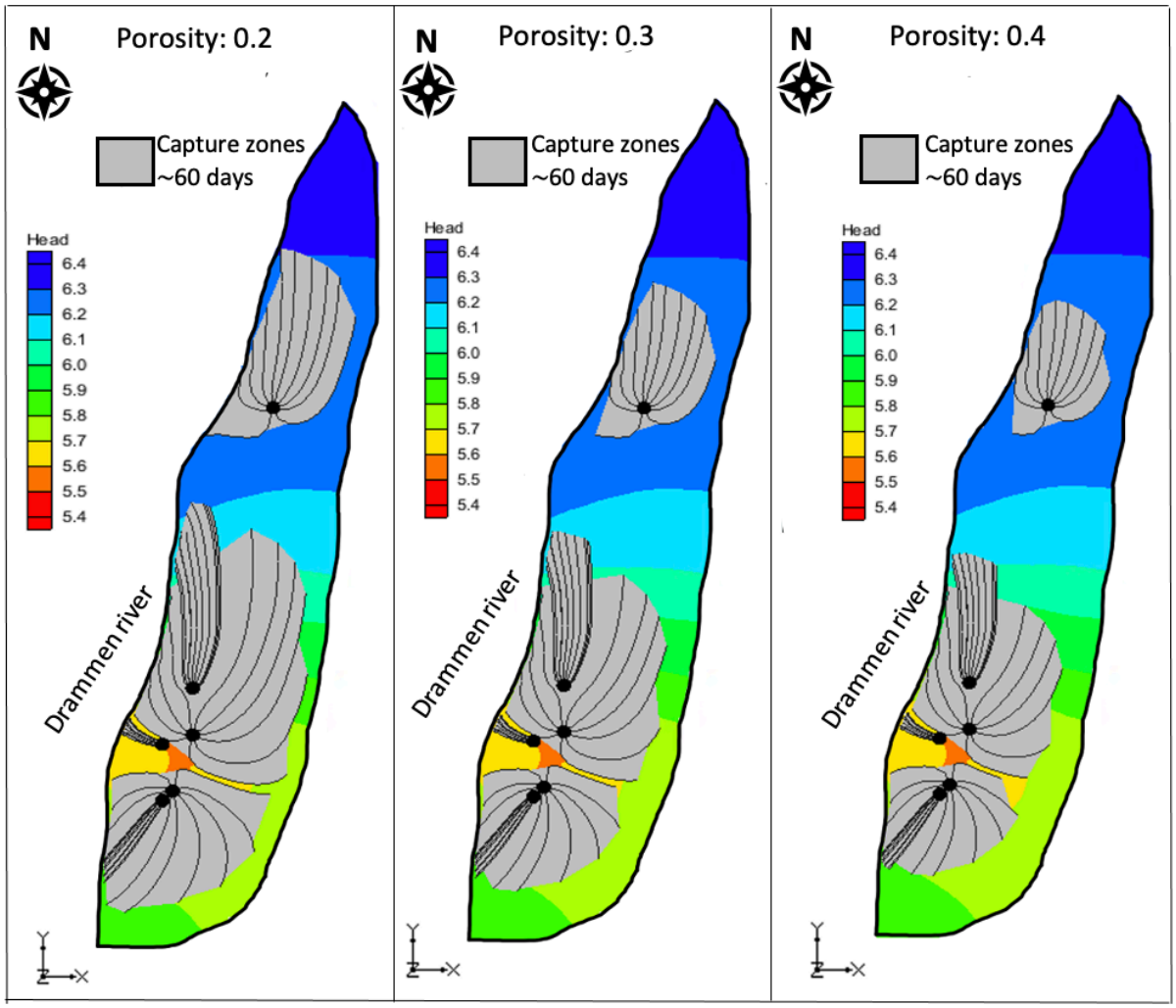

Figure 4.17. Model sensitivity to changes in porosity.

4.5.2.2 Calibration

The results of the calibration process shows an overall good agreement between the observed hydraulic heads from the field and the computed head values from the model (Figure 4.18). But there is not a good agreement between observed and computed heads for observation well G3 which can be seen as the observed and computed points are plotted further apart from each other with a deviation of -2.30m. Observation well G2 and did also have a deviation of -0.69m. The RMSE value for the calibrated model was 0.93 m which was considered as an acceptable error as the supply wells were pumping during measurements which affected

observation well G3 (Appendix 8). The RMSE value is 0.39m if observation well G3 is excluded.

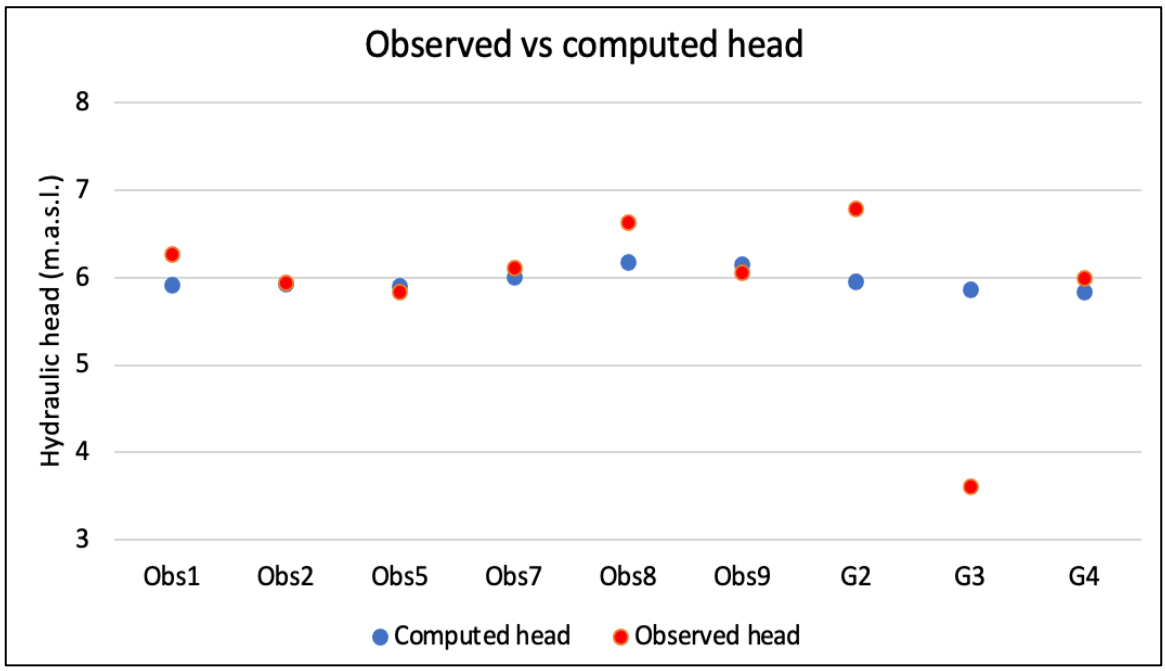

Figure 4.18. Plot of observed vs computed head values for the calibrated model.

4.5.2.3 Hydraulic conductivity assigned after calibration

The values used after calibration of the groundwater model in the different zones show that the northern part of the model has a higher hydraulic conductivity of 300 m/d than the southern part of 100 m/d. The result fit with the previous report from Asplan Viak (1995) as well as the grain size distribution analysis stating that the northern area has higher hydraulic conductivity than the southern area. But the grain size distribution analysis showed lower average hydraulic conductivity in both the northern and southern part of the model than what was used after calibration.

4.5.3 Water budget and groundwater flow simulations

The water budget with average pumping in 2020 showed 1248.49 m^3 of water is going into the groundwater with the most of it comes from daily surface recharge of 643.48 m^3while Drammen river feeds the system daily with an amount of 605.01 m^3. In addition, -1248.49 m^3 is going out from the groundwater system each day (Table 9).

Table 9. Water budget when wells are pumping their average value in 2020.

Sources/sinks	Flow in (m^3/d)	Flow out (m^3/d)
Constant head	0.0	0.0
Wells	0.0	-1248.49
Drammen river	605.01	0.0
Recharge	643.48	0.0
Total source/sinks	1248.49	-1248.49

The simulation of the groundwater flow when the wells was pumping was generated after the pumping rate was assigned according to Gurusoft reporting system retrieved from Rambøll for year 2020. Thus, the groundwater level is below the river. The groundwater level from the model is fitting with the water table map measured in field.

4.5.4 Testing different scenarios

4.5.4.1 River leakage by change in pumping rates

It was examined whether an increased pumping rate would lead to an increase in river leakage. The average amount pumped out of each supply well in 2020 were increased with 10%, 20% and 30%. The result show a linear relationship where the river leaks more water into the aquifer when the pumping rates are increased (Figure 4.19). According to the water table, the river leaks 605 m^3/d when the pumping rates of 2020 is used. If the pumping rate is increased by 10% is the river leaks an additional amount of 125m^3/d.

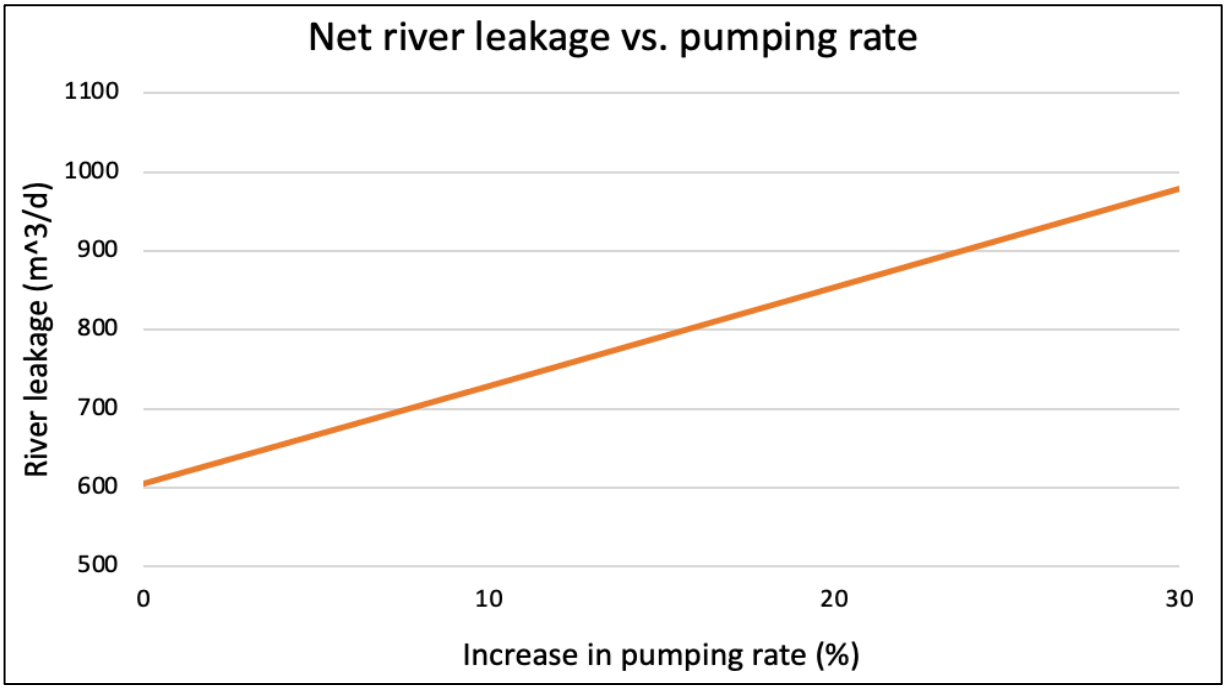

Figure 4.19. River leakage resulting from increased pumping rates in all supply wells in the waterworks.

4.5.4.2 River leakage by change in surface recharge

Changes in surface recharge was explored as it is an uncertain parameter that varies throughout the year. The originally calculated surface recharge was both increased and decreased by 50% when the supply wells were pumping their average amount in 2020. The results show an approximately linear relationship between surface recharge and river leakage (Figure 4.20). For each 100mm with surface recharge, the river leakage decreases with -9 m^3/d. When the original surface recharge increases by 50%, it leads to a decrease in river leakage of 6.63%.

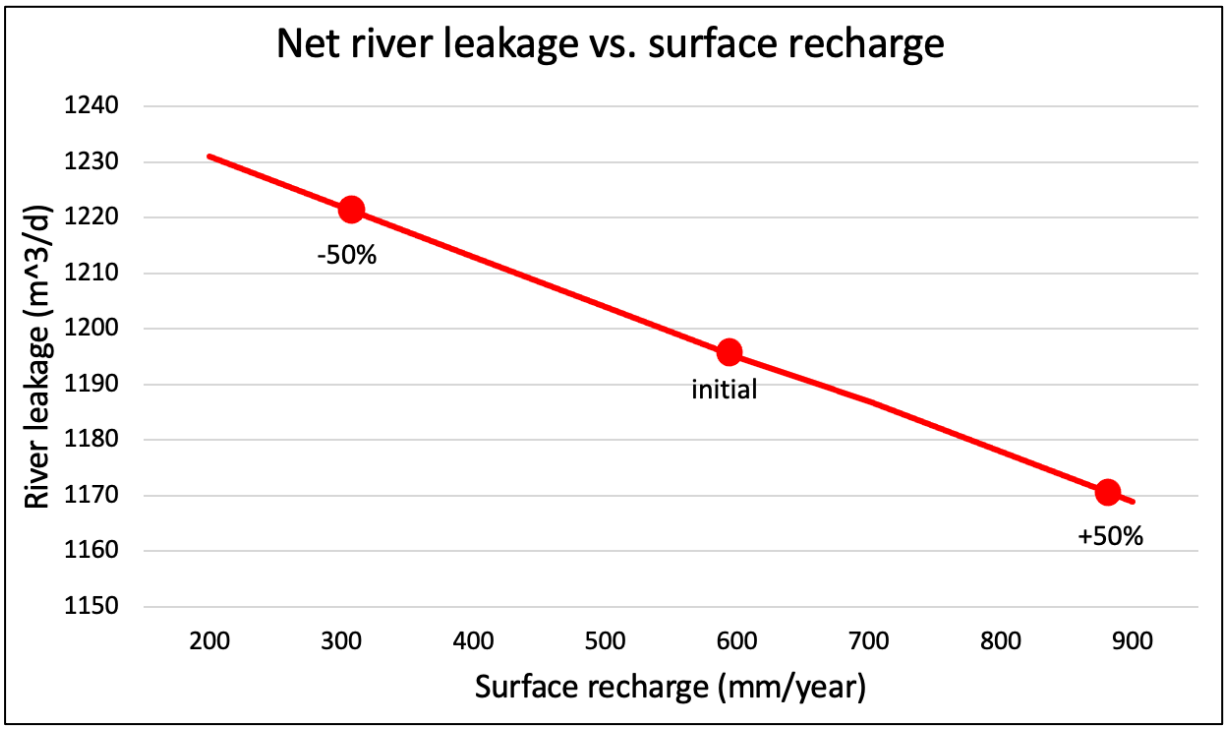

Figure 4.20. River leakage resulting from increased surface recharge in the waterworks. The red circles marks the decreased, the initial and the increased amount.

4.5.4.3 Well capture zones

MODPATH was used with particle tracking to investigate the direction in which the wells draw water from. All the wells draw water from the river, but SBM and SBS4 draw more water from the northern direction. SBS3 draws water from the river and from the northern and eastern direction. SUB draws water from the river and from the eastern and southern direction. SBS1 draws water from the river and the southern direction (Figure 4.21). The capture zone for each of the six supply wells shows the residence time of 60 days, which is the minimum limit the water can use between the river and a supply well to ensure that bacteria from the river die before they reach the well. The result shows that all wells meet the

60-day limit except for SBS5, which has a 50-day limit. SBS5 stands out from the other supply wells as it only draws water from the river and not from any other direction. A new supply well drilled in the north-eastern part of the study area south-east of SBM will maintain a residence time of 60 days and not influence the other existing supply wells (Figure 4.21)

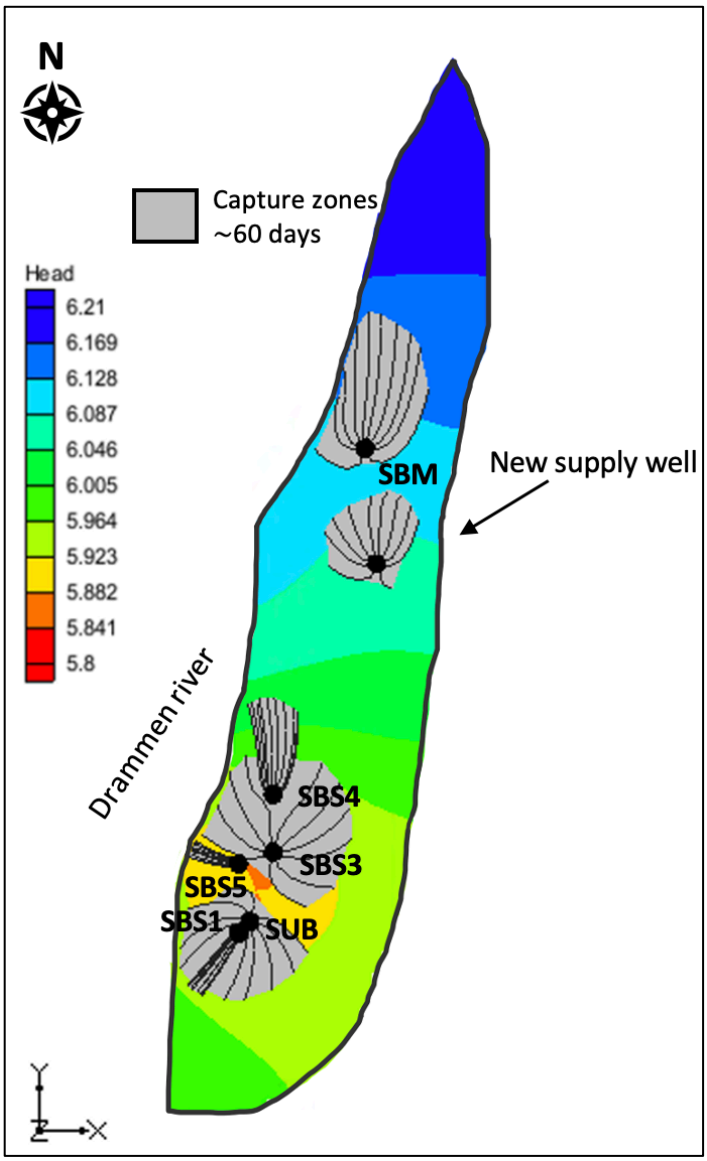

Figure 4.21. The well capture zones showing the residence time of 60 days and the groundwater direction.

4.6 Chemical properties of water

4.6.1 Iron and manganese concentrations in supply wells

From the iron and manganese samples collected in each well in 2019, SUB contains the highest concentrations of iron and also some manganese, but the concentrations is below the maximum limit value of 0.2 mg/l for iron and 0.05mg/l for manganese (Figure 4.22). SBS5 has also high concentrations of iron, but the manganese concentration differ greatly from the other wells with a concentration close to 0.10mg/l which is above the maximal limit. This well also stands out from the others as it only draws water from Drammen river and not from any other direction. In addition, the remaining wells all contain some iron but very little manganese. SUB is the deepest drilled well and has the highest concentrations of iron.

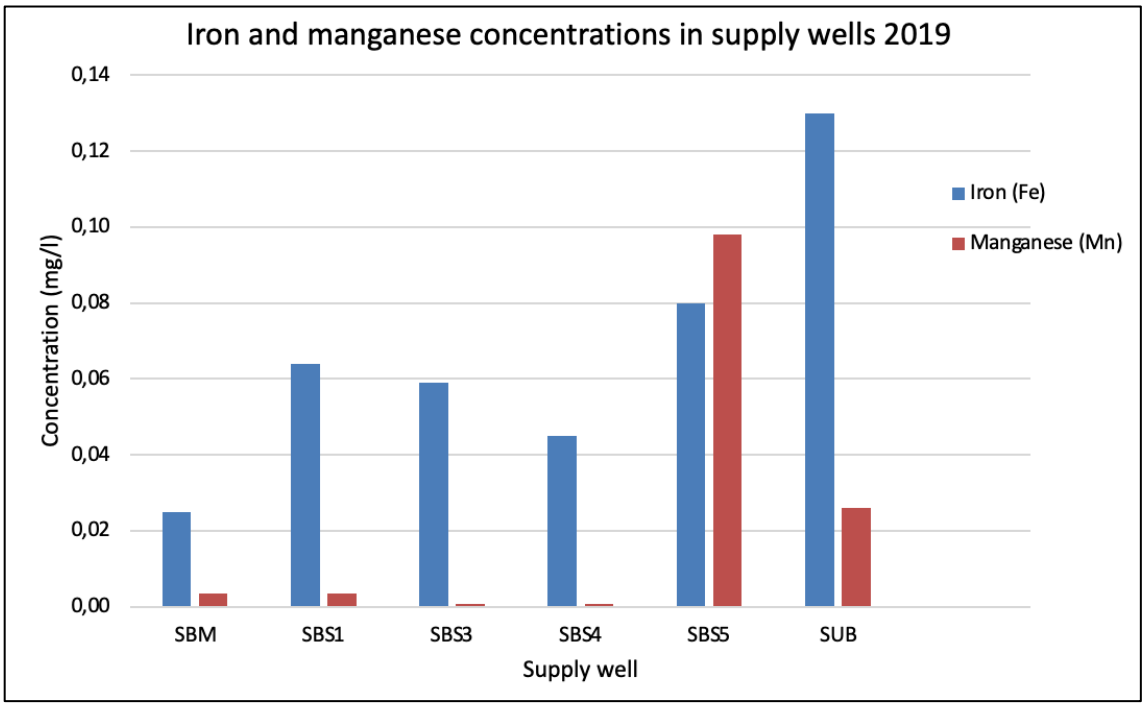

Figure 4.22. Iron and manganese concentration in each supply well July 2019.

4.6.2 Correlation between iron/manganese and precipitation

The iron and manganese concentrations in the groundwater at Strømbo in 2020 showed changes in time with several peaks (Figure 4.23). In relation to drinking water regulations (2022), the manganese concentrations are for long periods above the maximal limit value of 0.05 mg/l, while iron remains stable far below the maximal limit value of 0.2 mg/l. The highest concentration of manganese is detected in January and September and the lowest concentration is detected in August. It does not appear that there is any delay in the

manganese concentration after a period with more precipitation. While the concentration of iron fluctuates between 0.035 and 0.07 mg/l between January and August. The concentration drops in September before it rises slightly again towards the end of the year. Nor does it appear here that there is any delay in the iron concentration after a period with more precipitation. While the precipitation fluctuates between 0 and 20 mm from January and until October. Then it reaches a peak before dropping again towards the end of the year.

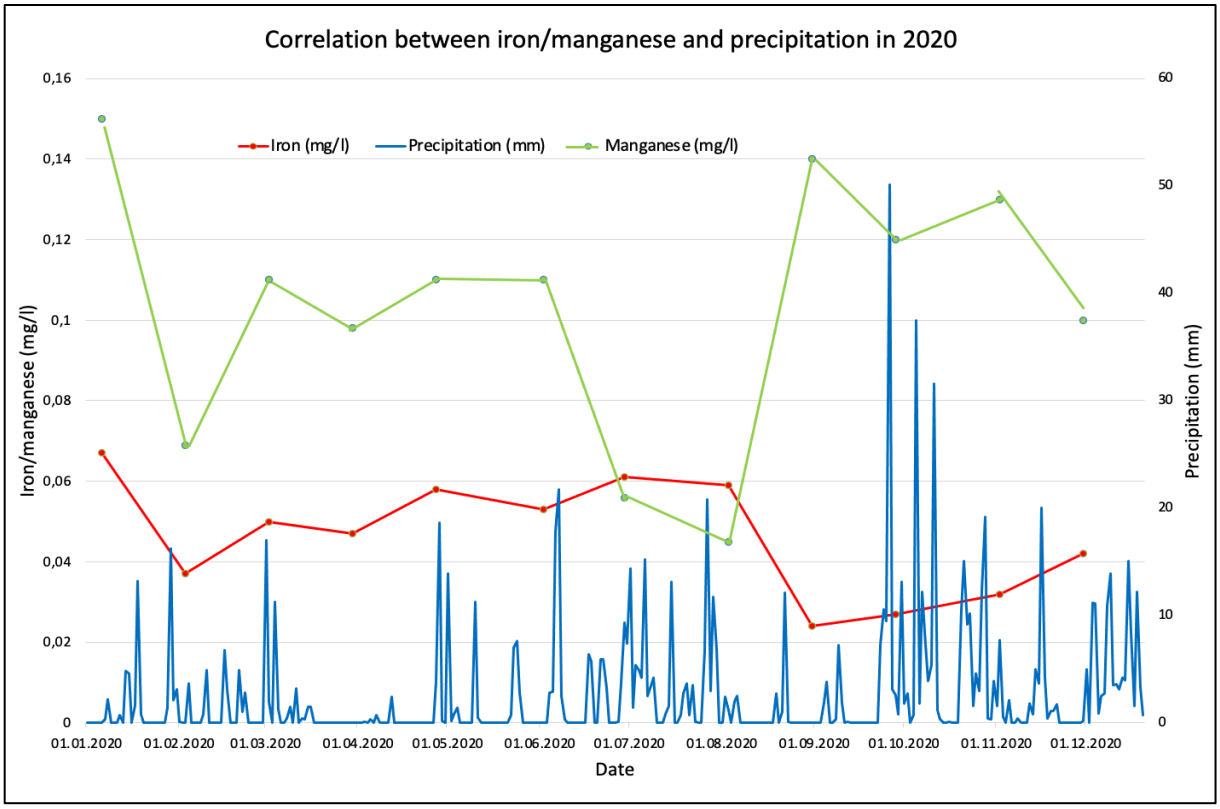

Figure 4.23. Plot of correlation between iron/manganese and precipitation in 2020.

Chapter 5
Discussion

5.1 Water balance

Data used in the water balance equation were retrieved from 2020 to correlate with pumping data for the same year. In the water balance, evapotranspiration was calculated from Tamm's formula assuming that radiation is the main factor for evapotranspiration. However, it does not consider plant cover, soil moisture or the composition of the soil in the area and is thus a major element of uncertainty. The storage term was excluded from the water balance as it is a common practice when considering longer periods like a year and since the model is working in steady state. In addition, the precipitation in the study area was 1077mm in 2020, which stands out from the last 5 years where the average precipitation during the years was 825mm. This may explain why a higher recharge rate was used in the local model after calibration.

5.2 Hydrogeological parameters

The hydraulic conductivity of the model was based on the grain size distribution analyses from 4 of the observation wells. However, there are a number of limitations on the accuracy of the method (Rogas *et al*., 2014). Few samples have been analyzed in relation to the size of the study area. Since the previous study from Norconsult (2011) and the samples collected showed sediments consisting of a mixture of sand and gravel, it was assumed that results from other areas in the model would have small differences. The results were compared to a previous study conducted by Asplan Viak (1995) which showed higher hydraulic conductivity in the northern part of the study area compared to the southern part. This agrees with the results from the grain size distribution analysis conducted in this study and was therefore assumed to be accurate. However, there is no geological reason supporting the difference in hydraulic conductivity between the northern and southern part. But the hydraulic conductivity can vary over several orders of magnitude for the same type of material or in the same aquifer (Murphy and Morrison, 2015). The grain size distribution analysis did also show quite big differences at different depths, which in turn leads to greater differences in the hydraulic conductivity. Most values ranges from 10^{-3} to 10^{-5} m/s which agrees with the values from Fetter (1994), where this interval represents well-sorted sand. To get an even better estimation of the hydraulic conductivity, pumping tests should be carried out.

5.3 Regional model

The interpolation of the bottom of layer 1 was one of the most challenging parts during the construction of the groundwater model. Most of the observation wells were drilled close to each other along Drammen river and some were drilled up the terrain, which led to a lack of bedrock information in large areas in the model. Especially the area north of the observation wells and the eastern area up the terrain had no available information. To interpolate the bedrock elevation, the drilling logs of the observation wells were used. It was intended to also use the geophysical surveys to define the bedrock, but they were limited to only 3 profiles (one in the north along Drammen river and two in the south/eastern area of the model) and not in the area up the terrain (Figure 3.7). In addition, the geophysical surveys only provided results based on intervals and not exact values. They had also several uncertainties as the signal quality was bad or since the profiles crossed obstacles affecting the results. Therefore, they were more difficult to use in the model. But they were compared with the drilling logs. The results did show greater differences between the drilling log and the geophysical survey for profile 1 which stretched along the Drammen river in the northern part of the model (Figure 4.5). The geophysical results showed a bedrock elevation between -8 to 8 m.a.s.l. The drilling log for Obs 8, which is located close to this profile, shows a completely different bedrock elevation of -18.46 m.a.s.l. However, there are uncertainties along the profile that made the bedrock difficult to interpret as the profile crossed a metal fence in the first 30 to 80 meters, affecting the result. In addition, the information retrieved from the drilling log only gives information from a discrete location and Obs8 was only close and not exactly on the profile. While the geophysical survey for profile 2, which extends from the north-eastern area of Obs6 towards the south-western area near Drammen river, shows a bedrock elevation between 15 to 30 m.a.s.l (Figure 4.6) The results from the drilling log of Obs6 located close to the start of the profile showed a bedrock elevation of 17.71 m.a.s.l. which is within the interval from the geophysical survey. The geophysical survey of profile 3 which crosses profile 2 from Drammen river in the west to the southeast and up the terrain in proximity to Obs1, Obs2, Obs3 and Obs4 also shows a bedrock elevation between 15 to 30 m.a.s.l (Figure 4.7). Several observation wells were drilled along this profile where Obs1 and Obs2 located near the start of the profile do not match the geophysical survey showing a much lower bedrock elevation. But the geophysical survey of profile 3 has a significant worse signal quality than the other profiles which may have influenced the result. In addition, there are uncertainties in the profile as the model could not be interpreted along shorter parts of the

profile as there occurred disturbances from fencing in the resistivity model. In addition, along the last 50m of the profile, the signal die under a superficial, flat reflector. But the drilling log of Obs3 and Obs4 located near this part of the model show a bedrock elevation of 26.41 m.a.s.l. and 19.9 m.a.s.l. which is within the result from the geophysical survey. Thus, profile 3 has a significantly worse signal quality than the other profiles. It is probable that poorer depth penetration of profile 3 can be linked to geological conditions, e.g., a rich occurrence of boulders, which is indicated by a large number of hyperbolas that leads to a spread signal.

The interpolation of the bedrock is the largest source of error in the stratigraphy interpretation and may have been both thinner and thicker in large parts of the regional model.
Simulating thin aquifers with large variance in topography is a challenging task for groundwater models, explaining why the regional model did not converge with only one layer. Thus, it is important to avoid thin layers to facilitate the convergence of the model. For this purpose, an additional layer was added to help the model converging by assigning the second layer a low hydraulic conductivity to keep it saturated with water. But as the model result was not efficient, it was decided to narrow the model to only include the area around the supply wells in the waterworks. In addition, the hydraulic head measurements showed that the 3 easternmost observation wells (Obs3, Obs4 and Obs6) were dry which led to the model being cut a little further to the west from these wells.

5.4 Local model

The local model is part of the regional model (Figure 3.14). The eastern boundary was modeled as a no-flow boundary. This choice was based on the results from the drilling logs of the observation wells and the geophysical surveys. They both showed that the bedrock rises steeply from outside the eastern boundary and up the terrain. In addition, the sediment map shows visible bedrock in the surface (Figure 2.2). It is therefore possible that the bedrock forms a hilltop that goes from the area with visible bedrock in the north to the area with visible bedrock in the middle part of the study area (Figure 4.13). The hilltop creates a physical barrier that pushes the water from the eastern border to the southwest and therefore south of the local model. In addition, the groundwater level map show that the hydraulic head is lower in the south-eastern part of the aquifer, which further supports the assumption that little, or no water comes from the eastern border (Figure 4.4) Thus, it was assumed that the local model will not receive any supply of water from the eastern part of the study area and

the boundary was therefore modeled as a no-flow boundary. If this is not the case and the study area is receiving a supply of water from the eastern border, the model result would be different.

5.4.1 Sensitivity analysis and calibration

The results from the sensitivity analysis for the uncalibrated local model showed that an increase in hydraulic conductivity of 30% led to a decrease in head value of 0.05m, while a decrease in hydraulic conductivity of 30% led to an increase in head value of 0.1m (Figure 4.15). While the sensitivity analysis for the recharge showed that an increase in recharge of 30% led to a decrease in head value of 0.1m and a decrease in recharge of 30% led to an increase in head value of 0.1m (Figure 4.16). Thus, the sensitivity analysis showed that the model is not very sensitive to either of the parameters, but some more sensitive to changes in recharge than hydraulic conductivity. Recharge is a difficult parameter to estimate as it is no direct measurement methods and since it depends on several different factors such as the amount of precipitation and climate. Thus, the recharge will vary throughout the year which can explain why the model is more sensitive to recharge. The model was assigned two hydraulic conductivity zones based on the average value of the results of the drilling logs of the observation wells. In reality, the hydraulic conductivity will vary trough the soil layer where the grain size distribution showed that the upper layer closer to the surface consist of sand while the lower layer closer to the bedrock consist of a mixture of sand and gravel. This may be the reason why the aquifer is some sensitive to changes in hydraulic conductivity. The hydraulic head measurements from all observation wells were used in the calibration of the local groundwater model. The groundwater level was measured in spring 2022, when it was assumed that the water level is high compared to autumn. The results show that there was a good agreement between the observed and calculated hydraulic heads, but observation well G3 had a discrepancy (Figure 4.18). This well is located right next to one of the supply wells and was probably affected by pumping when the measurement was collected. Observation well G2 also had a discrepancy, which may be due to the well not having lid. As a result, surface water can run down into the well and affect the groundwater or the well can become clogged.

5.4.2 Water budget and groundwater flow

Up to 60% of the inhabitants in Hokksund and Skotselv city get their drinking water from Strømbo waterworks. The water budget shows that the Drammen river is the largest source of infiltration in the aquifer, followed closely by recharge. The river is feeding the aquifer when the wells are pumping, and since river water contains more oxygen, the oxygen concentration increases in the groundwater which makes it easier for iron and manganese to dissolve. The water budget do also suggest that precipitation plays a major role as it accounts for a good part of the infiltration down to the groundwater. But the amount of precipitation will vary throughout the year. In seasons with less precipitation and thus a lower recharge rate, more water will leak from the river into the aquifer. While seasons with more precipitation leads to less water leaking from the aquifer into the river.

The direction of the groundwater flow depends on the pumping rate of the supply wells. The groundwater flow moves from the southwestern direction to the northeastern direction when the wells are turned off. This is caused by the topography in the area where the northern part of the study area has a lower surface elevation than the southern part. But the groundwater flow is changes when the wells are pumping causing the groundwater to move the opposite direction from northeast to southwest. Thus, the north-eastern part of the study area is the most suitable area to drill a new supply well.

5.5 Testing different scenarios

The results showed a linear relationship between the increase in pumping rate and the increase in river leakage. When the pumping is turned off, the river leakage is zero. An increase in surface recharge of 50% led to a reduction in river leakage of 6.63% where a higher surface recharge reflects higher groundwater level in the waterworks. Thus, river leakage to the aquifer is seasonal, where periods with more surface recharge result in less river leakage and vice versa. In addition, the results from the capture zones of the six supply wells show that all wells maintain a residence time of 60 days except for SBS5 with a residence time of 50 days (Figure 4.21). Thus, since this well is not holding the 60 days residence time is it less likely that all the bacteria from the river die before reaching this well. SBS5 is also drawing on more river water which increases the oxygen concentration around the well. In addition, neither a change in hydraulic conductivity nor recharge change the wells residence time. However, a change in porosity changes the well residence times where a lower porosity increases the

groundwater velocity and leads to larger capture zones and vice versa (Figure 4.17). If the wells residence time decreases, not all bacteria from the river will die which can explain why all supply wells contain manganese (Figure 4.22). In addition, the results show that the northernmost area is least affected by pumping. Close to this area near Drammen river, two supply wells have already been taken out of operation due to high concentrations of manganese. A new well should therefore not be established too close to the river so that the well does not only draw oxygen-rich water from the river and to ensure that the well's capture zone has a residence time of at least 60 days (Figure 4.21). The municipality also wants the new supply well to be placed close to the current pipeline network, which places restrictions on where the well can be established. Thus, the area north of the current supply wells becomes irrelevant as this area is too far from the pipeline network. Based on this, the most suitable area for a new supply well will be in the middle of the study area southeast of SBM and northeast of SBS4 (Figure 4.21). A new supply well in this area will draw most water from the northern direction and draw little water from the river, thereby reducing the supply of oxygen-rich water from Drammen River. The results show that it is the supply wells closest to the river that draw most water from it and have the highest concentrations of manganese.

5.6 Chemical properties of water

5.6.1 Iron and manganese concentrations in supply wells

Strømbo waterworks has occasionally had problems with high iron and manganese concentrations for a long time. This can lead to clogged well filters and pipeline networks as well as unwanted color and taste in the drinking water (Stensvik and Hilmo, 2020). Samples taken in July 2019 from each of the six supply wells show that all wells contained iron, some more than other where 4 of the 6 supply wells contain more iron than manganese. The Earth's crust consists of much more iron than manganese and may be a reason for higher concentrations of iron occur in the groundwater than manganese (Houben and Treskatis, 2007). A study carried out by Farnsworth and Hering (2011) shows that induced river infiltration will form a reducing zone near the riverbank. This leads to the oxygen in the river water being consumed by the decomposition of the organic material in the aquifer or infiltrated river water, which further produces reducing conditions and dissolution of iron and manganese. The wells located closest to the river contain the highest concentrations of manganese. Of all current supply wells, SBS5 is located closest to Drammen river and is also only drawing water from it. The river water is oxygen-rich which will make it easier for

manganese to oxidize which further can explain why this well have manganese concentrations above the maximal limit value of 0.05mg/l. In addition, two former supply wells (SBN1 and SBN2) located in the norther part of the study area were situated approximately at the same distance from the river as SBS5 but have been decommissioned as they had to high concentrations of manganese (Figure 2.4). These wells do also only draw on water from the river. Based on the results, the wells located closest to the river have the same problems with high concentrations of manganese.

5.6.2 Correlation between iron/manganese and precipitation

There was no clear correlation between iron/manganese concentrations and precipitation in 2020. Iron remained below its maximum limit value of 0.2mg/l throughout the year, while manganese was above its maximum limit value of 0.05mg/l for large parts of the year. The reason why this correlation was interesting is because precipitation have high oxygen content which can further lead the groundwater into an oxygen-rich state where iron and manganese will precipitate more easily. Rather, the results show that it is the oxygen-rich water from Drammen river that is responsible for the increase in manganese in the supply wells.

5.7 Further work

My final recommendations to Rambøll if the area is to be investigated further would be to achieve more geophysical profiles further east of the study area to gain a better estimation of the aquifer stratigraphy. Pumping test would give a better approximation to the hydraulic conductivity in the area which was only based on grain size distribution analysis in this thesis. In addition, several measurements of hydraulic head over time in the observation wells would give a better assessment of how the groundwater is affected by pumping and recharge. A more thorough investigation of the interaction between Drammen river and the groundwater could have been very interesting to get a better overview of the relationship between them, especially considering that they need to increase the capacity in the supply wells. Finally, daily data of the iron and manganese concentrations over a longer period of time would make it easier to find a definitive reason for the high concentrations. It would make it easier to compare the data with, for example, precipitation, where monthly values were used in this thesis. In would also be interesting to have daily data over the iron and manganese concentrations in each supply well in order to further compare this with meteorological factors.

Chapter 6
Conclusion

The Strømbo aquifer is one of the two sources of drinking water to Øvre Eiker municipality. The municipality wanted to investigate how the waterworks could increase the capacity by the end of summer 2022 to have enough drinking water for an increasing population growth. The groundwater flow model developed in this study has identified the flow pattern of the groundwater in the waterworks and investigated how the aquifer reacts to different pumping and recharge rates. The wells capture zones were also investigated to find the most suitable location for a new supply well that will help the municipality increase the capacity. A regional model was first created, but since there were problems converging it due to a very thin sediment layer, it was cut to a local model centered around the waterworks. The local model was assigned two hydraulic conductivity zones there the northern zone were given a hydraulic conductivity of 300 m/d and the southern zone of 80 m/d which corresponds to literature values for sand and gravel. The sensitivity analysis showed that the model was not very sensitive to either a change in hydraulic conductivity or recharge. An increase in hydraulic conductivity of 30% led to a decrease in groundwater level of 0.1m, and a decrease in hydraulic conductivity of 30% led to an increase in groundwater level of 0.1m. While an increase in recharge of 30% led to a decrease in head value of 0.1m and a decrease in recharge of 30% led to an increase in head value of 0.1m. Thus, the model was more sensitive to changes in recharge which may be due to recharge being a difficult parameter to estimate and since it will vary throughout the year. However, the sensitivity analysis showed that the well capture zones are sensitive to changes in porosity. The calibration process ended at a RMSE-value of 0.93m which is an accepted value based on literature. But the RMSE-value would have been lower (0.39m) if observation well G3 was excluded as this well is located next to one of the supply wells that were pumping during measurement. The local model showed that all supply wells is drawing water from Drammen river and that there is a linear relationship between an increase in pumping and an increase in river leakage. The model also showed that there is a linear relationship between surface recharge and river leakage, where an increase in surface recharge leads to a decrease in river leakage and vice versa. In addition, supply well SBS5 which is located closest to the river has the highest concentration of manganese and is also the only well that is drawing water from the river and no other

directions. Two supply wells north of the current wells at the same distance from the river as SBS5 were taken out of operation as the wells struggled with high concentration of manganese. These wells were also only drawing on water from the river. Thus, the wells located close to the river struggles with manganese concentrations above the maximum limit value. Since these wells are only drawing on oxygen-rich river water leads to a higher oxygen concentration in the groundwater near these wells where manganese dissolves faster compared to the other wells located further away from the river. In addition, the result do not show a correlation between iron/manganese and precipitation in 2020. Although an increase in precipitation will bring more oxygen-rich water into the aquifer, the results show that it is the oxygen-rich water from Drammen river that is responsible for the high manganese concentrations at Strømbo. Finally, a new supply well should not be located to close to the river to ensure that the well remains a capture zone of minimum 60 days. Since the municipality wants to establish the new well close to the pipeline network is southeast of supply well SBM found as the most suitable location.

References

Anderson, M.P and Woessner, W.W. (1992). *Applied Groundwater modeling: Simulation of Flow and Advective Trasport.* Academic Press, Inc., San Diego.

Anderson, M.P., Woessner, W.W., Hunt, R.J. (2015). *Applied groundwater modeling; Simulations of Flow and Advective Transport*, 2nd edition. Academic Press.

Alley, W.M., Reilly, T.E., Franke, O.L. (1999). *Sustainability of Ground-Water Resources.* U.S. Geological Survey Circular 1186. Denver, Colorado.

Alsharhan, A.S and Rizk. Z.E (2020). *Water Resources and Integrated Management of the United Arab Emirates.* The springer.

Asplan Viak (1995). *Compilation of pumping results from the groundwater wells at Strømbo.* Rapport nr. HK-95130/P.nr.94444. Kongsberg.

Bear, J and Verruijt, A. (2012). *Modeling groundwater flow and pollution (Vol. 2):* Springer Science & Business Media.

Bear, J. (2013*). Dynamics of Fluids in Porous Media.* Courier Corporation. New York, Dover. 45 pp.

Belk, T. (1994). Chapter 3: *Groundwater Contamination Wellhead Protection: A Guide for Small Communities*. DIANE Publishing. 10 pp.

Bruce, D.A. (1989). *Methods of overburden drilling in geotechnical construction – a generic classification.* Ground Engineering.

Campling, P., De nocker, L., Schiettecatte, W., Iacovides, A.I., Dworak, T., Kampa, E., Arenas, M.A., Pozo, C.C., Le Mat, O., Mattheib, V., Kervarec, F. (2008). *Assessment of alternative water supply options.*

Casanova, J., Devau, N., Pettenati, M. (2016). *Managed aquifer recharge: An Overview of Issues and Options*. In Book: Integrated Groundwater Management.

Colleuille, H and Kitterød, N-O. (1998). *2D simulering av strømningsforholdene i løsmassene på Sundreøya i Ål kommune*. NVE. Oppdragsrapport. Opplag 30.

Colleuille, H., Pedersen, T.S., Dimakis, P., Frengstad, B. (2004). *Elv og grunnvann. Analyse av interaksjon mellom et grunnvannsmagasin og Glomma på Rena, Hedmark (002.Z).* NVE. Rapport 2.

Colleuille. H., Wong. W.K., Dimakis. P. (2004*). Elv og grunnvann. Analyse av interaksjon mellom et grunnvannsmagasin og Glomma på Rena, Hedmark (002.Z).* NVE. Rapport 3. Grunnvannsmodellering.

Davis, J.C and Sampson, R.J. (1986*). Statistics and Data Analysis in Geology*. Third edition. Wiley New York. 295 pp.

Dingman, S.L. (2015). *Physical Hydrology*, 3rd ed. Waveland Press, Inc, Long Grove, Illinois. 133-253 pp

Evans, B.M and Myers, W.L. (1990). *A GIS-Based Approach to Evaluating Regional Groundwater Pollution Potential with DRASTIC.* Journal of Soil and Water Conservation, 45.

Fetter, C.W. (1994). *Applied Hydrogeology,* Third Edition. Prentice-Hall, Inc., Englewood Cliffs. 75-85 pp.

Fetter, C.W. (2001). *Applied Hydrogeology,* Fourth Edition. Prentice-Hall, Inc., Englewood Cliffs, NJ. 122-125 pp.

Fitts, C.R. (2002). *Groundwater science*. First Edition. Amsterdam. Elsevier Science Ltd. Academic Press. 13-14 pp.

Fitts, C.R. (2013). *Groundwater science*. Second Edition. Amsterdam. Elsevier Science Ltd. Academic Press. 8-155 pp.

Gaut, S. (2009). *Naturlige avsetninger som rensemedium. Hvilke mekanismer gjør at tilstrekkelig oppholdstid i umettet sone utgjør 2 hygieniske barrierer*. Vann nr. 1/2009.

Hansen, L., Rohr-Torp, E., Tønnesen, J.., Rønning, J.S., Mauring, E. (2005). *Grunnvann og grunnvarme fra dype dalfyllinger langs Glåma.* Trondheim. Rapport nr: 2002.082.

Harbaugh, A. W., Banta, E.R., Hill, M.C. and McDonald, M.G. (2000). *MODFLOW-2000, The U.S. Geological Survey Modular Groundwater Model- User Guide to Modularization Concepts and the Groundwater Flow Process*. Virginia: U.S. Geological Survey. Report 00-92.

Hashemi, H., Berndtsson, R., Kompani-Zare, M. and Persson, M. (2013). *'Natural vs. artificial groundwater recharge, quantification through inverse modeling'*, Hydrology and Earth System Sciences.

Houben, G.J and Treskatis, C. (2007). *Water Well: Rehabilitation and Reconstruction*. New York: McGrawHill.

McDonald. M.G and Harbaugh.A.W. (1988). *A modular three-dimensional finite-difference ground-water flow model.*

Morland, G. (1996). *Bruk av grunnvann i Norge*. NGU. Rapport 96.082. ISSN 0800-3416.

Murphy, B.L and Morrison, R.D. (2015). *Introduction to Environmental Forensics*. Third edition. Academic Press. 155 pp.

NGU (2022) *GRANADA – Nasjonal grunnvannsdatabase*. Available at: https://geo.ngu.no/kart/granada_mobil/ (Accessed: 2022).

NGF (1994). *Veiledning for utførelse av totalsondering. Melding nr.9*. Rev.Nr.1,2018. ISBN: 978-82-546-1002-2

Norconsult (2005). *Strømbo brønnfelt. Turbiditetsproblem. Årsakssammenheng og mulige løsninger.* Notat 2. Oslo.

Norconsult (2008). *Strømbo grunnvannsanlegg. Grunnundersøkelser. Etablering av produksjonsbrønner Sbs4 og Sbs5.* Rapportnr. 3991900.hg_r1. Oslo.

Norconsult (2011). *Forsøk: Infiltrasjon med råvann fra Drammenselva. Strømbo grunnvannsanlegg.* Notat 1. Oslo.

Geological Survey of Norway (2022*). Map services: Superficial deposits*. Available at: https://geo.ngu.no/kart/losmasse_mobil/ (Accessed: 2022)

Palmer, J.B. (2013). *Evaluation of MODPATH/MODFLOW for groundwater residence time estimation.* ICPRB Report No. ICP13-10. Interstate commission on the Protomac River Basin.

Pollock, D.W (1989). *Documentation of computer programs to compute and display pathlines using results from the U.S. Geological Survey modular three-dimensional finite-difference ground-water flow model.* Geological Survey Open-File Report, 89-381.

Pollock, D.W. (1994). *User's guide for MODPATH/MODPATHPLOT, version 3: A particle tracking post-processing package for MODFLOW, the U.S. Geological Survey finite-difference ground-water flow model*. U.S. Geological Survey Open-File Report, 6 ch. Technical Report, United States Geological Survey, 94-464.

Pollock, D.W (2012). *User guide for MODPATH version 6 - A particle-tracking model for MODFLOW*. Techniques and Methods 6-A41.

Rambøll (2021). *Oppsummering av kildeområdet og brønnkvalitet på Strømbo vannverk.* Notat nr. K-Not-008. Drammen.

Reilly, T and Harbaugh, A. (2004). *Guidelines for evaluating Ground-Water flow. Scientific Investigations.* U.S. Geological Survey. Report 2004-5038.

Reyne, T.W, Bradbury, K.R., Zheng, C. (2013). *Correct Delineation of Capture Zones Using Particle Tracking under Transient Conditions.*

Rogas, J., Lopez, O., Missimer, T.M., Coulibaly, K.M., Dehwah. A.H.A., Sesler, K., Lujan, L.R., Mantilla, D. (2014). *Determination of hydraulic conductivity from grain-size distribution for different depositional environments*. National groundwater association.

Rosas, J., Lopez, O., Missimer, T.M., Coulibaly, K. (2013). *Determination of Hydraulic Conductivity from Grain-Size Distribution for Different Depositinal Environments Reply.*

SeNorge (2022). *Klima. Øvre Eiker, Viken.* Available at: https://senorge.no/map (Accessed: 10.03.2022)

Statistics Norway (2022). *Kommunefakta. Øvre Eiker (Viken).* Available at: https://www.ssb.no/kommunefakta/ovre-eiker (Accessed: 01.04.2022).

Stenvik, L.A and Hilmo, B.O (2020). *Jern-og manganproblematikk ved grunnvannsuttak med eksempler fra Ringerike og Sunndal vannverk.* Vannforeningen.

Tesfaye, A. (2009) *Steady State Groundwater Flow and Contaminant Transport Modeling of Akaki Well Field and Its Surrounding Catchment (Addis Ababa, Ethiopia)*. Unpublished MSc Thesis, Addis Ababa University, Addis Ababa.

USGS (1997). *Modeling Ground-Water Flow with MODFLOW and Related Programs.* USGS Fact Sheet. FS-121-97.

Appendix

Appendix 1: Groundwater pumped from each well between 2010 and 2020.

Well	**SBS1**	**SBS3**	**SBS4**	**SBS5**	**SBM**	**SUB**
Year	**m³**	**m³**	**m³**	**m³**	**m³**	**m³**
2010	0	276 609	180 216	89 868	37 278	33 448
2011	0	279 648	171 275	33 291	72 715	66 568
2012	0	266 167	119 433	221 090	302 425	7 447
2013	0	81 936	111 263	188 790	272 091	18 159
2014	5 480	139 506	26 733	154 313	97 899	69 158
2015	8 683	267 862	68 099	56 645	266 807	95 192
2016	8 732	64 627	7 946	178 444	311 492	16 047
2017	8 672	178 603	8 629	145 528	202 166	52 236
2018	8 729	140 948	14 193	181 241	171 760	42 176
2019	8 565	194 455	36 032	56 550	19 227	136 141
2020	8 730	145 171	54 005	9 384	138 667	99 786
Average	**5 236**	**185 048**	**72 529**	**119 559**	**172 048**	**57 851**

Appendix 2: Precipitation record (mm) and temperature record (°C) of the study area in 2020.

	Precipitation (mm)	**Temperature** (°C)
January	51,0	2,3
February	28,1	1,9
Mars	40,4	3,4
April	26,1	7,3
May	46,2	10,5
June	95,8	18,7
July	131,6	15,6
August	24,0	17,7
September	112,2	13,1
October	196,8	7,5
November	52,4	4,5
December	241,5	1,4
Total	1046,1	8,6

Appendix 3. Calculated hydraulic conductivity by Hazen method for OBS1.

OBS1	d10	d60	U=d60/d10	Hazen K (m/s)	Hazen K (m/d)	Description
2-4m	0.164	0.984	6.00	2.83E-04	24	Poorly sorted sand low in fines
4-6m	0.434	2.603	5.99	2.00E-03	173	Poorly sorted gravel low in fines
6-8m	0.720	4.319	5.99	5.51E-03	482	Poorly sorted gravel low in fines
8-10m	0.093	0.555	5.96	9.11E-05	7,87	Poorly sorted sand low in fines
10-12m	0.090	0.541	6.01	8.66E-05	7,48	Poorly sorted sand low in fines
12-14m	0.199	1.192	5.98	4.19E-04	36	Poorly sorted sand low in fines
14-16m	0.062	0.372	6.00	4.09E-05	3,5	Poorly sorted sand low in fines
16-18m	0.478	2.869	6.00	2.43E-03	209	Poorly sorted gravel low in fines
18-20m	0.539	3.231	5.99	3.08E-03	266	Poorly sorted gravel low in fines

Appendix 4. Calculated hydraulic conductivity by Hazen method for OBS

OBS5	d10	d60	U=d60/d10	Hazen K (m/s)	Hazen K (m/d)	Description
10-11m	0.272	1.634	6.00	7.88E-04	68.08	Poorly sorted sand low in fines
11-12m	0.224	1.346	6.00	5.35E-04	46.22	Poorly sorted sand low in fines
12-13m	0.214	1.286	6.00	4.89E-04	42.25	Poorly sorted sand low in fines
13-14m	0.345	2.070	6.00	1.27E-03	109.73	Poorly sorted sand low in fines
14-15m	0.134	0.802	5.98	1.90E-04	16.42	Poorly sorted sand low in fines
15-16m	0.196	1.177	6.00	4,09E-04	35.34	Poorly sorted sand low in fines
16-17m	0.146	0.875	5.99	2.26E-04	19.53	Poorly sorted sand low in fines
17-18m	1.189	7.136	6.00	1.50E-02	1296	Poorly sorted sand low in fines
18-19m	0.204	1.226	6.00	4.44E-04	38.36	Poorly sorted sand low in fines
19-20m	0.116	0.696	6.00	1.43E-04	12.36	Poorly sorted sand low in fines
20-21m	0.178	1.071	6.01	3.39E-04	29.29	Poorly sorted sand low in fines
21-22m	0.067	0.404	6.02	4.28E-05	3.70	Poorly sorted sand low in fines
22-23m	0.590	3.543	6.00	3.71E-03	320.54	Poorly sorted sand low in fines
23-24m	0.051	0.308	6.03	2.79E-05	2.41	Poorly sorted sand low in fines
24-25m	0.023	0.137	5.95	5.57E-05	4.8	Poorly sorted sand low in fines
25-26m	0.090	0.540	6.00	8.61E-05	7.44	Poorly sorted sand low in fines
26-27m	0.071	0.420	5.91	5.39E-05	4.66	Poorly sorted sand low in fines

Appendix 5. Calculated hydraulic conductivity by Hazen method for OBS2.

OBS2	d10	d60	U=d60/d10	Hazen K (m/s)	Hazen K (m/d)	Description
0-1m	0.038	0.230	6.05	1.56E-05	1.35	Poorly sorted sand low in fines
1-2m	0.190	1.137	5.98	3,82E-04	33	Poorly sorted sand low in fines
2-3m	0.224	1.135	5.06	5.34E-04	46.14	Poorly sorted sand low in fines
3-4m	0.348	2.087	5.99	1.29E-03	111.46	Poorly sorted sand low in fines
4-5m	0.119	0.712	5.98	1.50E-04	12.96	Poorly sorted sand low in fines
5-6m	0.115	0.687	5.97	1.39E-04	12.01	Poorly sorted sand low in fines
6-7m	0.111	0.669	6.02	1.32E-04	11.40	Poorly sorted sand low in fines
7-8m	0.108	0.646	5.98	1.23E-04	10.63	Poorly sorted sand low in fines
8-9m	0.168	1.011	6.01	3.02E-04	26.09	Poorly sorted sand low in fines
9-10m	0.171	1.024	5.98	3.10E-04	26.78	Poorly sorted sand low in fines
10-11m	0.159	0.954	6.00	2.69E-04	23.24	Poorly sorted sand low in fines
11-12m	0.201	1.207	6.00	4.30E-04	37.15	Poorly sorted sand low in fines
12-13m	0.192	0.960	5.00	3.92E-04	33.87	Poorly sorted sand low in fines
13-14m	0.273	1.637	6.12	7.91E-04	68.34	Poorly sorted sand low in fines
14-15m	0.152	0.913	6.00	2.46E-04	21.35	Poorly sorted sand low in fines
16-17m	0.051	0.305	5.98	2.75E-05	2.38	Poorly sorted sand low in fines
17-18m	0.126	0.756	6.00	1.69E-04	14.60	Poorly sorted sand low in fines
18-19m	0196	1.176	6.00	4.09E-04	35.34	Poorly sorted sand low in fines
19-20m	1.158	9.501	5.99	2.67E-02	2306.88	Poorly sorted gravel low in fines
20-21m	0.812	4.870	5.99	7.00E-03	604.80	Poorly sorted gravel low in fines
21-22m	0.692	4.153	6.00	5.09E-03	439.48	Poorly sorted gravel low in fines
22-23m	0.403	2.419	6.00	1.73E-03	149.47	Poorly sorted gravel low in fines
24-25m	0.272	1.634		7.89E-04	68.17	Poorly sorted sand low in fines
25-26m	0.699	4.194		5.19E-03	448.42	Poorly sorted gravel low in fines
26-27m	0.361	2.164	6.00	1.38E-03	119.23	Poorly sorted sand low in fines
27-28m	0.199	1.194	6.00	4.21E-04	36.37	Poorly sorted sand low in fines
28-29m	0.712	4.272	6.00	5.39E-03	465.70	Poorly sorted gravel low in fines
29-30m	1.636	9.818	6.00	2.85E-02	2462.40	Poorly sorted gravel low in fines
30-31m	0.666	3.997	6.00	4.72E-03	407.81	Poorly sorted gravel low in fines
31-32m	0.613	3.680	6.00	4.00E-03	345.60	Poorly sorted gravel low in fines
32-33m	0.137	0.822	6.00	1.99E-04	17.19	Poorly sorted sand low in fines

Appendix 6. Calculated hydraulic conductivity by Hazen method for OBS9.

OBS9	d10	d60	U=d60/d10	Hazen K (m/s)	Hazen K (m/d)	Description
6-8m	0.088	0.525	5.96	8.15E-05	7.04	Poorly sorted sand low in fines
8-10m	0.280	1.681	6.00	8.35E-04	72.14	Poorly sorted sand low in fines
10-12m	0.138	0.827	5.99	2.02E-04	17.45	Poorly sorted sand low in fines
12-14m	0.534	3.202	5.99	3.03E-03	261.79	Poorly sorted gravel low in fines
14-16m	0.356	2.136	6.00	1.35E-03	116.64	Poorly sorted sand low in fines
16-18m	0.837	5.021	5.99	7.44E-03	644.54	Poorly sorted gravel low in fines
18-20m	0.523	3.137	5.99	2.91E-03	251.42	Poorly sorted gravel low in fines
20-22m	0.204	1.225	6.00	4.43E-04	38.28	Poorly sorted sand low in fines
22-24m	0.508	3.047	5.99	2.74E-03	236.74	Poorly sorted gravel low in fines
24-26m	1.303	7.817	5.99	1.80E-02	1555.20	Poorly sorted gravel low in fines

Appendix 7. Measurements and location of hydraulic head in observation wells.

Well	UTM WGS84 32V (N)	UTM WGS84 32V (E)	Well length TOC (m)	Bedrock depth (m)	Bedrock (masl)	Well diameter (mm)	Filter (m)	Depth water level from surface (m)	Elevation (masl)	Head (masl)
Obs1	6629814	549873	18.67	19.5	-3.78	42	none	9.45	15.72	6.27
Obs2	6629794	549904	36.43	34	0.61	168	31.40 - 34.40	28.34	34.29	5.95
Obs3	6629758	549955	13.94	14	26.41	42	none	no water	40.41	dry
Obs4	6629708	549983	16.68	15	19.90	168	12.50 - 14.50	no water	34.90	dry
Obs5	6629839	549911	28.14	26.7	-6.93	168	20.70 - 24.70	13.93	19.77	5.84
Obs6	669887	549969	16.43	14	17.71	168	11.30 - 14.30	no water	31.71	dry
Obs7	6629921	549917	26.27	25.2	-8.67	168	17.20 - 22.20	10.41	16.53	6.12
Obs8	6630130	549950	30.14	29	-18.46	168	none	3.9	10.54	6.64
Obs9	6630079	549945	25.4	27	-14.89	42	none	6.05	12.11	6.06
G2	6629892	549921	14.45					8.82	15.61	6.79
G3	6629840	549876	13.30					11.86	15.47	3.61
G4	6629869	549888	20.08					8.54	14.54	6.0
G5	6629845	549959	26.78					no water	34.29	dry
G6	6629819	549934	26.01					no water	34.68	dry

Appendix 8. Calculation of RMSE from calibration result.

Observation well	Computed head	Observed head	(h_m - h_s)	(h_m - h_s)^2
Obs1	5,919515	6,27	-0,350485	0,122839735
Obs2	5,930923	5,95	-0,019077	0,000363932
Obs5	5,905967	5,84	0,065967	0,004351645
Obs7	6,0078	6,12	-0,1122	0,01258884
Obs8	6,185941	6,64	-0,454059	0,206169575
Obs9	6,159211	6,06	0,099211	0,009842823
G2	5,954439	6,79	-0,835561	0,698162185
G3	5,866566	3,61	2,256566	5,092090112
G4	5,843854	6	-0,156146	0,024381573
		Sum:	0,494216	6,170790421
			RMSE:	0,938904409